

Wright State University

CORE Scholar

---

[Browse all Theses and Dissertations](#)

[Theses and Dissertations](#)

---

2010

## 2,3,7,8-Tetrachlordibenzo-p-dioxin Mediated Immune Suppression through Interactions at the 3'Immunoglobulin Heavy Chain Regulatory Region Enhancers

David Harold Ellis  
*Wright State University*

Follow this and additional works at: [https://corescholar.libraries.wright.edu/etd\\_all](https://corescholar.libraries.wright.edu/etd_all)



Part of the [Pharmacology, Toxicology and Environmental Health Commons](#)

---

### Repository Citation

Ellis, David Harold, "2,3,7,8-Tetrachlordibenzo-p-dioxin Mediated Immune Suppression through Interactions at the 3'Immunoglobulin Heavy Chain Regulatory Region Enhancers" (2010). *Browse all Theses and Dissertations*. 396.

[https://corescholar.libraries.wright.edu/etd\\_all/396](https://corescholar.libraries.wright.edu/etd_all/396)

This Thesis is brought to you for free and open access by the Theses and Dissertations at CORE Scholar. It has been accepted for inclusion in Browse all Theses and Dissertations by an authorized administrator of CORE Scholar. For more information, please contact [library-corescholar@wright.edu](mailto:library-corescholar@wright.edu).

2,3,7,8-TETRACHLORDIBENZO-P-DIOXIN MEDIATED IMMUNE SUPPRESSION  
THROUGH INTERACTIONS AT THE 3' IMMUNOGLOBULIN HEAVY CHAIN  
REGULATORY REGION ENHANCERS

A thesis submitted in partial fulfillment  
of the requirements for the degree of  
Master of Science

By

DAVID HAROLD ELLIS  
B.S., Ashland University, 1991

2010  
Wright State University

WRIGHT STATE UNIVERSITY  
SCHOOL OF GRADUATE STUDIES

October 22, 2010

I HEREBY RECOMMEND THAT THE THESIS PREPARED UNDER MY SUPERVISION BY David Harold Ellis ENTITLED 2,3,7,8-Tetrachlordibenzo-p-dioxin Mediated Immune Suppression Through Interactions at the 3'Immunoglobulin Heavy Chain Regulatory Region Enhancers BE ACCEPTED IN PARTIAL FULFILLMENT OF THE REQUIREMENTS FOR THE DEGREE OF MASTER OF SCIENCE.

---

Courtney Sulentic, Ph.D.  
Thesis Director

---

Mariana Morris, Ph.D.  
Chair  
Department of Pharmacology  
and Toxicology  
Boonshoft School of Medicine

Committee on Final  
Examination

---

Khalid Elased, Ph.D.

---

Nancy J. Bigley, Ph.D.

---

Andrew Hsu, Ph.D.  
Dean  
School of Graduate Studies

## **Abstract**

Ellis, David Harold. M.S., Department of Pharmacology and Toxicology, Wright State University, 2010. 2,3,7,8-Tetrachlordibenzo-*p*-dioxin mediated Immune suppression through interactions at the 3' Immunoglobulin Heavy Chain Regulatory Region Enhancers

2,3,7,8-Tetrachlordibenzo-*p*-dioxin (TCDD) is a potent toxin which inhibits the antibody response of B cells. The 3'IgHRR which is involved in transcriptional regulation of the heavy-chain polypeptide of antibodies is inhibited by TCDD. The hs1,2 enhancer region, isolated from the 3'IgHRR, is also inhibited while the isolated hs4 is activated by TCDD. This project sought to determine if that dichotomy in effects results from interactions at enhancer-specific binding sites for AhR, thought to mediate transcriptional effects of TCDD, and NFκB, a transcription factor involved in B cell activation. Here, I report a difference in the effect of TCDD on transcriptional activity of the 3'IgHRR and the isolated hs3b/hs4 enhancer pair, in the context of chromatin. I also demonstrate reduced binding of proteins to the hs1,2 and hs4 enhancer sequences containing both AhR and NFκB binding sites compared to single site sequences, suggesting that an interaction between the proteins alters their binding to the enhancers.

## Table of Contents

Introduction.....	1
The Immune System .....	1
2,3,7,8-Tetrachlorodibenzo-p-dioxin .....	5
Aryl Hydrocarbon Receptor.....	11
3'Immunoglobulin Heavy-Chain Regulatory Region.....	14
Hypothesis and Strategic Aims .....	21
Methods and Materials.....	22
Materials .....	22
Cell Model, Culture Conditions, Viability, and Transfection.....	23
Producing the Parental Cell Line .....	25
Real-Time PCR Testing for $\gamma$ 2b-LoxPhs3a1,2 Incorporation .....	27
Producing the Deletion Derivative Clones .....	29
PCR for Confirmation of hs3a and hs1,2 Enhancer Deletion.....	30
Screening for LPS-Inducible $\gamma$ 2b and the Effect of TCDD .....	31
Enzyme Linked Immunosorbent Assay (ELISA) for $\gamma$ 2b.....	33
The Electrophoretic Mobility Shift Assay (EMSA): .....	34
Nuclear Protein Isolation .....	34
Labeling Probes: .....	36
EMSA: .....	37
EMSA/Western .....	39
Statistical Comparisons:.....	40
Results and Discussion .....	41
Conclusions.....	103
Bibliography .....	105

## Table of Figures

Figure 1 The Ig Heavy Chain Gene Locus. ....	2
Figure 2 Class Switched Heavy Chain Gene Locus .....	4
Figure 3 The Aryl Hydrocarbon Receptor (AhR) Signaling Pathway.....	12
Figure 4 The Ig Heavy Chain Gene Locus with 3-Prime Enhancer Region.....	14
Figure 5 The $\gamma$ 2b Transgene before and after Cre-Recombination.....	26
Figure 6 Restriction Enzyme Digestion of the $\gamma$ 2b-LoxPhs3a1,2 and pEGFP-CRE Plasmids.....	41
Figure 7 Restriction Enzyme Digest and Linearization of the $\gamma$ 2b-LoxPhs3a1,2 and NEO Plasmids .....	43
Figure 8 Real-Time PCR of DNA from CH12.LX. $\gamma$ 2b-LoxPhs3a1,2 Cells .....	45
Figure 9 LPS-Induced $\gamma$ 2b Expression in CH12.LX. $\gamma$ 2b-LoxPhs3a1,2 Clones .....	48
Figure 10 Inhibition of LPS-Induced $\gamma$ 2b Expression by 10 nM TCDD .....	49
Figure 11 Restriction Enzyme Digestion of the pEGFP-CRE Plasmid.....	51
Figure 12 FACS of GFP-Expressing Cells .....	52
Figure 13 PCR Test for Deletion of the hs3a and hs1,2 Enhancers from Cell Isolates Collected after Limiting Dilution of GFP-Expressing Cells .....	56
Figure 14 PCR Test for the Presence of the hs3a and hs1,2 Enhancers in Cell Isolates Collected after Limiting Dilution of GFP-Expressing Cells .....	57
Figure 15 PCR Test for the Presence of hs3a and hs1,2 Enhancers in Proposed Deletion Derivatives .....	58
Figure 16 PCR Test for hs3a and hs1,2 Deletion from Proposed Deletion Derivatives ...	59
Figure 17 PCR Test for hs3a and hs1,2 Deletion from Proposed Deletion Derivatives ...	60
Figure 18 PCR Test for hs3a and hs1,2 Deletion from Proposed Deletion Derivatives ...	61
Figure 19 PCR Test for the Presence of the hs3a and hs1,2 enhancers in Proposed Deletion Derivatives.....	62
Figure 20 PCR Test for the Presence of the hs3a and hs1,2 enhancers in Proposed Deletion Derivatives.....	63
Figure 21 LPS-Induced $\gamma$ 2b-Expression and Inhibition by TCDD in CH12.LX. $\gamma$ 2b- LoxPhs3a1,2-pC13 Cells.....	69
Figure 22 LPS Does not Induce D1 Deletion Derivative to Express $\gamma$ 2b .....	70
Figure 23 LPS Induced $\gamma$ 2b Expression in CH12.LX. $\gamma$ 2b-LoxPhs3a1,2-pC14 and – pC15 Cells .....	71
Figure 24 First Study of the Effect of LPS and TCDD on Deletion Derivative D2-29 and Its Parental pC13 .....	72
Figure 25 Second Study of the Effect of LPS and TCDD on Deletion Derivative D2-29 and Its Parental pC13 .....	74
Figure 26 The Effect of LPS and TCDD on Various Deletion Derivatives and Their Parental pC13 .....	76
Figure 27 Initial EMSA Optimization with Variable Reagent Concentrations .....	80
Figure 28 Initial EMSA Optimization Showing Variable Reagent Concentrations and Imager Anomalies .....	81
Figure 29 Optimization of the EMSA for the hs4 probe.....	82
Figure 30 Optimization and Characterization of the hs4 Probe with an Overhang .....	83
Figure 31 EMSA with hs4 and DRE3 probes .....	84

Figure 32	EMSA with the hs4 and DRE3 Probes and Various Unlabeled Competitors ..	88
Figure 33	EMSA with the hs4 and DRE3 Probes and Unlabeled Competitors at a 30 nM TCDD Treatment .....	89
Figure 34	EMSA/Western to Study the Binding of AhR and RelA.....	90
Figure 35	EMSA/Western with 4% or 6% Polyacrylamide Gels .....	92
	Figure 36: EMSA Comparing 100 and 130 mM KCl and 10 and 30 nM TCDD with the hs4 and DRE3 Probes .....	94
Figure 37	Optimization of the KCl Concentration for EMSA of the hs1,2 Probe.....	96
Figure 38	EMSA with the hs4 Probe and Cells Treated with AhR Ligands .....	97
Figure 39	Re-optimization of the hs4 and hs1,2 Probes .....	99
Figure 40	EMSA with Mouse and Human hs1,2 Probes .....	100
Figure 41	EMSA Comparing the Binding of Altered hs4 Sequences.....	101

## Table of Tables

Table 1 EMSA Probes .....	37
Table 2 Thershold Crossing ( $C_T$ ) Values from Real Time PCR.....	44
Table 3 Results of PCR testing of CH12.LX. $\gamma$ 2b-LoxPhs3a1,2 clones.....	55
Table 4 Results of PCR testing of the D2 Subclones.....	64
Table 5 Results of PCR testing of the Various Subclones.....	65
Table 6 Results of PCR testing of the Various Subclones 2.....	66
Table 7 Results of PCR testing of the Various Subclones 3.....	67
Table 8 Results of Subclone Testing for $\gamma$ 2b Transgene Modification.....	68

# Introduction

## The Immune System

The immune system defends the body from infectious organisms and protects it from damage by foreign molecules. It is composed of the innate and the adaptive immune responses. Innate immunity is the body's immediate response to threats. It includes the epithelial barrier which blocks entry to the body; phagocytic cells which engulf microbes, foreign materials, and dead cells; natural killer cells which destroy infected or foreign cells; and the complement system which opsonizes or marks microbes for removal or kills them directly. Adaptive immunity is the body's response to specific threats and includes the activity of lymphocytes and their effector molecules: antibodies and cytokines. Adaptive immunity can be divided into humoral and cell-mediated immunity. Humoral immunity is directed by B cells and involves production and secretion of antibodies, or soluble immunoglobulin molecules.

Immunoglobulins (Ig) are polypeptides made of two heavy and two light chain peptides linked by disulfide bonds. They are produced by all B cells as membrane-bound, B Cell Receptors (BCR). When a B cell is activated by binding of its BCR by antigen and accessory receptor binding, B cells proliferate and produce soluble Ig which is secreted to extracellular spaces so it can opsonize and neutralize antigens, activate the complement cascade, and activate phagocytic cells. One heavy and one light chain come together to

form each arm of an antibody. The heavy and light chains on the Ig are each composed of a constant region and variable region (Ig structure and function reviewed by (Schroeder, et al., 2010). On each arm of the antibody, a light chain variable region ( $V_L$ ) and heavy chain variable region ( $V_H$ ) create an antigen binding pocket. Antigen specificity or idiotype is generated by a series of genetic rearrangements which occur in maturing or activated B cells. Germline rearrangement or somatic recombination of V and J genes in the  $V_L$  and the V, D, and J genes of the  $V_H$  is the first step in creating a diverse array of immunoglobulin binding pockets. That diversity is increased by “junctional diversity” through which the nucleotide sequence at the recombined junctions can be altered during somatic recombination. These events occur during B cell maturation. When a mature B cell is stimulated, somatic hypermutation can also change the antigen binding site through random point mutations during B cell proliferation. While somatic recombination and junctional diversity increase antigen binding diversity in the B cell repertoire, somatic hypermutation can increase the binding affinity of an antigen-specific antibody. The isotype or class of an antibody is determined by which heavy chain constant region is expressed. There are five main classes of antibody: IgM, IgD, IgG, IgA, and IgE encoded by constant regions within the heavy chain gene locus (Figure 1).

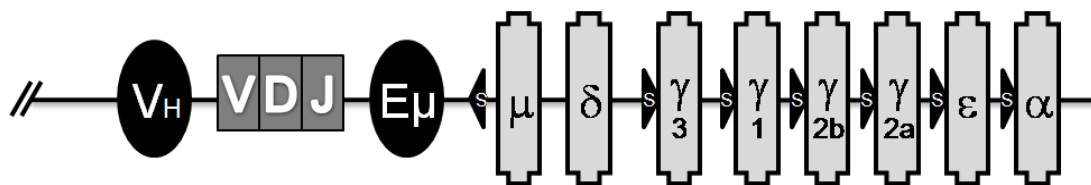


**Figure 1 The Ig Heavy Chain Gene Locus:**  $V_H$  – variable heavy chain promoter;  $VDJ$  – variable region defining antigen specificity;  $E_\mu$  - mu enhancer;  $s$  – switch region for class switch recombination;  $\mu$ ,  $\delta$ ,  $\gamma_3$ ,  $\gamma_1$ ,  $\gamma_{2b}$ ,  $\gamma_{2a}$ ,  $\epsilon$ ,  $\alpha$  – heavy chain constant region isotypes producing IgM, IgD, IgG3, IgG1, IgG2b, IgG2a, IgE, and IgA respectively.

The first gene downstream of VDJ in the germline sequence is  $\mu$  which produces the IgM isotype, a large pentameric antibody with lower specificity and limited function compared to other isotypes. IgD mainly exists as a membrane receptor. IgG is smaller, has greater antigen specificity, and is more flexible than other isotypes. IgG is the most common isotype and can easily move in to extracellular spaces and across the placental barrier. IgA is produced in the greatest abundance, mainly on mucosal surfaces where it controls bacterial populations. IgE is associated with allergic reactions and can produce a strong inflammatory response and may also be important against parasites. Each Ig class has different characteristics giving the antibody particular functions. The first heavy chain gene downstream of the rearranged VDJ region determines the class of antibody produced. The class of antibody produced by a B cell can change upon activation through class switch recombination. During recombination, regions within the heavy chain gene are shifted, irreversibly removing some heavy chain regions and placing a different region immediately downstream of the VDJ (Figure 2). Class switch recombination allows B cells to produce antibody with greater affinity for a specific antigen and a class with optimal physical characteristics for that antigen.

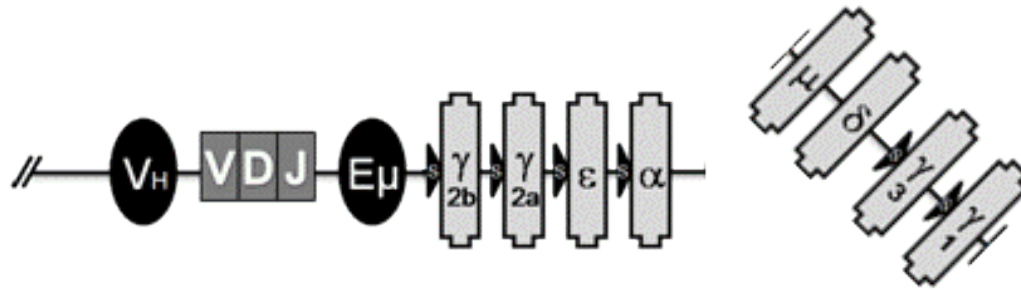


**Figure 2 Class Switched Heavy Chain Gene Locus:** heavy chain constant regions  $\mu$  through  $\gamma 1$  have been cleaved from the locus and  $\gamma 2b$  has become the first constant region downstream of the VDJ. The cell will now produce antibody with the same idiotype but of the  $\gamma 2b$  isotype.

B cells require two signals for activation leading to antibody secretion. Some antigens can provide both signals themselves by binding more than one receptor and/or cross linking BCRs (Vos, et al., 2000). They are called T- independent antigens. Other antigens must be processed and displayed on the B-cell surface through major histocompatibility complex (MHC) receptor so that a T cell will bind and activate the B cell (Bishop, et al., 2001). They are called T-dependent antigens. When a B cell is activated, it produces soluble antibodies and proliferates, undergoing somatic hypermutation in attempt to increase binding affinity for the antigen which caused B-cell activation. For T-dependent antigens, the activated T cell will produce cytokines which stimulate the B cell to increase antibody production. The activated B cell will proliferate, undergo class switch recombination, and differentiate: some of the new cells will become short-lived plasma cells whose only function is to produce and secrete antibody while other daughter cells will become long-lived memory B cells, able to respond quickly with high affinity antibody during future encounters with the same antigen.

Cell-mediated immunity is directed by T cells. When activated, T cells produce signals which can activate phagocytic cells to kill internalized microbes, infected cells to undergo apoptosis, and other immune cells to migrate in to the tissue and initiate an immune response. T cells have membrane-bound receptors (TCR) similar to the Ig receptors of B cells (Rojo, et al., 2008) with antigen binding diversity generated by the same mechanisms (Livák, 2004). The T cell is activated when the TCR binds antigens displayed on MHC proteins of antigen presenting cells such as dendritic cells, macrophages, or B cells, and an accessory receptor is activated by its ligand on the target cell (Bonilla, et al., 2010). Activated T cells proliferate and produce cytokines. Daughter cells can become one of various forms of short-lived effector T cells, producing cytokines appropriate for immune response to the activating antigen, or long-lived memory T cells cable of quickly expanding and producing cytokines in response to future encounters with the same antigen.

The immune system protects the body from foreign molecules and microbes but that function can be affected by xenobiotics which target immune tissues or the vital functions of those tissues. Since immune responses rely on a variety of processes such as receptor activation, signal transduction, cellular proliferation, activation of transcription, and protein production, it is susceptible to modulation by xenobiotics that target any one of those processes. Environmental contaminants such as halogenated aromatic hydrocarbons are known to alter immune function.

## 2,3,7,8-Tetrachlorodibenzo-p-dioxin

2,3,7,8-Tetrachlorodibenzo-p-dioxin (TCDD) is a halogenated aromatic hydrocarbon of natural and synthetic origin with potent toxic effects. It is best known as

a manufacturing by-product in the pesticide, herbicide, and paper industries, but it can be produced anytime an organic substance is burned in the presence of chlorine (Altarawneh, et al., 2009; Dyke, et al., 1997; Huang, et al., 1995). Chlorine is ubiquitous, so TCDD can be produced during most combustion processes including the burning of petroleum based fuels, waste incineration, forest fires, or smoking tobacco. There is a great potential, therefore, for repeated TCDD exposure in the natural environment. TCDD is persistent in the body (Geusau, et al., 2002). Its elimination half-life in humans can range from 1 to 10 years, increasing with age and body fat content but inverse to concentration in the body (Kerger, et al., 2006; Pirkle, et al., 1989; van der Molen, et al., 1998). Due to its long half-life and lipid partitioning, TCDD can bioaccumulate, increasing total body burden with each subsequent exposure (Körner, et al., 2002), which introduces another route of human exposure: from food animals which have accumulated TCDD in their tissues. Many, if not all of TCDD's effects are mediated by the Aryl Hydrocarbon Receptor (AhR) (Okey, et al., 1994; Fernandez-Salguero, et al., 1996). Since it is the most potent AhR ligand known, TCDD is used as a prototype to study AhR ligands in general. Other ligands include pollutants such as other halogenated and polycyclic aromatic hydrocarbons (HAH and PAH), polychlorinated dibenofurans (PCDF) and polychlorinated biphenyls (PCB); and natural compounds such as the flavenoids (found in fruits, vegetables, green tea, and wine), tetrapyrroles (e.g. bilirubin), and indoles (from cruciferous vegetables) (Denison, et al., 2003; Phelan, et al., 1998; Fukuda, et al., 2007; Medjakovic, et al., 2008; Sinal, et al., 1997). The AhR-mediated effects of TCDD might also be associated with these other ligands. It is, therefore, important that we understand those effects and the mechanism by which they are

accomplished so we can better predict the risks associated with exposure to TCDD and other AhR ligands.

In animals or in animal cell models, TCDD causes a host of adverse effects ranging from chloracne or chloaracne-like lesions to mortality (Poland, et al., 1982; Pohjanvirta, et al., 1994). Immunological effects were recognized as early as 1972 when Buu-Hoï *et. al.* (Buu-Hoï, et al., 1972) reported hematological changes and thymic atrophy in rats associated with a single dose of TCDD. The thymus is the principal organ for production and maturation of T cells which, as discussed above, have roles in both cell-mediated and humoral immunity. Gupta *et. al.* (Gupta, et al., 1973) and Harris *et. al.* (Harris, et al., 1973) identified thymic atrophy as the most sensitive indicator of TCDD exposure in guinea pigs and mice and rats. Small spleen size and loss of lymphoid cells from the spleen and lymph nodes also resulted from TCDD exposure. The spleen filters antigens and spent red blood cells from the blood while lymph nodes trap antigens in the lymphatic system; both facilitate an immune response by fostering the interaction of antigens, B cells, and T cells.

TCDD was shown in those early studies to effect two lymphoid tissues important for immune response and alter the number of immune cells present in the blood and lymphatic system. In addition, Vos *et. al.* (Vos, et al., 1973) connected those changes in immune tissues to functional deficits by reporting that TCDD can suppress both cell-mediated and humoral function in guinea pigs and cell-mediated immunity in mice. In the guinea pig, there was clearly a dose dependent decrease in tetanus toxoid secondary response antibody levels (humoral) and in the tuberculin toxin delayed skin hypersensitivity test (cell-mediated) during the course of 8 weekly doses of TCDD. In

mice, the cell-mediated response of splenocytes from a TCDD-treated donor to an untreated, hybrid host's lymph node (graft versus host assay - GVH) was inhibited in a dose dependent manner, suggesting a decrease in cell-mediated immunity. Further studies by Thigpen *et. al.* (Thigpen, et al., 1975) demonstrated that TCDD increased susceptibility of mice to *Salmonella bern.* As little as 1 µg of TCDD per Kg body weight per week (µg/Kg/wk) caused an increase in mortality yet the typical TCDD-related lesions of the liver and thymus did not occur at doses below 10 µg/Kg/wk. The ability of mice to fight *S. bern* infection was inhibited, therefore, at doses which did not produce lesions typical of TCDD toxicity. *S. bern* is an intracellular pathogen which normally can only be cleared by a cell-mediated immune response, suggesting that cell-mediated immunity was affected; however, there was no change in susceptibility to *Herpesvirus suis*, a viral pathogen susceptible to both cell-mediated and humoral immune response. In addition, the bacterial or viral load in that infection model was artificially inflated to lethal levels. It is not clear whether humoral or cell-mediated immunity is more dominant in response to such a challenge. Finally, Vos *et. al.* (Vos, et al., 1978) demonstrated that increased susceptibility to endotoxin-producing pathogens (*S. Bern*) may be caused by a decrease in detoxification of endotoxin, not by inability to clear the infection. It is not clear, therefore, if the humoral or cell-mediated systems, or both were affected. Nor is the mechanism of effect clear since it could be caused by either a loss of immune cells (T-cell, B-cell, phagocytic cells) or cell function; however, Vos *et. al.* (Vos, et al., 1974) studied the change in blood cell counts in mice and found that while 4 weekly doses of 25 µg/Kg caused an increase in neutrophil counts, thymic lesions, and reduced thymic

weight, there was no change in lymphocyte or monocyte blood counts, suggesting that immune suppression is more likely caused by loss of function than loss of immune cells.

Vecchi *et. al.* (Vecchi, et al., 1980) demonstrated in mice that antibody production is inhibited by TCDD but they did not find an effect on cellular proliferation or cell-mediated immunity. Primary antibody production in response to both a T-cell-dependent antigen (sheep red blood cells – SRBC) and a T-cell-independent antigen (Type II pneumococcal polysaccharide) was suppressed by TCDD treatment. Since T cells are only involved in T-cell-dependent humoral response, this suggests that TCDD targeted B cells. Contradiction in results of the GVH assay to test cell-mediated immunity with those of Vos *et. al.* (Vos, et al., 1973) can be explained by their difference in controls: Vecchi injected inactivated cells for the control while Vos injected vehicle alone, thus the effect measured by Vos was probably inflated due to inadequate control of background host response. In a second study, Vecchi *et. al.* (Vecchi, et al., 1983) confirmed that TCDD suppressed humoral but not cell-mediated immunity.

Further evidence that TCDD targets B cells comes from a series of experiments by Dooley and Holsapple. First, they confirmed that immune suppression occurs at lower concentrations than other typical lesions (Holsapple, et al., 1986) and that antibody production is suppressed without affecting cell proliferation (Hosapple, et al., 1986). Similar to Vecchi's results, TCDD inhibited antibody production in response to both T-cell-dependent (SRBC) and T-cell-independent (LPS and DNP-Ficoll) antigens. B cells are necessary for both reactions but T cells are only necessary for reaction to the SRBC. If antibody inhibition was due to an effect on T cells, only the SRBC reaction would be affected. Since both reactions were affected, this suggested that B cells were the principal

target for inhibiting humoral immunity. To test this, they treated mice with TCDD or vehicle and isolated splenic B cells, T cells, and macrophages (Dooley, et al., 1988). By recombining the untreated cell types with TCDD-treated cell types and stimulating the various cell combinations with DNP-Ficol or SRBC, they determined that antibody secretion was only suppressed when the B cells in the recombined population had been exposed to TCDD. IgM secretion was not affected in the recombined population of T cells treated with TCDD and untreated B cells. While those results convincingly identified B cells as the target of TCDD-mediated immune suppression, a follow-up study (Dooley, et al., 1990) found that antigen-specific activation of T cells was inhibited by TCDD. This suggests that T cells are still affected even if B cells are the principle target of TCDD-mediated immune suppression.

Warren *et. al.* (Warren, et al., 2000) demonstrated in mice that a single dose of TCDD one day prior to sublethal pulmonary infection by influenza A virus caused class-specific differences in Ig expression and greater lethality. They also reported tissue specific changes in T cell differentiation and cytokine production, but T cells from treated animals were still able to stimulate lysis of infected macrophages equivalent to those from control animals. The changes noted in T cell function, therefore, may be less important than the changes in antibody isotype switching for clearance of the virus. In a follow up study, Vorderstrasse *et. al.* (Vorderstrasse, et al., 2003) reported a similar conclusion: suppression of T cell function did not fully explain increased susceptibility to sublethal viral infection, and impaired antibody class switching may have an impact. Based on this and other studies (Kerkvliet, 2009), TCDD can clearly inhibit the function

of T cells; however, TCDD clearly affects B cells directly and that direct effect appears have a greater impact on host susceptibility to immune challenges.

## Aryl Hydrocarbon Receptor

The Aryl Hydrocarbon Receptor (AhR), as already explained, likely mediates the effects of TCDD. The hallmark effect by which AhR signal transduction has been determined is the induction of P450 metabolizing enzyme, Aryl Hydrocarbon Hydroxylase (AHH) or CYP1A1. AhR is a ligand-activated, DNA-binding protein, and a member of the basic helix-loop-helix transcription factor family (Lees, et al., 1999). In the cytoplasm, AhR is bound by a chaperone complex consisting of two heat shock 90 proteins (hsp90)(Perdew, 1988; Wihelmsson, et al., 1990; Pongratz, et al., 1992), which stabilize AhR in a highly sensitive ligand-binding conformation; the X associated protein 2 (XAP2) (also known as ARA9 or AIP)(Kazlauskas, et al., 1999; Kazlauskas, et al., 2000; Lees, et al., 2003), which inhibits nuclear translocation and ubiquitination of AhR and stabilizes the chaperone complex; and p23 (Kazlauskas, et al., 1999; Kazlauskas, et al., 2000), which stabilizes the hsp90/AhR complex and promotes nuclear translocation (Figure 3). When AhR is bound by a ligand, XAP2 disassociates and the remaining complex translocates to the nucleus. In the nucleus, p23 and the hsp90 proteins are displaced by the Aryl-Hydrocarbon Nuclear Translocator (ARNT) protein (Wihelmsson, et al., 1990; McGuire, et al., 1994). The AhR/ARNT heterodimer binds DNA at a Dioxin Responsive Element (DRE) and alters transcription of genes in which the DRE resides (Jones, et al., 1986; Jones, et al., 1986; Durrin, et al., 1987).

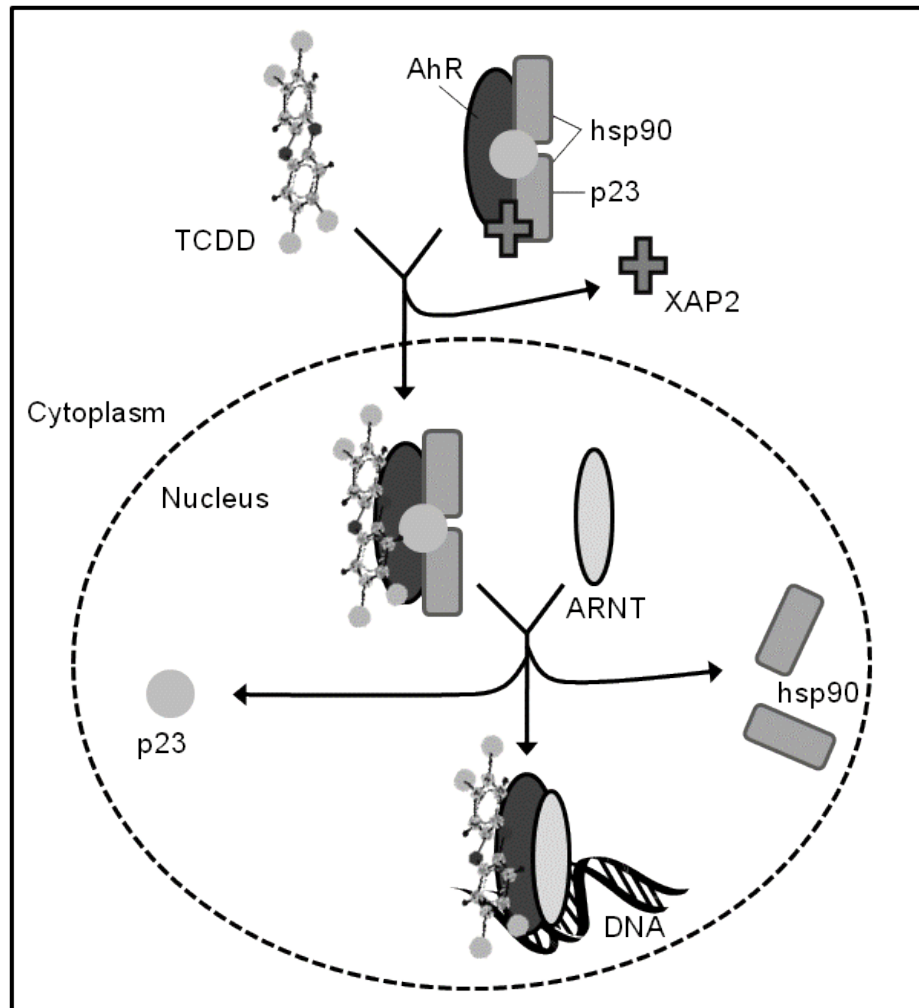


**Figure 3 The Aryl Hydrocarbon Receptor (AhR) Signaling Pathway:** Cytosolic AhR is bound to p23, XAP2, and two hsp90 proteins. AhR ligand (TCDD) displaces XAP2 allowing nuclear translocation of the remaining complex. In the nucleus, ARNT displaces p23 and the hsp90 proteins and the AhR/ARNT complex binds to Dioxin Response Elements (DRE) and affects transcription of genes.

If the effects of TCDD are mediated by the AhR and TCDD affects B-cells function, so one would expect to find AhR expressed in B cells and activated after TCDD exposure. Williams *et. al.* (Williams, et al., 1996) found that AhR and ARNT proteins are both constitutively expressed in mouse splenocytes. Using the Electrophoretic Mobility Shift Assay (EMSA) with a DRE probe, they showed that TCDD induced two DNA binding complexes (representative of the two known alleles of AhR), suggesting that ligand activated AhR is functional in mouse splenocytes. Interestingly, a third,

constitutive binding complex was also present suggesting the presence of an unreported, third AhR allele or an alternative binding multi-mer. Marcus *et. al.* (Marcus, et al., 1998) demonstrated that LPS (T-independent) activation of mouse splenocytes also induced AhR, ARNT, and CYP1A1 expression, indicating that AhR can be activated in B cells without an exogenous ligand present. Moreover, Crawford *et. al.* (Crawford, et al., 1997) demonstrated by inducing greater binding to a DRE- containing probe, that activated B cells with increased levels of AhR and ARNT may be even more sensitive to TCDD than resting B cells. Functional AhR is also induced in CD40L-activated human B cells (Allan, et al., 2005) without an exogenous ligand.

While these studies demonstrate that AhR and ARNT can be expressed in splenocytes, and many effects of TCDD are mediated by the AhR, these studies do not prove a link between TCDD-mediated suppression of antibodies and the AhR. Sulentic *et. al.* (Sulentic, et al., 1998) demonstrated that link using two B cell lines which differ in susceptibility to TCDD toxicity: CH12.LX cells expressed constitutive and inducible AhR and ARNT, while BCL-1 cells expressed ARNT but not AhR. As expected, TCDD induced CYP1A1 expression and inhibited LPS-induced IgM secretion in CH12.LX but not in the AhR deficient BCL-1 cells. Subsequently, Sulentic *et. al.* (Sulentic, et al., 2000) demonstrated that in the CH12.LX cell line, four different AhR ligands induce CYP1A1 and inhibit LPS-induced IgM secretion in correlation with their affinity for AhR. The transcriptional effects of AhR are likely transduced through binding of a recognition sequence in DNA, so there is likely a DRE binding site within one of the Ig regulatory regions. One potentially affected regulatory region is the 3' Immunoglobulin Heavy-Chain Regulatory Region.

## 3'Immunoglobulin Heavy-Chain Regulatory Region

The 3' Immunoglobulin Heavy-chain Regulatory Region (3'IgHRR) is a group of enhancers located 3-prime of the heavy-chain constant regions (Figure 4).

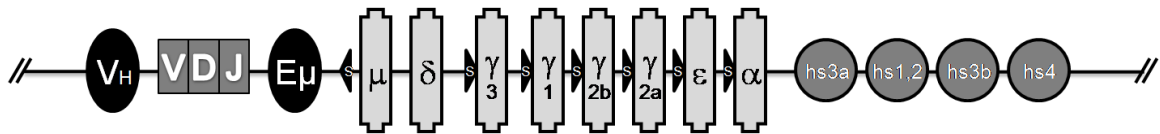


**Figure 4 The Ig Heavy Chain Gene Locus with 3-Prime Enhancer Region:** “hs” numbers refer to regions of DNA that are hypersensitive to DNase I cleavage.

The 3'IgHRR was discovered in the rat B cell (Pettersson, et al., 1990) and thereafter identified in mouse (Dariavach, et al., 1991; Lieberson, et al., 1991) and human B cells (Mills, et al., 1997). The 3'IgHRR was found to have DNase I hypersensitivity sites which are uniquely active in B cells, being highly methylated in immature B cells but demethylated at different stages of B cell maturity, and hypomethylated in dysregulated (myeloma) cells (Giannini, et al., 1993).

Madisen and Groudine (Madisen, et al., 1994) identified the 3'IgHRR as a locus control region able to enhance expression of a human growth hormone reporter construct. Arulampalam *et al.* (Arulampalam, et al., 1994) demonstrated that when mature B cells are activated by LPS or 12-O-tetradecanylphorbol 13-acetate (TPA) the 3'IgHRR enhanced transcription of a transgenic human  $\beta$ -globin reporter gene. The enhancer activity of the 3'IgHRR was shown to be restricted to B cells by lack of activity after transient transfection of reporter constructs into T cells (Michaelson, et al., 1995).

Lieberson *et al.* (Lieberson, et al., 1995) demonstrated that IgG2a production is dependent on the 3'IgHRR. Their results were confounded by use of a replacement fragment containing the neomycin resistance gene which was later found to affect transcription (Seidl, et al., 1999), by fragments of the replacement vector being found in non-target locations, by multiple (inactive) copies of the 3'IgHRR being found on different chromosomes, and their deletion segment including only two of the enhancer regions (hs1,2 and part of hs3a). Nevertheless, they demonstrated a connection between the 3'IgHRR and Ig gene expression. Arulampalam *et al.* (Arulampalam, et al., 1996) confirmed those results by producing mice with rearranged IgH transgenes with and without the enhancer region. Mice with the 3'IgHRR produced 5 to 7 fold more Ig than those without the enhancer region. Ong *et al.* (Ong, et al., 1998) studied the relative contribution of enhancers to Ig gene transcription in cell lines representing different developmental stages of B cells. Using transient reporter constructs, they reported a shift in the relative contribution of the 3'IgHRR and its individual enhancer regions as B cells differentiate, but that the full 3'IgHRR was more active than cut constructs at every developmental stage. Furthermore, while the full 3'IgHRR and pairs of enhancers (hs1,2/hs3a or hs4/hs3b) markedly enhanced transcription, the enhancers had little or no effect individually. Chauveau *et al.* (Chauveau, et al., 1998) confirmed the relative contributions of the enhancers, demonstrating greatest activity with the full 3'IgHRR in its natural orientation. Shi and Eckhardt (Shi, et al., 2001) further studied enhancer activity at different stages of B cell development through stable transfection of reporter constructs. Their constructs had CRE-recombinase recognition sites that allowed post-transfection deletion of either the hs1,2 and hs3a enhancer pair or the hs4 and hs3b

enhancer pair. They discovered that the hs4/hs3b pair was active at both stages of development while the hs1,2/hs3a pair was active only in the later Ig-secreting stage.

Manis *et al.* (Manis, et al., 1998) showed that the 3'IgHRR is also important for class switch recombination. Their results were confounded by replacement of enhancer segments with a neomycin resistance gene cassette known to affect transcription (Seidl, et al., 1999), but the importance of an uncut 3'IgHRR for class switch recombination was sufficiently demonstrated. This was confirmed by Pinaud *et al.* (Pinaud, et al., 2001) who deleted enhancer elements without using a replacement sequence and isotype switching was also inhibited in their study. TCDD was shown to inhibit IgH class switching in the studies by Warren *et al.* (Warren, et al., 2000) and Vorderstrasse *et al.* (Vorderstrasse, et al., 2003) discussed earlier, strengthening the argument that TCDD may target the 3'IgHRR.

TCDD inhibits IgH gene transcription and isotype switching and the 3'IgHRR is important in both those function, so it is not surprising that Sulentic *et al.* (Sulentic, et al., 2000) reported finding DRE-like sites in the 3'IgHRR. Using EMSA/Western, they demonstrated that AhR and ARNT from the nucleus of TCDD-treated B cells bound those DRE-like sites within the hs1,2 and hs4 enhancers. Binding of AhR to the promoter regions of genes, however, might induce or inhibit transcription, but there is no evidence for transcription of the 3'IgHRR, so how could binding of the AhR/ARNT complex to the 3'IgHRR interfere with its enhancer activity? While the mechanism by which the 3'IgHRR is involved in Ig heavy-chain gene expression and rearrangement is not well understood, there is evidence of physical interaction between the heavy-chain gene locus

and the 3'IgHRR (Ju, et al., 2007). Binding of the enhancer could interfere with that interaction. Alternatively, if that interaction is mediated by certain transcription factors, then perhaps AhR-mediated inhibition involves interference with the binding of other transcription factors. Several transcription factors bind the 3'IgHRR and affect IgH transcription. Michaelson, *et. al.* (Michaelson, et al., 1996), showed that B cell Specific Activator Protein (BSAP), Octamer, and Nuclear Factor kappa B, Rel proteins (NFκB/Rel) bind the hs1,2 and hs4 enhancer regions. Furthermore, they demonstrated using B-cell lymphoma cell lines at different stages of development that NFκB appears to inhibit hs1,2 enhancer activity in mature B cells but activates it in plasma cells, while the hs4 enhancer was activated by NFκB at all stages of B cell development. The binding of NFκB/Rel proteins to the 3'IgHRR, therefore, is likely important for B cell function.

The NFκB family consists of 5 protein subunits: RelA or p65, RelB, c-Rel, p50 or NF-κB1, and p52 or NF-κB2. The subunits, or NFκB/Rel proteins, form homo- or heterodimers and bind κB sites within regulated genes to affect transcription of that gene. They are important in immune function, having roles in B cell differentiation (Feng, et al., 2004; Liou, et al., 1994), B cell survival and proliferation (Tumang, et al., 1998; Grumont, et al., 1998), and B cell activation and Ig class switch recombination (Bhattacharya, et al., 2002; Gerondakis, et al., 1998; Gugasyan, et al., 2000; Lin, et al., 1998).

Not only do NFκB/Rel proteins bind sites on the 3'IgHRR, but their binding changes after TCDD exposure. Puga *et. al.* (Puga, et al., 2000) demonstrated using EMSA that in mouse Hepa1 cells, TCDD induces DNA binding of NFκB/Rel proteins. In

addition, EMSA/Western showed that the binding complex consisted mainly of p50 homodimers; however, only p65 and p50 were probed in the Western analysis.

Baglolle *et. al.* (Baglolle, et al., 2008) demonstrated a similar effect in mouse primary lung fibroblast cells. The cells were transfected with a NFκB-luciferase-reporter plasmid and activated with TPA after AhR induction using cigarette smoke extract. The NFκB-regulated reporter plasmid was inhibited when AhR was induced in competent mouse cells, but not in AhR-null cells, suggesting that AhR suppresses NFκB-regulated transcription. Moreover, they showed that when AhR was induced, RelB expression and nuclear localization decreased, but again, only two of the NFκB/Rel proteins were probed (RelA and RelB).

AhR appears to also interact directly with NFκB/Rel proteins. Vogel *et. al.* (Vogel, et al., 2007) found using the EMSA supershift assay, that AhR and RelB mutually bind a site they termed the “RelBAhRE” site in the IL-8 promoter. They did not find ARNT or RelA in the binding complex. Further study with co-immunoprecipitation revealed that AhR and RelB physically associate, and ChIP analysis confirmed that the AhR/RelB complex was bound to the RelBAhRE site in the IL-8 promoter. In that study, TCDD and forskalin (an adenylate cyclase activator) induced binding of the AhR/RelB complex to the IL-8 promoter, but LPS did not; however, LPS did induce binding to a mutant probe that more closely resembled a consensus κB site but the proteins in that binding complex were not identified.

Tian *et. al.* (Tian, et al., 1999) indentified physical interaction between AhR and RelA in reciprocal co-immunoprecipitation experiments. When they activated NFκB by

TNF $\alpha$  treatment or over expressed RelA, an AhR-regulated reporter plasmid was inhibited, indicating that the RelA/AhR interaction may inhibit AhR-mediated transcription. Likewise, activation of AhR by  $\beta$ -naphthoflavone or TCDD inhibited activation of a NF $\kappa$ B-regulated reporter plasmid, indicating that AhR and RelA-mediated transcription are mutually inhibited by the AhR/RelA interaction. Perhaps RelA has a greater affinity than ARNT for AhR, sequestering AhR from its transcription partner. They used whole cell lysates, which brings to question the difference between AhR and RelA in the cytoplasm versus the nucleus, but Kim *et. al.* (Kim, et al., 2000) compared cytoplasmic and nuclear extracts and found that a greater amount of AhR co-precipitated with RelA in cytoplasmic protein extracts than in nuclear protein extracts. This suggests that RelA is displaced by ARNT in the nucleus, so it may not have greater affinity for AhR than ARNT. Using EMSA supershift, three  $\kappa$ B binding complexes were identified: p50 homodimer, p65/p50 heterodimer, and AhR/p65 heterodimer, suggesting that either the AhR/p65 complex is inhibitory, or that sequestering of p65 in complex with AhR allows a greater amount of p50 homodimer binding, which is generally an inhibitory complex.

It is clear from these studies that AhR and the NF $\kappa$ B/Rel proteins can associate with each other and affect their respective transcriptional activities, and in B cells, Sulentic *et. al.* (Sulentic, et al., 2004) demonstrated using the EMSA/Western assay, a TCDD-induced increase in binding of AhR and p65, and possibly RelB and cRel to the hs4 enhancer region. The assay was conducted with nuclear proteins from resting (not activated by antigen) cells, suggesting that both the AhR and NF $\kappa$ B/Rel proteins were activated by TCDD exposure and translocated to the nucleus. The DRE and  $\kappa$ B sites in

the hs4 enhancer region overlap, but those sites in the hs1,2 enhancer are separated. Knowing now, that the AhR and NF $\kappa$ B/Rel proteins can interact and alter each other's transcriptional regulation, it would be interesting to compare how binding changes after TCDD exposure and after activation by antigen between the distant sites in the hs1,2 and overlapping sites in the hs4 enhancers. In fact, Sulentic *et. al.* (Sulentic, et al., 2004) found that TCDD exposure had a different effect on the hs1,2 and hs4 regions of the 3'IgHRR when isolated from each other. They used luciferase reporter plasmids regulated by either the 3'IgHRR or the hs1,2 enhancer or the hs4 enhancer. TCDD inhibited 3'IgHRR-regulated and hs1,2-regulated transcription, but synergistically activated hs4-regulated transcription. Mutating the hs4 DRE or  $\kappa$ B site reduced LPS activation with and without TCDD. In a follow up study, Sulentic *et. al.* (Sulentic, et al., 2004) made new reporter plasmids with the hs4 enhancer region reduced to the 42 base pairs surrounding the overlapping DRE and  $\kappa$ B sites in order to eliminate the effect of other transcriptional elements that bind the enhancer. In this study, TCDD alone induced transcriptional activity, which was greatly increased by LPS treatment; activity was again eliminated by mutation of the DRE or  $\kappa$ B site. I propose, therefore, that the dichotomy in the effects of TCDD on the hs1,2 and hs4 enhancers of the 3'IgHRR is mediated by an AhR-mediated alteration in NF $\kappa$ B/Rel proteins binding within the enhancers.

## Hypothesis and Strategic Aims

My hypothesis is that the dichotomy in the effects of TCDD on the hs1,2 and hs4 enhancers of the 3'IgHRR is mediated by an AhR-mediated alteration in NFκB/Rel proteins binding within the enhancers. I used two specific aims to test this hypothesis. First, the dichotomy in effect was discovered in transient expression experiments, so I sought to demonstrate that the TCDD-induced dichotomy in hs4 and hs1,2 activity seen in a transient expression model is reflective of 3'IgHRR transcriptional regulation in the context of chromatin. I made clones of CH12.LX cells that stably expressed a γ2b mini-locus consisting of variable heavy chain coding sequences and γ2b constant region sequences regulated by the variable heavy chain promoter and four of the 3' enhancers. LoxP sites were located 5-prime of the hs3a and 3-prime of the hs1,2 enhancers. Cre-recombinase cut the transgene at each LoxP site and recombined the DNA, excising the targeted sequence to form the γ2bΔhs3a1,2 transgene. I tested those recombined clones for the effect of TCDD on the transgene which, after cre-recombination, was regulated by the hs3b and hs4 enhancers only.

The second aim was to demonstrate that TCDD causes a qualitative shift in the NFκB/Rel proteins that bind κB sites within the hs1,2 and hs4 enhancers using the Electrophoretic Mobility Shift Assay with Western Blot analysis (EMSA/Western). The EMSA makes it possible to predict the binding of nuclear proteins to specific DNA sequences and the Western allows the identification of specific proteins bound to the DNA.

# Materials and Methods

## Materials

RPMI 1640, nonessential amino acids, sodium pyruvate, 2-mercaptoethanol, penicillin, and HBSS were from Mediatech, INC. (Manassas, VA). HEPES, DMSO, ethidium bromide, and G418 disulfate were from Sigma (St Lewis, MO). Hyclone bovine calf serum (BCS) was from ThermoScientific (Rockford, IL). EcoR1 and Not 1 restriction digest enzymes and React buffers were from Invitrogen (Carlsbad, CA). HindIII restriction digest enzyme was from BioRad (Hercules, CA). Pvu1 and Xho1 enzymes for linearizing plasmids were from Promega (Madison, WI). IGEPAL CA630 was from MP Biomedicals (Aurora, OH). Complete-Mini Protease Inhibitor Cocktail, Poly[d(I-C)], and ABTS were from Roche (Indianapolis, IN). Bovine Serum Albumin (BSA) was from Calbiochem (La Jola, CA). TCDD was from AccuStandard (New Haven, CT). GAM (goat anti-mouse) capture antibody and GAM-HRP conjugate used in the ELISA were from Southern Biotech (Birmingham, AL). Purified moust IgG2b, and GAM-HRP conjugate used in the Western was from Bethyl Laboratories (Montgomery, TX). Anti-AhR antibodies were from Abcam (Cambridge, UK). Anti-Rel antibodies were from Santa Cruze Biotechnology (Santa Cruze, CA). HotMaster Taq DNA polymerase and buffers were from 5 Prime (Gaithersburg, MD). sNTP solutions were from Applied Biosystems (Foster City, CA). Easytides Adenosine 5'-triphosphate [ $\gamma$ -<sup>32</sup>P] was from Perkin Elmer (Boston, MA). Select-D G25 STE spin columns were from IBI Scientific (Peosta, IA). pEGFP-CRE plasmid,  $\gamma$ 2b-LoxPhs3a1,2 plasmid, and NEO plasmid were all kind gifts from Dr. Laural Eckhardt, City University of New York (New York, NY).

CH12.LX cells were a generous gift from Dr. Geoffrey Haughton (University of North Carolina, Chapel Hill, NC) via Dr. Norbert Kaminski (Michigan State University, East Lansing, MI).

## Cell Model, Culture Conditions, Viability, and Transfection

CH12.LX cells are a B cell lymphoma line derived from an in vitro culture of CH12 lymphoma cells (Bishop, et al., 1986) which itself was derived by intraperitoneal transfer of hyperimmunized spleen cells to a thymectomized and irradiated mouse (Arnold, et al., 1983; Lanier, et al., 1982). The CH12.LX cells and their derivatives were cultured at 37<sup>0</sup>C in a humidified, CO<sub>2</sub>-enriched (5%) atmosphere using RPMI 1640 growth medium supplemented with 13.5 mM HEPES, 0.1 mM nonessential amino acids, 1 mM Sodium Pyruvate, 50 mM 2-mercaptoethanol, 100 U/mL streptomycin, 100 U/mL penicillin, and 10% HyClone BCS.

Viability and cell concentration were measured on the ViCell cell viability analyzer (Beckman Coulter, Fullerton, CA). Culture flasks were vigorously swirled to suspend cells and divide cell clumps then a 10 mL serological pipet was used to pipette the culture up and down to further divide cell clumps and mix the culture before transferring 1 mL of culture to a ViCell cuvette for automated counting. In smaller cultures or samples, cells were thoroughly mixed and clumps divided using a pipette and an appropriate aliquot was diluted to a total of 1 mL in 1x PBS (137 mM NaCl, 2.7 mM KCl, 4.3 mM Na<sub>2</sub>HPO<sub>4</sub> x 7 H<sub>2</sub>O, 1.4 mM KH<sub>2</sub>PO<sub>4</sub>) in a ViCell cuvette.

All transfections were accomplished by electroporation using an ECM 360 Electro Cell Manipulator (BTX, Hawthorne, NY). Cells were cultured to near-confluence

in complete medium and viability and concentration were measured on the ViCell. An appropriate volume containing  $1.10 \times 10^7$  viable cells per transfection cuvette was transferred to a centrifuge tube and the cells pelleted by centrifugation at 200 to 300 x g for 5 minutes. The pellet was resuspended in a total of 220  $\mu$ L of fresh culture medium per transfection cuvette with an appropriate amount of linearized or circular plasmid DNA. Transfection cuvettes with a 1 cm gap width received 200  $\mu$ L of the cell and plasmid solution ( $1.0 \times 10^7$  cells). The cells were pulsed (2 cuvettes at once) with the ECM 360 set for 250 volts, 250  $\mu$ Farad, and 300 ohms resistance. The actual voltage delivered and pulse length was recorded. After electroporation, a 200  $\mu$ L aliquot of complete culture medium was added to the cuvette(s) and the entire solution transferred and pooled from each cuvette to an appropriate volume of pre-warmed, complete growth medium.

Transfected cell stocks were stored in liquid nitrogen. The cells were cultured to approximate confluence in 10 mL of complete growth medium, pelleted by centrifugation (300xg, 5 min) and resuspended in 2.5 mL of BCS which was then mixed with 2.5 mL of complete medium containing 20% dimethylsulfoxide (DMSO). Aliquots of that cell solution were transferred to 1 mL cryo-vials, packed in Styrofoam and frozen overnight at  $-80^{\circ}\text{C}$ . The vials were then transferred to a liquid nitrogen storage. The cells were recovered from storage by transfer to a  $40^{\circ}\text{C}$  water bath until almost completely thawed. Then the cells were transferred to a culture tube containing 0.2 mL of complete medium at room temperature. At 3 minute intervals, with occasional swirling to mix, increasing volumes (0.4, 0.8, 1.6, and 3.2 mL) of complete medium were added. After a final 3 minute incubation at room temperature, the cells were pelleted by centrifugation (200xg,

5 min), resuspended in 1 mL of complete medium, and transferred to 10 mL of complete medium in a 75 cm<sup>2</sup> culture flask and incubated at 37 °C under 5% CO<sub>2</sub>.

## Producing the Parental Cell Line

CH12.LX cells were co-transfected with a  $\gamma$ 2b-LoxPhs3a1,2 and NEO plasmids. The  $\gamma$ 2b-LoxPhs3a1,2 plasmid has been described previously (Shi, et al., 2001). Briefly, the mini-locus consists of variable heavy chain coding sequences and  $\gamma$ 2b constant region sequences regulated by the variable heavy chain promoter and four of the 3'IgHRR enhancers. LoxP sites are located 5-prime of the hs3a and 3-prime of the hs1,2 enhancers so that cre-recombinase enzyme will delete the hs3a and hs1,2 enhancers (Figure 5). Plasmid integrity was tested by restriction digest with Hind III enzyme and with a combination of Eco R1 and Not1 enzymes. The circular plasmid was linearized with Pvu1 prior to transfection. The NEO plasmid produces aminoglycoside phosphotransferase, conferring resistance to neomycin and to Geneticin (G418). It is a 2kb-Not1 fragment with LoxP sites surrounding the NEO gene which was inserted to the Not1 site of a pBS-SK(Spe1/HindIII). It was linearized with Xho I prior to transfection.

For restriction enzyme digestion and linearization, 1  $\mu$ L of each enzyme, 1  $\mu$ L of the appropriate buffer, and 1  $\mu$ g plasmid DNA were mixed in a total volume (with deionized, filtered water) of 10  $\mu$ L and incubated one hour at 37 °C. DNA was visualized on 0.7% or 1% agarose gel in 1x TBE with 0.5% Ethidium Bromide.

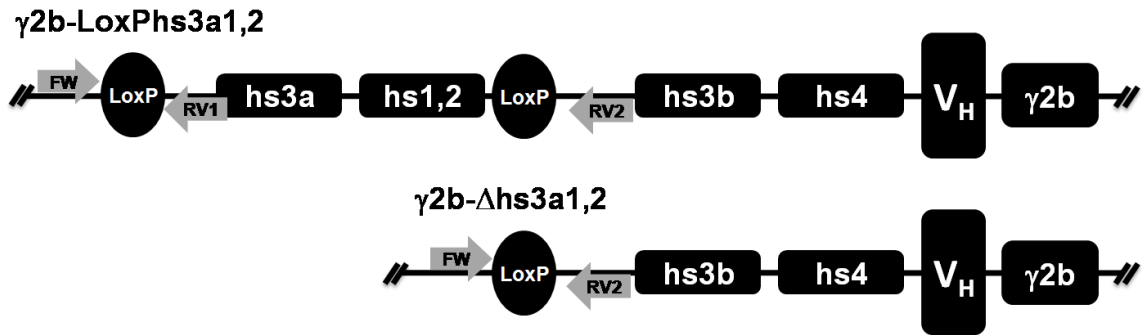


**Figure 5 The  $\gamma 2b$  Transgene before and after Cre-Recombination:** The  $\gamma 2b$  transgene on the  $\gamma 2b$ -LoxPhs3a1,2 plasmid consists of variable heavy chain coding sequences and  $\gamma 2b$  constant region sequences regulated by the variable heavy chain promoter and four of the 3' enhancers. LoxP sites are located 5-prime of the hs3a and 3-prime of the hs1,2 enhancers. Cre-recombinase will cut the transgene at each LoxP site and recombine the flanking DNA, excising the targeted sequence to form the  $\gamma 2b\Delta hs3a1,2$  transgene. FW is the annealing location for the forward PCR primer used to test for successful Cre-recombination. RV1 is the reverse primer annealing location for PCR product indicating that the hs3a and hs1,2 enhancers were not deleted. RV2 is the reverse primer annealing location for PCR product indicating successful deletion of the enhancers.

Transfection was accomplished by electroporation using 20  $\mu\text{g}$  of  $\gamma 2b$ -LoxPhs3a1,2 plasmid and 5  $\mu\text{g}$  of NEO plasmid per  $1.0 \times 10^7$  cells. Four times more LoxPhs3a1,2 plasmid than NEO plasmid was used to ensure that cells incorporating the NEO plasmid would also incorporate the  $\gamma 2b$ -LoxPhs3a1,2 plasmid. After electroporation, transfected cells were transferred to 100 mL of complete culture medium and aliquoted to wells of 96-well plates at 100  $\mu\text{L}$  per well. Plates were incubated at 37  $^{\circ}\text{C}$  in 5%  $\text{CO}_2$  for 48 hours before addition of 100  $\mu\text{L}$  per well of complete culture medium containing 4 mg/mL G418. After 6 days in culture, 100  $\mu\text{L}$  of medium was carefully removed from each well and replaced with 100  $\mu\text{L}$  of fresh medium containing 4 mg/mL of G418. Every 3 days thereafter, 100  $\mu\text{L}$  of culture medium was similarly replaced. When a colony of cells became visible to the naked eye, it was transferred to a well of a 12 well plate, labeled to identify its plate and well of origin to prevent duplicate colony sampling, and cultured in 2 mL of fresh medium containing 2 mg/mL G418.

When the cell population in those wells became dense (about 6 days) they were transferred to 75 cm<sup>2</sup> culture flasks with 10 mL of fresh culture medium containing 2 mg/mL G418. When the viable cell population exceeded 3.0 x 10<sup>5</sup> cell/mL, an aliquot containing 5 x 10<sup>6</sup> cells was removed for storage in liquid nitrogen. Subsequent culture and testing were done in the absence of G418. Successful incorporation of the  $\gamma$ 2b-LoxPhs3a1,2 transgene and estimation of the number of copies incorporated was accomplished by real-time PCR (described below). Transgene function was confirmed by LPS treatment and measurement of  $\gamma$ 2b by ELISA (described below).

## Real-Time PCR Testing for $\gamma$ 2b-LoxPhs3a1,2 Incorporation

Real-time PCR was used to estimate the number of  $\gamma$ 2b-LoxPhs3a1,2 loci incorporated in each parental clone. Genomic DNA was extracted from clones using GeneElute Mammalian Genomic DNA MiniPrep Kit (Sigma) and quantified using a NanoDrop ND-1000 Spectrophotometer (NanoDrop Technologies, Wilmington, DE). Real-time PCR was conducted using an AB 7500 Real Time PCR System (Applied Biosystems, Foster City, CA) with SYBR Green reporter dye (Applied Biosystems SYBR Green PCR Master Mix) in 96-well format. 20 ng of DNA and 10 pmol each of forward and reverse primers were amplified with the following thermal profile: 2 minutes at 50<sup>0</sup>C; 10 minutes at 95<sup>0</sup>C; 40 cycles of 15 seconds at 95<sup>0</sup>C then 1 minute at 60<sup>0</sup>C after which fluorescence was measured. DNA from each clone was amplified using primers for the  $\gamma$ 2b or NEO or  $\beta$ -actin (see below). Threshold Cycle (C<sub>T</sub>), the cycle at which fluorescence becomes greater than a threshold value, was calculated by Sequence Detection Software (SDS v 1.2.3)(Applied Biosystems) relative to  $\beta$ -actin amplification. A dissociation run was conducted to disqualify wells with multiple or questionable

products: if a well had a lower melting temperature than like-product wells and/or more than one peak in the dissociation plot, it was omitted from the analysis. Untransfected CH12.LX cells were used as a negative control while C3 cells (CH12.LX.  $\gamma$ 2b-LoxPhs3b4, stably transfected with a similar transgene but with LoxP sites surrounding the hs3b and hs4 enhancers) were used as positive controls. If the  $C_T$  for  $\gamma$ 2b in a parent was less than or equal to the  $C_T$  for  $\gamma$ 2b in CH12.LX then it was estimated to have one or more copies of the  $\gamma$ 2b transgene, since CH12.LX cells have undergone class-switch to produce IgA and should not contain the  $\gamma$ 2b gene. If  $C_T$  for  $\beta$ -actin in a parental was less than its own  $C_T$  for  $\gamma$ 2b, it was estimated to have less than two copies of the  $\gamma$ 2b transgene, since each cell should have two copies of the  $\beta$ -actin gene. Each parental clone and control was tested in duplicate; outliers were determined by Sequence Detection Software protocol and disqualified from calculations.

Primers were obtained from the Macromolecular Structure Facility, Michigan State University (East Lansing, MI). The primers for  $\gamma$ 2b with a 229 base pair product were forward 5'-CACCCATCGAGAGAACCATC-3' (CEWS63) and reverse 5'-CCAGGCAAGTGAGACTGACA-3' (CEWS64). The primers for NEO were forward 5'-TGAATGAACTGCAGGACGAG-3' (CEWS37) and reverse 5'-ATACTTTCTCGGCAGGAGCA-3' (CEWS38). The primers for  $\beta$ -actin with a 122 base pair product were forward 5'-GCTACAGCTTCACCACCACA-3' (CWS65) and reverse 5'-TCTCCAGGGAGGAAGAGGAT-3' (CEWS66).

## Producing the Deletion Derivative Clones

Enhancer deletion and isolation of deletion derivatives (CH12.LX.γ2b-Δhs3a1,2) was accomplished by transient expression of CRE-recombinase (CRE) and green fluorescent protein (GFP) and with fluorescence assisted cell sorting (FACS). Transient CRE and GFP expression was accomplished by transfection of cells with a pEGFP-CRE plasmid which encoded CRE and a GFP variant with brighter fluorescence and silent mutations for compatibility with mammalian cells (Dikici, et al., 2009). The integrity of the plasmid was tested by restriction digest with Hind III. The circular plasmid was introduced to cells by electroporation with actual voltage delivered at 236 volts for 1.3 milliseconds. Transfected cells were transferred to 50 mL of complete medium and cultured overnight at 37 °C with 5% CO<sub>2</sub>. The cells were pelleted by centrifugation at 300 xg for 5 minutes and resuspended in 2 mL of complete medium for cell sorting. Cells expressing GFP were separated by FACS from non-expressing cells by the Core Flow Cytometry Facility at Cincinnati Children's Hospital (Cincinnati, OH). Cells expressing GFP were transported from the facility in 2 mL of complete medium. Upon return, cells were pelleted by centrifugation at 200 xg for 5 minutes, resuspended in 1 mL of complete medium and either underwent limiting dilution (diluted to 5 cells per mL in complete medium) such that 100 μL transferred to wells of a 96-well culture plate contained an estimated 0.5 cells, or were cultured in 5 ml of complete medium over night or for six days after which they underwent another limiting dilution to 0.5 cells per well. When a cell clump became visible to the naked eye, it was transferred to a well of a 6-well plate with 5 mL of complete medium and labeled with plate and well of origin to prevent duplicate sampling of a clonal isolate. When cells appeared confluent in 6-well plates,

they were transferred to a 75 cm<sup>2</sup> culture flask with 10 mL of complete medium and assigned a new designation: Dx, where x is the isolate number. An aliquot of near confluent cells in 75 cm<sup>2</sup> culture flasks was removed for storage of cells in liquid nitrogen while another aliquot was used to isolate DNA for confirmation of enhancer deletion.

## PCR for Confirmation of hs3a and hs1,2 Enhancer Deletion

Deletion of the hs3a and hs1,2 enhancers was verified by PCR amplification of sequences specific for the  $\gamma$ 2b mini-locus before and after deletion. This was accomplished by using one forward primer which annealed upstream from the most 5-prime LoxP site (preceding the hs3a enhancer), and one of two reverse primers (RV1 and RV2, Figure 5). RV1 annealed inside the targeted deletion so that only clones with an intact  $\gamma$ 2b mini-locus would have a PCR product (UNCUT). RV2 annealed downstream from the most 3-prime LoxP site (located after the hs1,2 enhancer) so that only clones which have the cut  $\gamma$ 2b mini-locus will have a PCR product (CUT). If the hs3a and hs1,2 enhancers were not deleted, the sequence separating RV2 from the forward primer was too long (5389 base pairs) for a PCR product to form. The parental clone (pC13) served as a positive UNCUT control and a negative CUT control, while CH12.LX which does not contain the mini-locus was also used for a negative control.

Primers were designed using Primer Blast ([www.ncbi.nlm.nih.gov/tools/primer-blast/](http://www.ncbi.nlm.nih.gov/tools/primer-blast/)) and made by the Macromolecular Structure Facility, Michigan State University (East Lansing, MI). Several primers were designed, ordered, and tested to find the proper specificity. The forward primer used had the sequence 5'-

GCCGCTAATTCCGATCATATT-3' (CEWS143). The UNCUT reverse primer (RV1) had the sequence 5'-TTGGCTGGACGTAAACTCCT-3' (CEWS161). The UNCUT primer pair (CEWS143+161) should amplify a 100 base pair product from the mini-locus only if the enhancers were not deleted. The CUT reverse primer (RV2) had the sequence 5'-TTGCCCCAATATCCCTTAGAT-3' (CEWS144). The CUT primer pair (CEWS143+144) should amplify a 122 base pair product from the cut mini-locus with enhancers deleted but nothing from the uncut mini-locus.

DNA was isolated using the GeneElute Mammalian Genomic DNA MiniPrep Kit (Sigma). PCR amplification was conducted in an Eppendorf Mastercycler (Eppendorf AG, Hamburg, Germany) thermocycler with HotMaster Taq DNA polymerase. 200 ng of genomic DNA was mixed with 0.2 mM dNTP mix, 0.2 mM forward primer, 0.2 mM reverse primer, 1.25 U of Taq, and 2.5  $\mu$ L of 10x HotMaster Buffer, in a total volume (with deionized, filtered water) of 25  $\mu$ L. Where the DNA yield was low, the total volume was increased to 50  $\mu$ L with appropriate increase in buffer and as close to 200 ng of DNA as possible. PCR products were visualized by electrophoresis in a 2% agarose gel in 1x TAE with 0.5% Ethidium Bromide, and imaged with a Foto/Eclipse (Fotodyne, Hartland, WI) dark box, COHU (Poway, CA) high performance CCD camera, and Scion Image 1.60c software (Scion, Frederick, Maryland).

## Screening for LPS-Inducible $\gamma$ 2b and the Effect of TCDD

Cells were seeded to 12-well culture plates at  $3.13 \times 10^4$  cell/mL in 2 mL of complete growth medium. For LPS-induced  $\gamma$ 2b expression in parental clones,  $2.5 \times 10^5$  cells were pelleted by centrifugation (200 xg, 5 minutes), resuspended in 8 mL of

complete medium, and aliquots transferred to the culture plate. One aliquot was left untreated while the others were treated with either 0.01 or 0.1 or 1.0  $\mu\text{g}/\text{mL}$  of *E. coli* lipopolysaccharide (LPS) by addition of 2  $\mu\text{L}$  of LPS at the appropriate concentration. For the effect of TCDD in parental clones,  $1.25 \times 10^6$  cells were pelleted by centrifugation (200  $\times g$ , 5 minutes), resuspended in 40 mL of complete medium, and 10 mL aliquots transferred to culture tubes. One tube was left untreated (control), another was treated with 0.01% DMSO (Vh), another with 0.01% DMSO and 1  $\mu\text{g}/\text{mL}$  LPS (LV), and the last tube was treated with 30 nM TCDD in DMSO (final is 0.01% DMSO) and 1  $\mu\text{g}/\text{mL}$  LPS (LT). 2 mL aliquots from each tube were then transferred to each of four wells of a 12-well plate. For testing of deletion derivative clones, 6.5 mL aliquots at  $3.13 \times 10^4$  cell/mL were transferred to new tubes and treated with 1x PBS (NA) or 0.01% DMSO (Vh), or 0.01 nM, 0.1 nM, 1.0 nM, or 10 nM TCDD (T) in DMSO (final 0.01% DMSO) or 0.001  $\mu\text{g}/\text{mL}$ , 0.01  $\mu\text{g}/\text{mL}$ , 0.1  $\mu\text{g}/\text{mL}$ , 1.0  $\mu\text{g}/\text{mL}$ , or 10  $\mu\text{g}/\text{mL}$  LPS (L) or an appropriate combination of 1x PBS, LPS, DMSO, and TCDD (LV or LT). 2 mL aliquots were transferred from each tube to duplicate wells of a 12-well culture plate

Treated culture plates were incubated at 37  $^{\circ}\text{C}$  with 5%  $\text{CO}_2$  for 48 hours. Then cells were packed on the well bottoms by centrifugation at 3000 rpm (1811  $\times g$ ) for 10 minutes so that 1.5 mL of supernatant could be removed and discarded without losing cells. 0.5 mL of 1x PBS was added to each well and cells resuspended by pipetting. The entire volume was then transferred to a 1.5 mL centrifuge tube and the cells were pelleted by centrifugation at 2000 rpm for 5 minutes. The supernatant was discarded and then cells resuspended in 50  $\mu\text{L}$  of mild lysis buffer (150 mM NaCl, 2 mM EDTA, 10mM  $\text{NaPO}_4$ , 1% IGEPAL CA630) with Complete-Mini Protease Inhibitor Cocktail (Complete-

Mini) by vortexing. The lysed cell solutions were stored at  $-80^{\circ}\text{C}$  at least overnight. The lysate was then thawed on ice, vortexed to mix, cleared of cellular debris by centrifugation at 14000 rpm (20817  $\times g$ ) for 10 minutes, and transferred to a new storage tube. Samples were then assayed for  $\gamma 2b$  protein by Enzyme Linked Immunosorbent Assay (ELISA).

## Enzyme Linked Immunosorbent Assay (ELISA) for $\gamma 2b$

Total protein in the samples was measured by Bio-Rad Protein assay following the manufacturer's instructions, in 96-well format using a Spectramax Plus 384 plate reader (Molecular Devices, Sunnyvale, CA) with Softmax Pro software version 4.0. An aliquot of each sample was diluted to  $0.01 \mu\text{g}/\mu\text{L}$  in 1 x PBS for use in the ELISA. ELISA was conducted in 96-well format using an ELx50 auto strip washer (Bio-Tek Instruments, Winooski, VT) and the Spectramax Plus 384 plate reader. The plates were coated with goat anti-mouse immunoglobulin capture antibody by incubating at  $4^{\circ}\text{C}$  overnight with  $100 \mu\text{L}$  of  $3 \mu\text{g}/\text{mL}$  antibody solution (0.1 M Carbonate-Sodium Bicarbonate buffer). Three wells were left empty as negative controls. The plates were rinsed with 1x PBS containing 0.05% TWEEN20 (PBS/TWEEN) and then with deionized, filtered water, then blocked for one hour with  $200 \mu\text{L}$  per well of 3% BSA in 1x PBS with 0.05% TWEEN20 at room temperature. The plates were rinsed again with PBS/TWEEN and water, and then stored at  $-20^{\circ}\text{C}$  until use. Standards (prepared by serial dilution of purified mouse IgG2b) and diluted samples were added to coated ELISA plates in duplicate at  $100 \mu\text{L}$  per well and incubated for 1 to 1.5 hours at  $37^{\circ}\text{C}$ . Three wells coated with capture antibody were incubated with saline as "no protein" negative controls while a random protein sample was added to 3 wells lacking capture antibody for

“no capture” controls. After incubation, solutions were discarded and the plates rinsed with PBS/TWEEM and water. The detection antibody, goat anti-mouse Ig  $\gamma$ 2b conjugated to horseradish peroxidase was diluted 1:60,000 in 3% BSA in 1x PBS containing 0.05% TWEEN20 and then a 100  $\mu$ L aliquot transferred to each well. The plate was then incubated another 1 to 1.5 hours at 37  $^{\circ}$ C and rinsed with PBS/TWEEN and water. 100  $\mu$ L of ABTS substrate pre-warmed to about room temperature, was then added to each well and the rate of substrate conversion at 37  $^{\circ}$ C was monitored for one hour using the Spectramax Plus 384 plate reader.

## The Electrophoretic Mobility Shift Assay (EMSA):

### Cell Treatment:

Cells were seeded in complete growth medium and cultured to confluence. Cell viability and concentration were measured by ViCell, and then split to 3 culture flasks of 120 mL each, at approximately  $5.0 \times 10^5$  cells/mL. The flasks were either treated with 30 nM TCDD (T) in DMSO (final DMSO concentration 0.019%), or 0.01% DMSO (Vh), or 1 x PBS (NA). After 5 minutes, each of the flasks was swirled to mix and resuspend the cells, and then 60 mL was transferred to another flask and treated with 1  $\mu$ g/mL LPS (L and LV and LT). The flasks were incubated at 37 $^{\circ}$ C with 5% CO $_2$  for one hour. Cultures were transferred to conical-bottom tubes and cells collected by centrifugation at 300 xg for 5 minutes.

### Nuclear Protein Isolation

CH12.LX cell pellets collected after treatment were washed with 1x PBS and pelleted again by centrifugation at 200 xg for 5 minutes. For the homogenizer method,

cellular membranes were swelled by incubation in 10 mM HEPES (10 mM HEPES, pH 8, 1 mM DTT, and Complete-mini) for 10 minutes on ice. When isolating proteins from splenocytes, HB (10 mM HEPES, pH 8, 1.5 mM MgCl<sub>2</sub>, Complete-mini) was used to swell membranes instead of 10 mM HEPES and Hank's Buffered Saline Solution (HBSS) was used in place of 1 x PBS. Cells were pelleted again to remove the HEPES or HB, resuspended in MDH (25 mM HEPES, pH 8, 3 mM MgCl<sub>2</sub>, 1 mM Dithiothreitol (DTT), Complete-mini), and transferred to a Dounce homogenizer (B pestle). Cellular membranes were lysed with 10 slow pestle strokes while the homogenizer was kept on ice and the lysed cells were transferred to a conical tube.

For the non-ionic detergent method, CH12.LX cell or splenocyte pellets collected after treatment were washed with HBSS and pelleted again, and then resuspended in HB and incubated on ice for 10 minutes to swell the cellular membranes. HB+IGEPAL (HB + 1.5% IGEPAL CA630) was then added to achieve a final IGEPAL CA630 concentration of 0.5% and samples incubated another 5 minutes on ice.

The nuclei were collected after either method of membrane lysis by centrifugation at 1000 xg for 5 minutes and the cellular fraction (supernatant) discarded. The nuclear pellets were washed twice with MDHK (25 mM HEPES, pH 8, 3 mM MgCl<sub>2</sub>, 100 mM KCl, 1 mM DTT, Complete-mini), then resuspended in HEDK (25 mM HEPES, pH 8, 1 mM EDTA, 400 mM KCl, 1 mM DTT, Complete-mini). Tubes were rocked on ice or rotated at 4 °C for 30 to 40 minutes for high-salt extraction of nuclear proteins. Nuclear debris was pelleted by centrifugation at 14000 xg for 15 minutes, and the supernatant (nuclear proteins) were transferred to new tubes. Protein concentrations were measured using a BCA Protein Assay Kit (Thermo Scientific Pierce) by following the

manufacturer's instructions, either immediately from fresh samples or from an aliquot stored separate from the sample. Samples and protein aliquots were stored at  $-80^{\circ}\text{C}$ .

### Labeling Probes:

Single stranded nucleic acid sequences and their anti-sense complements were ordered from the Macromolecular Structure Facility, Michigan State University (East Lansing, MI). The sequence for each of the probes used is shown in Table 1.

Complementary oligomers were annealed by combining 1000 pmol of each and incubating them at  $88^{\circ}\text{C}$  for 5 minutes in a heat block and then removing the block from its heat source and allowing it to cool to room temperature slowly. Annealed oligomers were end-labeled with  $^{32}\text{P}$  by reaction with T4 Kinase using the Ready-to-Go T4 Polynucleotide Kinase Kit (Amersham Biosciences, Piscataway, NJ): 10 pmol of annealed oligomer was incubated with T4 Kinase and 20  $\mu\text{Ci}$  of Easytides Adenosine 5'-triphosphate [ $\gamma\text{-}^{32}\text{P}$ ] (Perkin Elmer, Boston, MA) for 30 minutes at  $37^{\circ}\text{C}$ . Select-D G25 STE spin columns were used to remove  $^{32}\text{P}$  not bound to DNA. The activity of the radio-labeled probe was measured by liquid scintillation spectrometry using a TRI-CARB 1900 TR Liquid Scintillation Counter (Packard Instrument Corp, Meridian, CT).

<b>Name (CEWS + anti-sense CEWS numbers) and Description</b>	<b>Nucleotide Sequence (5' to 3')</b>
<b>hs4 (23+24) Mouse hs4 enhancer sequence</b>	<b>AGCAGAGGGGGGACTGGCGTGGAAAGCCCCATTACCCAT</b>
<b>hs4s (21+22) Shorter version of the mouse hs4 enhancer sequence</b>	<b>GGGACTGGCGTGGAAAGCCCCATTCA</b>
<b>hs1.2 (84+85) Mouse hs1.2 enhancer sequence</b>	<b>GGAAGAACTAOCCTTAGGGGTCTATTAAGTACCACGCTAGG</b>
<b>hs4muDRE (120+121) hs4 probe with a mutated DRE site</b>	<b>AGCAGAGGGGGGACTGGATCGGAAAGCCCCATTACCCAT</b>
<b>hs4muKB (122+123) hs4 probe with a mutated κB site</b>	<b>AGCAGAGGGGGGACTGGCGTGGAAAGTTATATTACCCAT</b>
<b>DRE3 (86+87) sequence with a DRE site from the mouse CYP1A1 promoter</b>	<b>GATCCGGAGTTGCGTGAGAAGAGCCA</b>
<b>DRE4 (104+105) sequence with a DRE sites from the mouse CYP1A1 promoter</b>	<b>GATGCACGIGGCGTGTGTC</b>
<b>consensus κB (124+125) a sequence containing a consensus κB binding site</b>	<b>GATCTCTCGGGGATTCOCCCTGTA</b>
<b>huhs1.2 (78+79) human hs1.2 enhancer sequence from α1A R3</b>	<b>CCCCTCCCCCAGCGTGGCCAGGCTGGCTCAGGCCCTCCAGATTGGGGACACCCCCCG</b>
<b>huhs1.2kb (80+81) κB site from the human hs1.2 enhancer α1A R3</b>	<b>CTCCAGATTGGGGACACCCCCCGCCCCCT</b>
<b>huhs1.2DRE (82+83) DRE site from the human hs1.2 enhancer α1A R3</b>	<b>CCCCTCCCCCAGCGTGGCCAGGCTGGCTCA</b>

**Table 1 EMSA Probes (top or sense strand):** The oligonucleotides radio-labeled or used as unlabeled probes were ordered as complementary, single stranded DNA. Shown here is the sequence for the top or sense strand.

## EMSA:

Short oligonucleotide probes were designed to include DRE and κB binding sites from the hs4 and hs1,2 enhancer regions and were labeled as previously described. The probes sequences are shown in Table 1. Activity of the radio-label in counts per minute

(CPM) on the day of an EMSA experiment was determined by calculating the number of half-lives that past ( $p$ ) since the probe was labeled and dividing the CPM at the time of label by 2 raised to the  $p$  power ( $CPM \div 2^p$ ). The probe was then diluted in HED (25 mM HEPES, pH 8, 1 mM EDTA ) to 10,000 CPM/ $\mu$ L.

Nuclear proteins were diluted to 10  $\mu$ g/30  $\mu$ L with HED and HEDK such that the final KCl concentration in the 30  $\mu$ L binding reaction would be 80 mM for the hs1,2 enhancer probes and 100 mM for the hs4 enhancer probes. The nuclear proteins were incubated at room temperature with 1 to 2  $\mu$ g of Poly[d(I-C)] in 25 mM HEPES, pH 8, 1 mM EDTA, 1 mM DTT, and 80 or 100 mM KCl , for 15 minutes to engage non-specific binding prior to addition of radio-labeled probe. Note that earlier studies used 10 mM HEPES instead of 25 mM. In later studies the reaction buffer was brought to 10% glycerol by addition of HEDG where HED had been added previously. Antibodies for a supershift assay or unlabeled competitor probes, when used, were included in the last 5 minutes of that incubation. 40,000 CPM of probe in 4  $\mu$ L was added and the reaction incubated another 45 minutes to 1 hour at room temperature. The entire 30  $\mu$ L reaction volume was then loaded to a 4%, 6%, or 8% polyacrylamide gel in 1x TAE (6.7 mM Tris, pH 8, 3.3 mM Sodium Acetate, 1 mM EDTA) in a Model P10DS Owl vertical gel apparatus (Owl Separation Systems, Portsmouth, NH). In earlier studies, prior to the addition of 10% glycerol to the reaction, loading dye was added to the reaction before transfer to the gel. 120 volts of electricity was applied for 6 to 10 hours, refreshing the upper reservoir of TAE about every 3 hours. The gel was then dried on 3 mm filter paper (Whatman) with one side covered by common plastic wrap and exposed to autoradiography film in an autoradiography cassette at -80  $^{\circ}$ C for 4 to 36 hours which

was then developed and scanned for digital documentation. In the earliest optimization experiments, the dried gel was exposed to a phosphoimaging plate (BASIII) overnight at room temperature, which was developed in a FujiFilm FLA 5100 (FujiFilm, Valhalla, NY) phosphoimager. During optimization of the EMSA, the concentration of KCl or Poly[d(I-C)] was varied along with the percent of polyacrylamide in the gel and timing of electrophoresis. Antibodies specific for AhR or one of the NFκB/Rel subunits were used to try and supershift (cause a greater shift in mobility through the gel than binding of the protein alone) a probe and reveal which proteins were bound. Unlabeled probes (double stranded oligonucleotides annealed in the process of making a radio-labeled probe, but not added to a labeling reaction) were added to a reaction to compete with labeled probe such that proteins that bind sites on the unlabeled probe will no longer bind the labeled probe.

#### EMSA/Western

The EMSA reaction for an EMSA/Western was conducted as described above except that some of the samples were only incubated with un-labeled probe so that the portion of gel containing un-labeled probes could be separated from the rest prior to drying. The un-labeled portion of gel was rocked in transfer buffer (48 mM Tris, 39 mM Glycine, 0.4% SDS, 20% Methanol) at room temperature for 20 minutes, then transferred to PVDF membrane at 20 volts overnight. The membrane was then probed for AhR or one of the NFκB/Rel subunits using specific antibodies. Anti-AhR was used at a 1:2000 dilution. Anti-Rel specific for each NFκB/Rel subunit was used at a 1:1000 dilution. The blocking buffer used during Western Blot analysis was 1% dry non-fat milk in TBS-T (2mM Tris, pH 7.6, 13.7 mM NaCl, 0.1% TWEEN20) and TBS-T was used for rinses.

The secondary antibody was goat anti-mouse immunoglobulin (GAM) conjugated to HRP at a 1:4000 dilution. SuperSignal West Pico Chemiluminescent Substrate (Thermo Scientific) was applied to the membrane which was then covered with common plastic wrap and exposed to autoradiography film for 5 seconds to 5 minutes. The film was developed and digitally documented as described earlier. During initial studies, some Western blots were visualized using a FujiFilm LAS 3000 Image Reader (FujiFilm).

### Statistical Comparisons:

Statistical comparisons were made using Prism 5 for Windows (GraphPad) version 5.02. Significance was set at 95% confidence. Differences in variance were compared using 2-way analysis of variance (ANOVA) with a Bonferroni post-test to compare treatments. When only one clone was tested, a 1-way ANOVA and Bonferroni post-test were used.

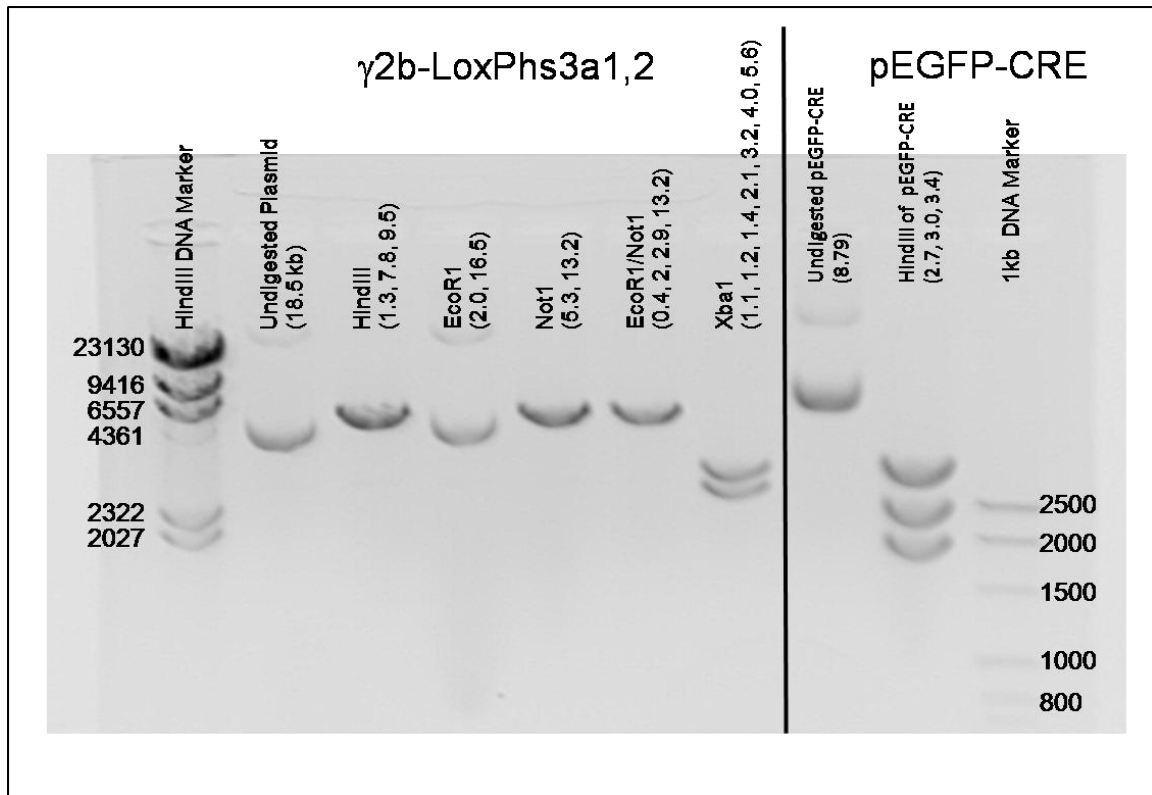


**Figure 6 Restriction Enzyme Digest of the  $\gamma 2b$ -LoxPhs3a1,2 and pEGFP-CRE Plasmids:** The integrity of the plasmids was tested by restriction enzyme digest and agarose gel electrophoresis. Column labels show the restriction enzyme used and in parenthesis, the expected DNA fragment sizes after digestion with that enzyme.

## Results and Discussion

The first specific aim asserting that a dichotomy in the effects of TCDD between the hs1,2 and hs4 enhancers observed in transient transfection studies (Sulentic, et al., 2004) was also true in the context of chromatin, was tested by stable transfection of CH12.LX cells with a hs3b/hs4-regulated,  $\gamma 2b$  reporter construct. Previous studies (Fernando, unpublished) demonstrated inhibition of the hs3a/hs1,2-regulated construct after stable transfection, similar to the transient transfection study.

Prior to transfection, the plasmid underwent restriction fragment digestion to confirm its integrity. The expected restriction fragments were not produced when digesting the initial preparation of the  $\gamma$ 2b-LoxPhs3a1,2 plasmid ( Figure 6). The expected results were as follows: Hind III, bands expected at 1.3, 7.8, and 9.5 kb; Eco R1, bands expected at 2.0 and 16.5 kb; Not 1, bands expected at 5.3, 13.2 kb; Eco R1 + Not 1, bands expected at 0.4, 2.0, 2.9, and 13.2 kb; and Xbam 1, bands expected at 1.1, 1.2, 1.4, 2.1, 3.2, 4.0, and 5.6 kb. A new preparation of the plasmid was correctly digested and linearized prior to transfection (Fernando, personal communication). The NEO plasmid which was co-transfected for selection of successfully transfected cells did not appear linearized at the time of transfection (Fernando, personal communication) even though it was previously linearized by Xho 1 (Figure 7 Restriction Enzyme Digest and Linearization of the  $\gamma$ 2b-LoxPhs3a1,2 and NEO Plasmids: The integrity of the  $\gamma$ 2b-LoxPhs3a1,2 plasmid was verified by restriction enzyme digest (column labels with expected fragment size in parenthesis) and agarose gel electrophoresis along with linearization of the  $\gamma$ 2b-LoxPhs3a1,2 (Pvu1) and NEO (XhoI) plasmids.). Since circular DNA can also be incorporated to the genome and its efficiency of incorporation can be better or worse than linear DNA depending mainly on the cell line (Neumann, et al., 1886; Xie, et al., 1993; Xie, et al., 1992; Kumar, et al., 1994; Liu, et al., 2008), the Xho 1 digested NEO was used regardless of its conformation. The reporter construct and NEO were co-transfected to cells by electroporation at a ratio of 2:1, to ensure that cells transfected with NEO were also likely to have been transfected with the reporter. After selection in G418-supplemented medium, 19 individual cell colonies were isolated; however, some isolates (pC9, pC11, pC18, pC19) were lost during passage to a larger volume of medium.

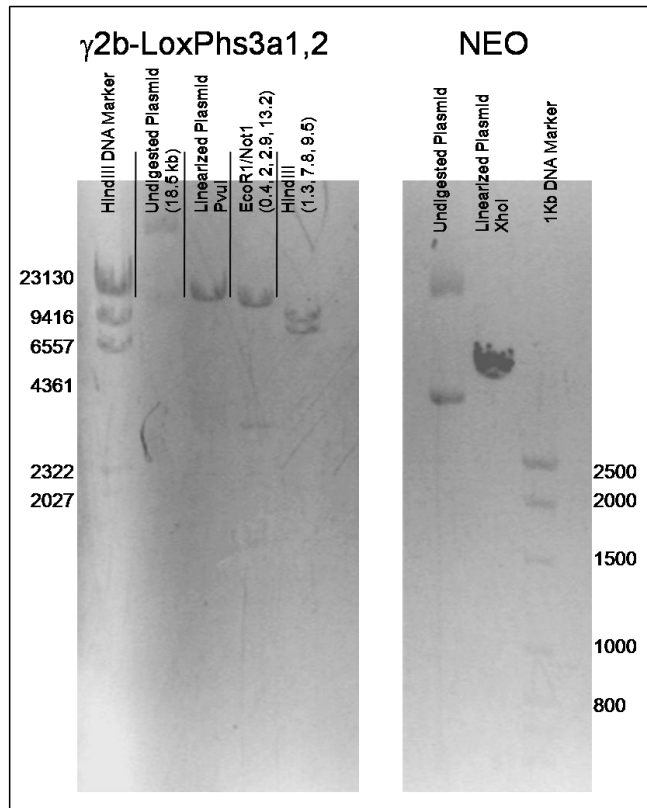


**Figure 7 Restriction Enzyme Digest and Linearization of the  $\gamma$ 2b-LoxPhs3a1,2 and NEO Plasmids:** The integrity of the  $\gamma$ 2b-LoxPhs3a1,2 plasmid was verified by restriction enzyme digest (column labels with expected fragment size in parenthesis) and agarose gel electrophoresis along with linearization of the  $\gamma$ 2b-LoxPhs3a1,2 (Pvu1) and NEO (XhoI) plasmids.

Real-time PCR was used to estimate the number of reporter constructs successfully transfected to parental clones. By selecting clones with only one copy of the reporter, I hoped to ensure efficient CRE-recombinase modification of the construct. The  $C_T$  values for each of the parental clones (CH12.LX. $\gamma$ 2b-LoxPhs3a1,2 designated pCx , where  $x$  is the clonal isolate number), for the negative control (untransfected CH12.LX cells), and for the positive control (C3 cells) are shown in Table 2 with associated graphs in Figure 8. A  $C_T$  value for  $\gamma$ 2b in the sample which was greater than that for the negative control but less than the  $C_T$  for the  $\beta$ -actin gene in the same sample was assumed to indicate incorporation of a single copy of the reporter construct.

Sample	Mean $\beta$ -actin $C_T$	$\beta$ -act $C_T$ Standard Error	Mean $\gamma$ 2b $C_T$	$\gamma$ 2b $C_T$ Standard Error	Mean NEO $C_T$	NEO $C_T$ Standard Error
NO DNA	none	*	none	*	36.5	*
C3 Cells	21.0	*	25.3	*	22.8	0.41
CH12.LX	21.0	1.42	30.7	0.55	31.1	0.10
pC1	28.0	*	30.2	*	29.8	*
pC2	27.7	*	30.0	*	29.2	*
pC3	26.1	*	28.5	*	27.9	*
pC4	23.5	0.29	26.1	0.44	24.4	0.29
pC5	28.1	0.07	30.1	*	29.2	0.32
pC6	27.0	0.09	29.6	0.00	31.1	3.21
pC7	27.0	0.08	29.0	0.31	28.2	0.06
pC8	27.2	0.05	29.3	0.14	29.1	0.09
pC10	23.0	0.04	26.0	0.21	24.3	0.02
pC12	23.3	0.08	33.7	*	25.2	*
pC13	24.2	0.09	27.0	0.03	25.5	0.18
pC14	23.4	0.02	25.7	0.07	25.1	0.47
pC15	23.3	0.06	25.5	0.12	25.0	0.16
pC16	22.0	0.58	22.7	0.78	23.6	0.18
pC17	22.7	*	24.0	*	24.9	1.22
* less than two samples used to calculate mean						

**Table 2 Threshold Crossing ( $C_T$ ) Values from Real Time PCR:** Listed are the mean  $C_T$  values for  $\beta$ -actin,  $\gamma$ 2b, and NEO genes in  $\gamma$ 2b-LoxPhs3a1,2 parental clones, CH12.LX  $\gamma$ 2b-negative controls, and C3 Cell  $\gamma$ 2b-positive controls.

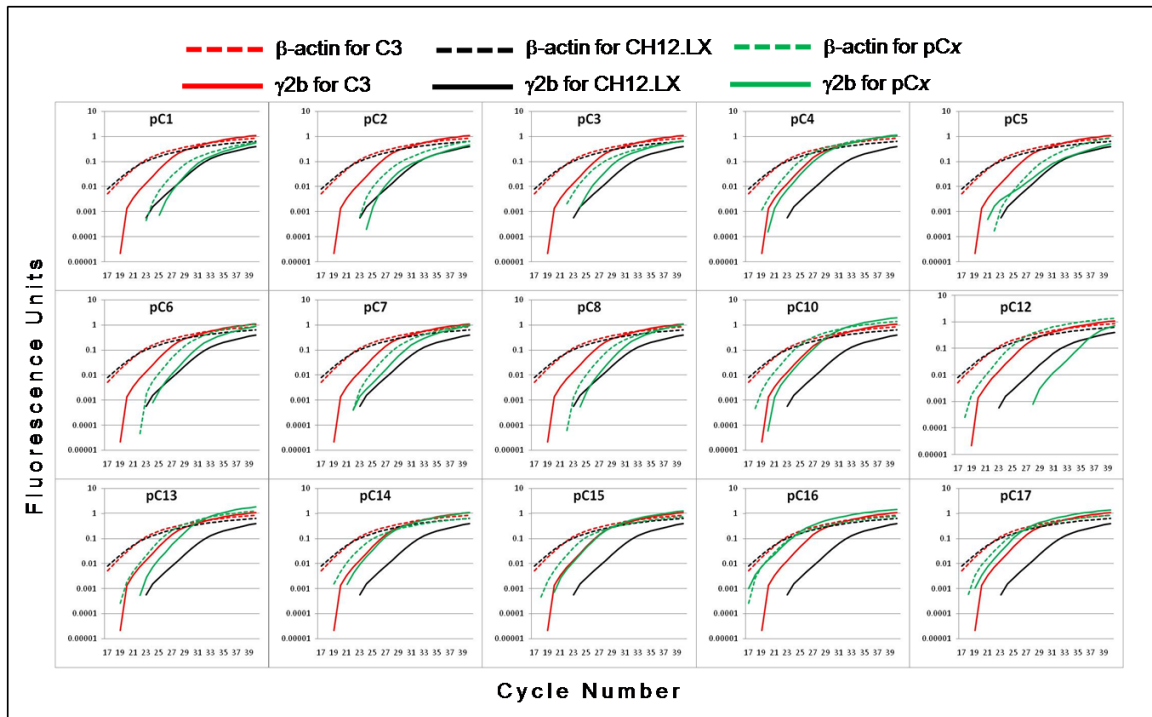


**Figure 8 Real-Time PCR of DNA from CH12.LX.γ2b-LoxPhs3a1,2 Cells:** Single-copy integration of the  $\gamma 2b$  mini-locus was estimated by real-time PCR using primers for  $\gamma 2b$  and  $\beta$ -actin. Shown here is fluorescence from the last 14 cycles of real-time PCR where  $C_T$  occurred for each clone. Copy number was estimated by comparison to a 2-copy control ( $\beta$ -actin) and a  $\gamma 2b$  negative control (CH12.LX cell DNA) as well as a single-copy positive control (C3 cell DNA).

The  $C_T$  value for  $\gamma 2b$  in one parental (pC12) was greater than that for CH12.LX. Since the CH12.LX cell line produces IgA, it has undergone class switch recombination and its DNA should not contain a  $\gamma 2b$  constant region; however, IgM can be measured in CH12.LX cells, suggesting that some cells may not have undergone class switch recombination, or that only one copy of the heavy chain gene locus has been recombined, so that cells still retain a copy of the  $\gamma 2b$  gene. This explains why real-time PCR revealed a  $C_T$  value (30.7) for  $\gamma 2b$  in the negative control, CH12.LX cells. In order to estimate single copy incorporation for the reporter plasmid, the  $C_T$  for  $\gamma 2b$  in CH12.LX cells was

defined as one copy or less of the  $\gamma$ 2b gene. Since the pC12 clone had a greater  $C_T$  value than CH12.LX, it was assumed to have less than one copy of the  $\gamma$ 2b transgene and was dropped from further characterization. Thirteen clones were estimated to have incorporated one copy of the  $\gamma$ 2b transgene. Three of the  $C_T$  values for the NEO transgene (No DNA, CH12.LX cells, and pC6) were greater than the  $C_T$  value for  $\gamma$ 2b in CH12.LX cells, suggesting less than one copy was present, which was expected in the No DNA and CH12.LX controls. Since G418 selective pressure was removed after initial characterization, pC6 was not disqualified for appearing to have less than one copy of the NEO transgene. No  $C_T$  value for  $\gamma$ 2b was less than the  $C_T$  value for  $\beta$ -actin in the same cell, suggesting that none of the clones had more than two copies of the  $\gamma$ 2b mini-locus in its genome. pC16 was not characterized further because its  $C_T$  value for  $\gamma$ 2b was less than one cycle from its  $C_T$  for  $\beta$ -actin, suggesting that it may have incorporated 2 copies of the  $\gamma$ 2b mini-locus.

In summary, the transfection was successful: 1 of 15 clones tested incorporated the NEO plasmid but not the  $\gamma$ 2b mini-locus; 1 of 15 incorporated more than one copy of the NEO plasmid; and 1 of the 15 tested may have incorporated more than one copy of the  $\gamma$ 2b mini-locus. Twelve of the 15 clones tested incorporated one NEO plasmid and one  $\gamma$ 2b mini-locus. Although this seems like overwhelming success, transfection of 4 fold more  $\gamma$ 2b plasmid than NEO may have increased the probability of selection for  $\gamma$ 2b-positive clones, and using 20  $\mu$ g of  $\gamma$ 2b plasmid per  $1 \times 10^7$  cells was apparently a good ratio to ensure single-copy incorporation.

The transgene copy number could have been determined with greater confidence by an alternative method, such as making a standard curve of the transgene by calculating its molecular weight and using an estimated molecular weight for CH12.LX genomic DNA to determine input concentration (Reisinger, et al., 2008). Alternatively, a method calculating the relative quantification of gene copy could have been employed (Cawthon, 2002). Since I only needed to estimate that one transgene copy was present to ensure deletion of the hs3a and hs1,2 enhancers in every copy present, the method I employed was adequate.

Clones which successfully incorporated the  $\gamma$ 2b transgene (CH12.LX. $\gamma$ 2b-LoxPhs3a1,2 or parental clones) were tested for LPS-inducible  $\gamma$ 2b expression by addition of LPS to culture medium and measurement of  $\gamma$ 2b in cell lysate by ELISA. The results for the 14 parental clones tested are shown in Figure 9. At the lowest LPS concentration (0.01  $\mu$ g/mL),  $\gamma$ 2b expression was unchanged for one clone (pC1) and increased between 1.8 and 4 fold over unstimulated levels in the other clones. Expression of  $\gamma$ 2b increased between 2 and 10 fold over unstimulated at an LPS concentration of 0.1  $\mu$ g/mL. With a LPS concentration of 1.0  $\mu$ g/mL,  $\gamma$ 2b expression increased between 2 and 10 fold over unstimulated except for pC4 which showed a 20 fold increase. Clone pC10 appeared to not express  $\gamma$ 2b. In three clones,  $\gamma$ 2b expression appears to decrease at higher concentrations of LPS; however, pC5 at 1  $\mu$ g/mL had high variability during total protein determination (CV=32%); therefore, the total amount of protein used in the ELISA may have been less than 1  $\mu$ g. The decrease in  $\gamma$ 2b for pC7 and pC16 were unexpected. Given the overall low level of  $\gamma$ 2b expression in pC16 and its lower expression at high

concentrations, and its potential to have more than one copy of the  $\gamma 2b$  transgene, it was disqualified from further testing.

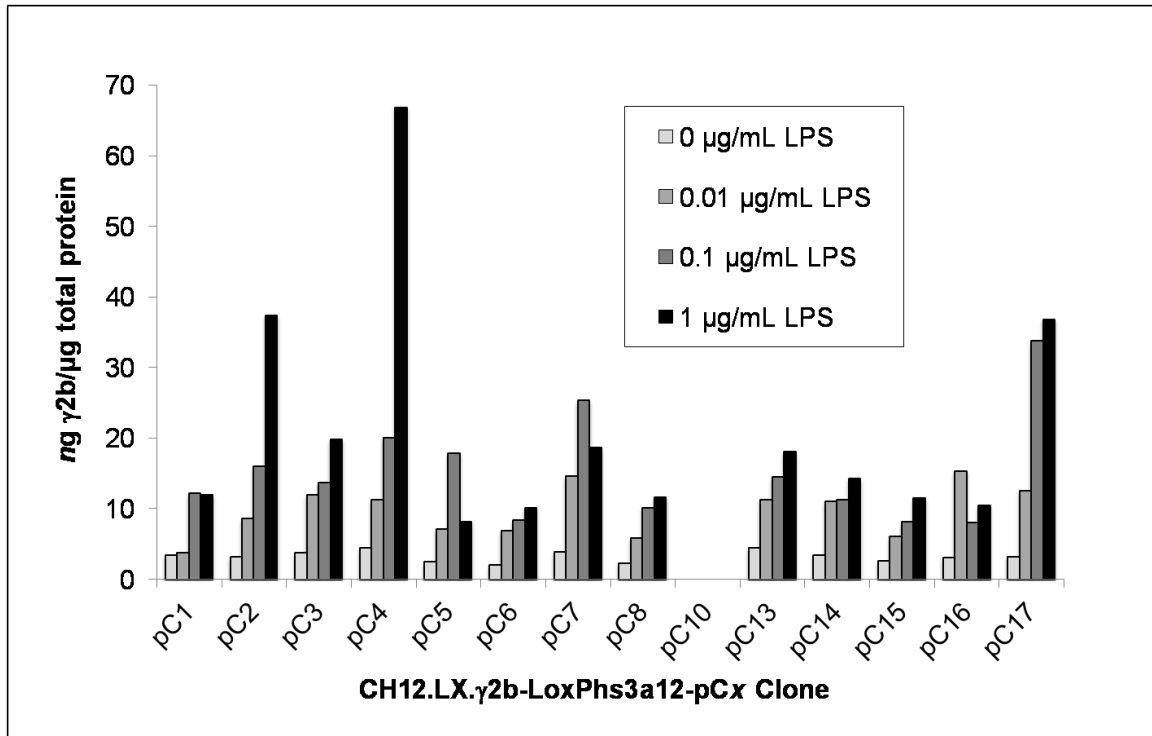


**Figure 9 LPS-Induced  $\gamma 2b$  Expression in CH12.LX. $\gamma 2b$ -LoxPhs3a1,2 Clones:** Clonal isolates of cells after introduction of the  $\gamma 2b$ -LoxPhs3a1,2 and NEO plasmids were screened by ELISA for  $\gamma 2b$  expression after treatment with LPS. Bars are representative of a single treatment with the indicated LPS concentration, making statistical comparisons unfeasible.

Six parental clones (pC2, pC3, pC4, pC5, pC13, and pC17) were screened for the effect of TCDD on  $\gamma 2b$  expression and compared to C3 cells as a positive control. These clones were chosen because they displayed a concentration dependent increase in  $\gamma 2b$  expression, appeared to each have a single copy of the transgene, and had no obvious reasons to be disqualified. The results are shown in Figure 10. With 95% confidence, each LPS+DMSO is significantly greater than its corresponding NA or DMSO, and each LPS+TCDD is significantly less than its corresponding LPS+DMSO.

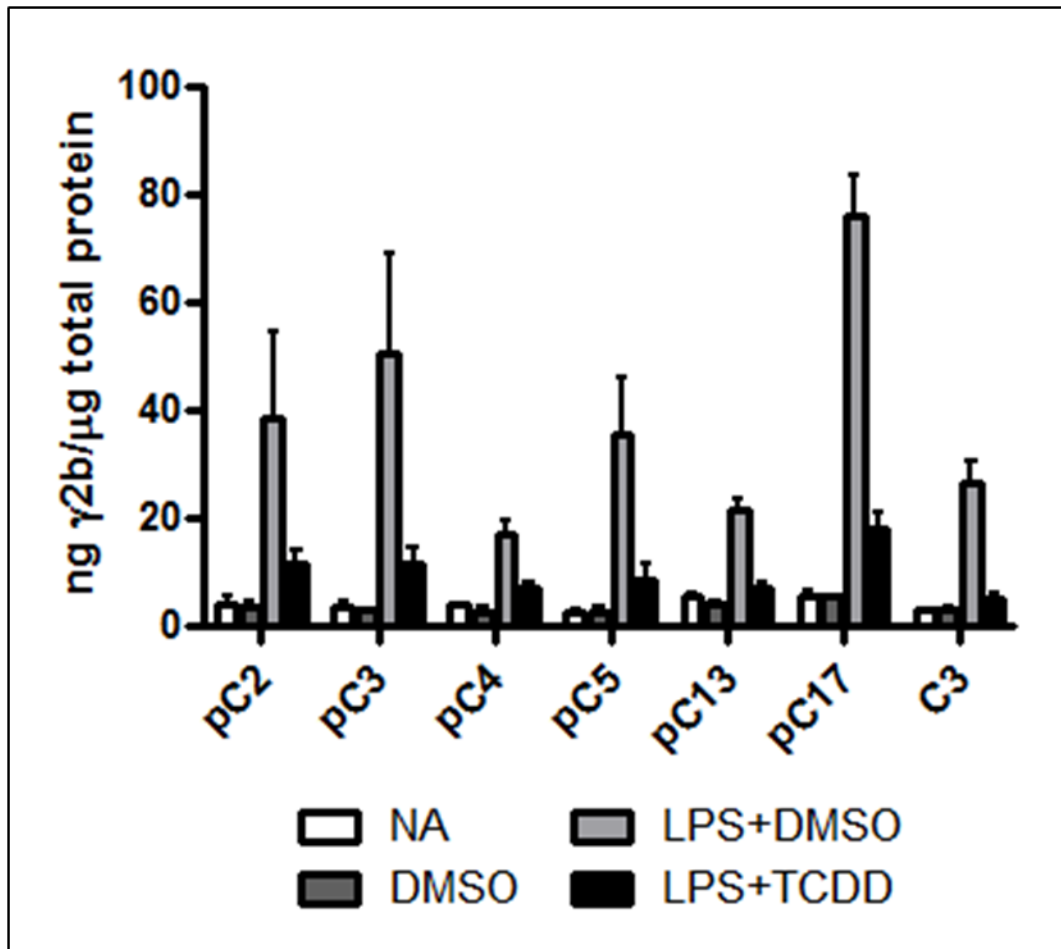


**Figure 10 Inhibition of LPS-Induced  $\gamma$ 2b Expression by 10 nM TCDD:** Six  $\gamma$ 2b-LoxPhs3a1,2 clones were screened for the effect of 10 nM TCDD (in DMSO) on  $\gamma$ 2b expression. Each clone was induced by LPS to express  $\gamma$ 2b (each LPS+DMSO is significantly greater than its corresponding NA or DMSO), and that expression is inhibited by TCDD (each LPS+TCDD is significantly less than its corresponding LPS+DMSO) ( $\alpha=0.05$ ). Each bar represents 4 replicates and error bars represent the standard deviation.

This means that each clone was stimulated by LPS to produce  $\gamma$ 2b and that stimulation was inhibited by TCDD. Only pC17 had a LPS+TCDD significantly different from (greater than) its corresponding NA and DMSO, suggesting that in all tested clones except pC17, TCDD inhibited  $\gamma$ 2b expression back to baseline, or pre-stimulation levels. pC13 was chosen as parent for the deletion derivatives because it had the least variability

in  $\gamma$ 2b expression and was similar to the C3 positive control in this screen for inhibition by TCDD. Cells were not treated with LPS alone for comparison to LPS+DMSO treatment in this screening, but previous studies and subsequent studies have shown that 0.01% DMSO does not significantly alter LPS-mediated activation of CH12.LX cells.

The hs3a/hs1,2 enhancer pair were removed from the CH12.LX. $\gamma$ 2b-LoxPhs3a1,2 reporter transgene by transient expression of CRE-recombinase enzyme. The enzyme and Green Fluorescent Protein (GFP) reporter were transfected on a pEGFP-CRE plasmid by electroporation. The plasmid was linearized by digestion with Hind III (bands expected at 2.7, 3.0, and 3.4 kilobases). Figure 7 shows the results of a restriction digest conducted several months prior to transfection while Figure 11 shows results of a digest just prior to transfection. Successfully transfected cells were identified by expression of GFP and sorted by FACS. Graphical results of cell sorting are presented in Figure 12. About 71,000 GFP-expressing cells were recovered. Clonal selection was accomplished by limiting dilution in 96-well plates; however, cells that were diluted on the day of sorting did not grow. Experience from culturing CH12.LX cells suggests that the cells have greater viability when in contact with other cells. I speculate that being electroporated on the previous day, sorted through a flow cytometer, and then diluted to isolate single cells was too much stress and the cells could not grow. Perhaps mitogenic stimulation would have produced clonal isolates from that first batch of cells. Subsequent limiting dilutions yielded many colonies, but only 19 were collected with high confidence that they came from a single clone instead of a clump of cells.

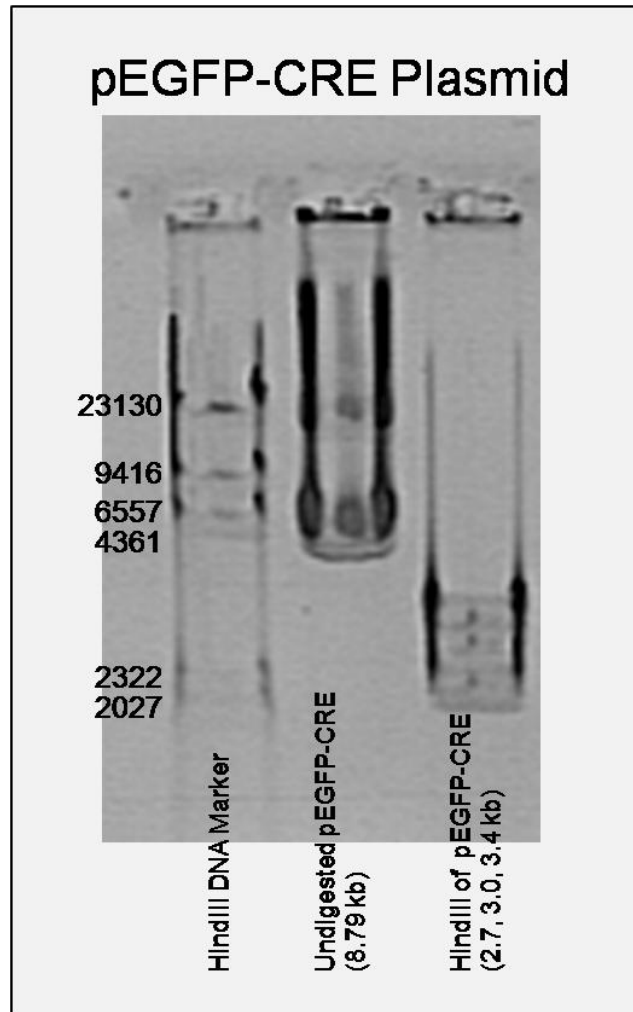


**Figure 11 Restriction Enzyme Digestion of the pEGFP-CRE Plasmid:** The integrity of the pEGFP-CRE plasmid was re-verified just prior to transfection. Column labels show the restriction enzyme used and in parenthesis, the expected DNA fragment sizes after digestion with that enzyme.

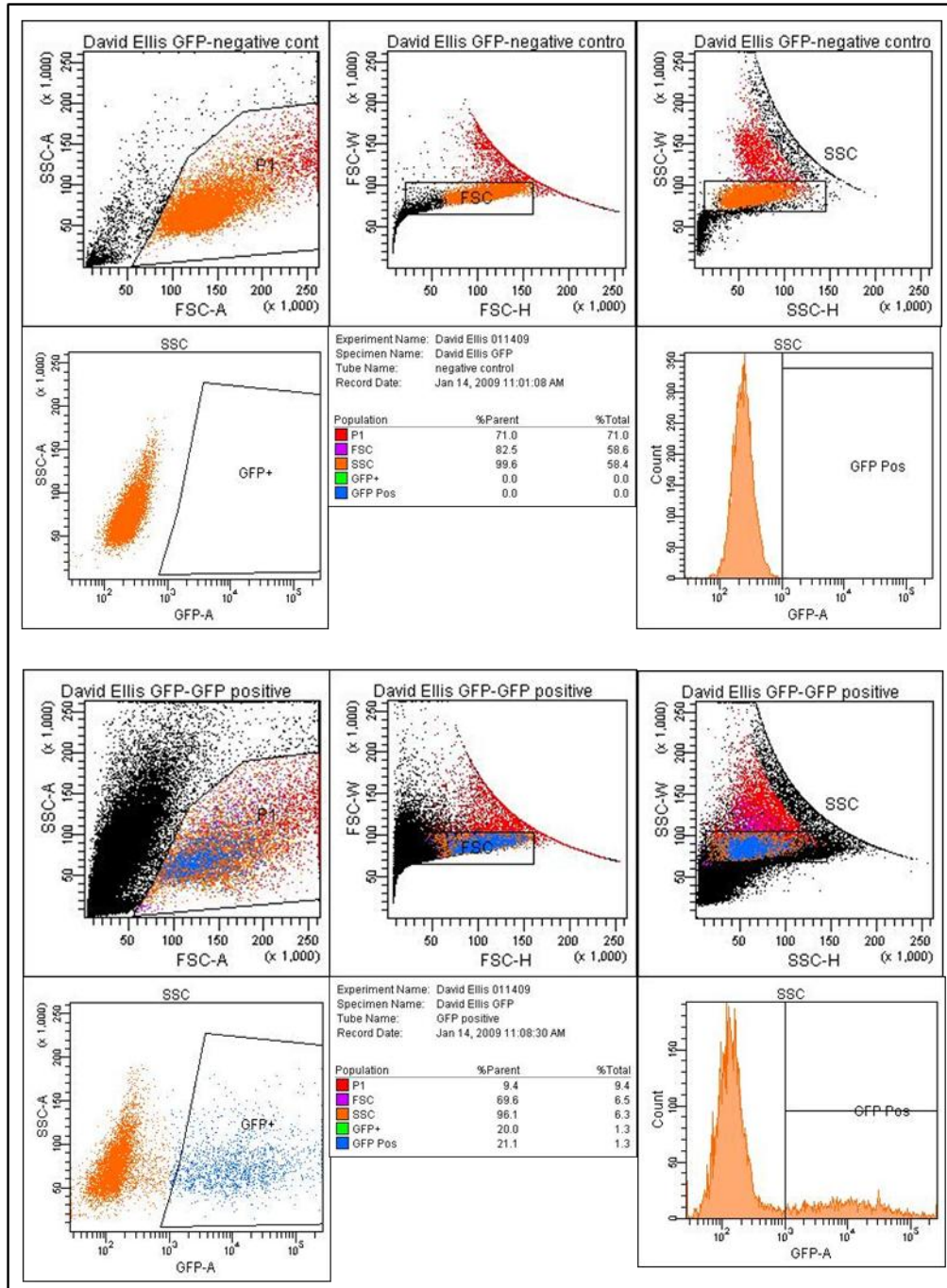


**Figure 12 FACS of GFP-Expressing Cells:** After transfection with the pEGFP-CRE plasmid, cells expressing GFP were separated from non-expressors by the Core Flow Cytometry Facility at Cincinnati Children’s Hospital (Cincinnati, OH), who provided these graphics. Untransfected CH12.LX cells were used as negative control (top 6 panels). Stringent gating to ensure precise collection of GFP expressing cells rendered less than 2% of the total cells (lower 6 panels).

Deletion of the hs3a/hs1,2 enhancer pair was confirmed by PCR using primers that flanked the two LoxP sites (CUT), amplifying a DNA sequence only if the long enhancer pair was removed; or primers that amplified part of the sequence inside the LoxP-surrounded enhancers (UNCUT), amplifying a sequence only if the enhancer pair was not removed. Results of PCR analysis are shown in Figure 13, Figure 14, Figure 15, and Figure 16 and summarized in Table 3. The pC13 (parental) negative cut control had a product with UNCUT primers and did not have a product with CUT primers. Also in this test, the CH12.LX (LX) negative PCR control (which should not have any sequence from the transgene present to amplify) had a product with the UNCUT primers (Figure 13). This could have been caused by contamination or from spill-over between wells on the agarose gel which was noted during gel loading in the initial PCR tests when the entire reaction volume was loaded to gels. Only 15  $\mu$ L was loaded from later tests, no spill-over was noted, and the LX did not have a product with the UNCUT primers (Figure 15). In addition, the first PCR test used an old stock of Taq DNA polymerase which was at or past its expiration date. Only one of the deletion derivative clones isolated from limiting dilution (D15) was positive for CUT and negative for UNCUT, indicating the  $\gamma$ 2b mini-locus was correctly cut in those cells to remove the hs3a and hs1,2 enhancers. Five of the clones (D12, D13, D14, D17 and D18) were positive for UNCUT and negative for CUT, indicating that the  $\gamma$ 2b mini-locus in those cells was not cut. The remaining clones were positive for both CUT and UNCUT, indicating either that they had more than one copy of the mini-locus, some of which was correctly cut by CRE-recombination and some of which was not, or that there was a mixed population of cut and uncut cells. This result could not be caused by the deleted segment being reintegrated to the genomic DNA

because the forward PCR primer was outside of the deleted segment. Initially, D1 did not have a product with UNCUT primers (Figure 14); however, when tested again to confirm this finding, it did have a product (Figure 15).

Seven of the double positive (CUT and UNCUT) clones (D1, D2, D3, D4, D5, D16, and D19) underwent the same limiting dilution as the initial proposed deletion derivatives and their clonal isolates underwent PCR confirmation. The results are shown in Figure 17, Figure 18, Figure 19, and Figure 20, and summarized in Table 4, Table 5, Table 6, and Table 7. The majority of those clonal isolates were either correctly cut or uncut, with a few still showing both characteristics. The numbers of isolates correctly cut, uncut, and mixed are summarized in Table 8. Since the clones could be separated in to populations (cut or uncut), there was likely a mixed population of cut and uncut in the original deletion derivative isolates.

<b>CH12.LX.γ2b-Ahs3a1,2 clone number</b>	<b>Primers CEWS 143+144 CUT</b>	<b>Primers CEWS 143+161 UNCUT</b>
D1	+	-/+
D2	+	+
D3	+	+
D4	+	+
D5	+	+
D6	+	+
D7	+	+
D8	+	+
D9	+	+
D10	+	+
D11	+	+
D12	-	+
D13	-	+
D14	-	+
D15	+	-
D16	+	+
D17	-	+
D18	-	+
D19	+	+
pC13	-	+
LX(CH12.LX)	-	+/-
C3	large	+

**Table 3 Results of PCR testing of CH12.LX.γ2b-LoxPhs3a1,2 clones:** Clones were tested by PCR using primers that surround the LoxP sites of the target deletion to identify correctly cut transgenes (CUT) and primers that surround only the 5-prime LoxP site to identify uncut transgenes (UNCUT). “+” indicates the presence of a PCR product while “-” indicates absence of PCR product. “+/-” indicates that different results were obtained in replicate tests. “Large” indicates the product observed was too large for that primer pair.

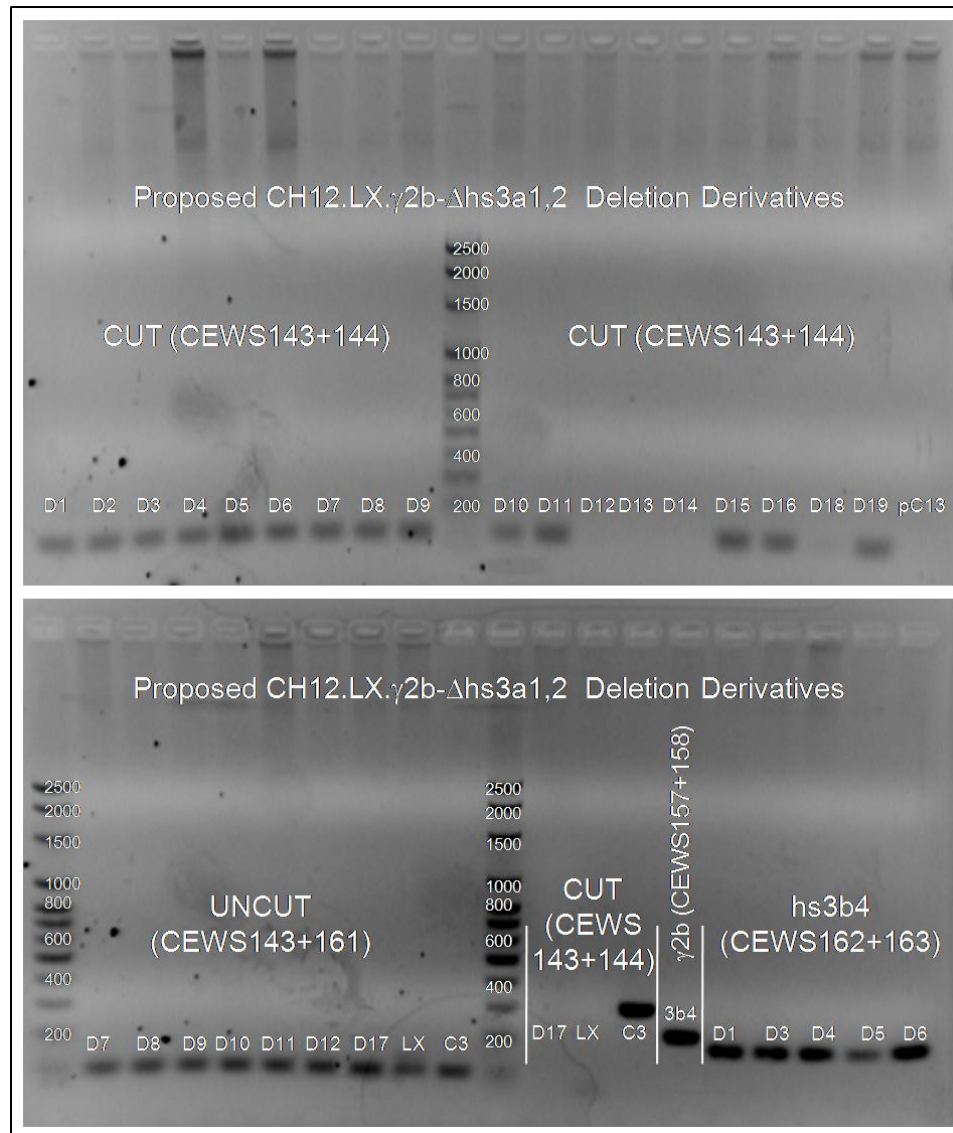


**Figure 13 PCR Test for Deletion of the hs3a and hs1,2 Enhancers from Cell Isolates Collected after Limiting Dilution of GFP-Expressing Cells:** Isolates were screened by PCR for presence of the hs3a and hs1,2 enhancer region which was targeted for deletion by cre-recombination. The primers CEWS143+144 were found to accurately amplify DNA which had been cut while CEWS143+161 accurately amplified DNA which was not cut. In addition, CEWS162+163 accurately identified the presence of the hs3b and hs4 enhancer region and CEWS157+158 identified a  $\gamma$ 2b sequence in an hs3b and hs4 deletion derivative (3b4). Many of the same clones tested positive for being CUT and UNCUT.

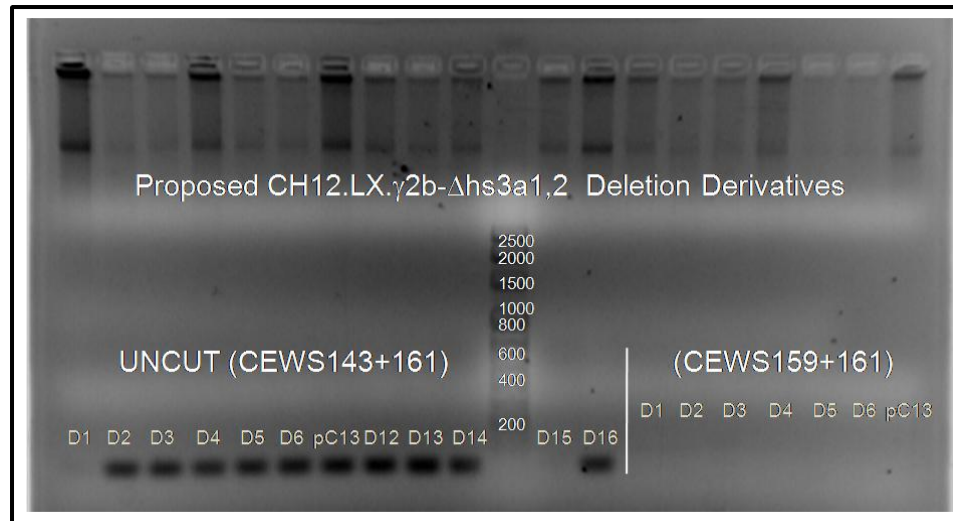


**Figure 14 PCR Test for the Presence of the hs3a and hs1,2 Enhancers in Cell Isolates Collected after Limiting Dilution of GFP-Expressing Cells:** Isolates were screened by PCR for presence of the hs3a and hs1,2 enhancer region which was targeted for deletion by cre-recombination. The primers CEWS143+161 were found to accurately amplify DNA which was uncut. CEWS159+163 were unable to identify UNCUT clones.

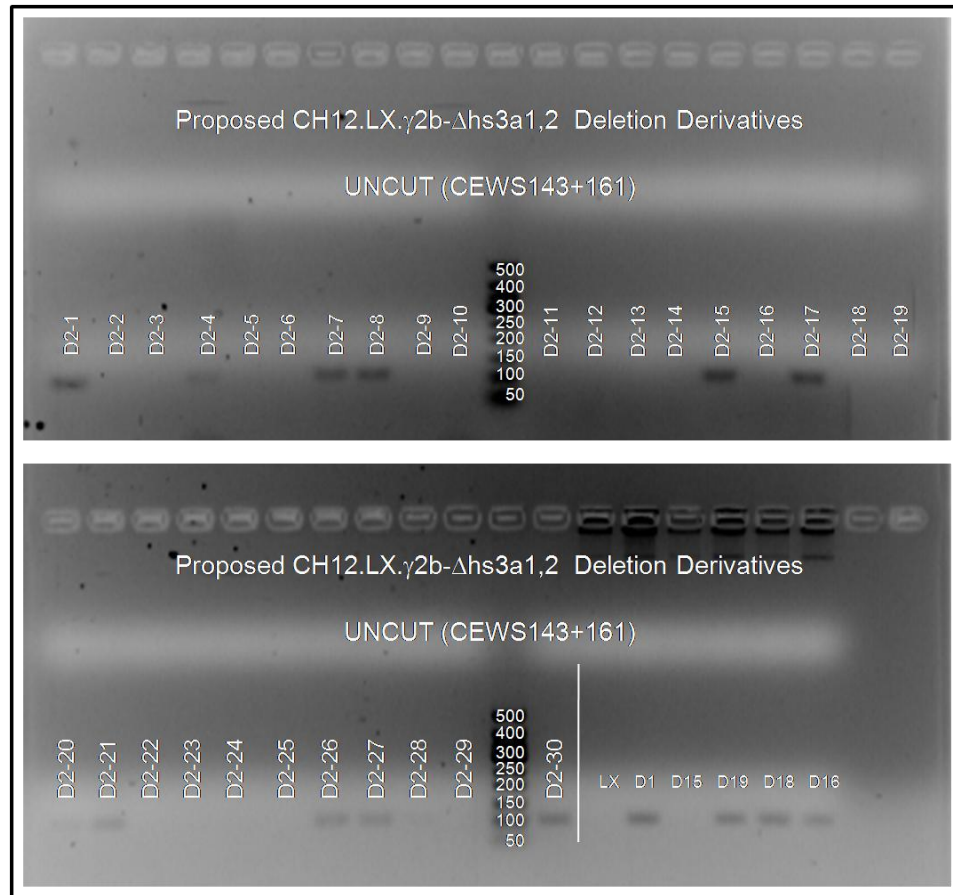


**Figure 15 PCR Test for the Presence of hs3a and hs1,2 Enhancers in Proposed Deletion Derivatives:** Cells which were isolated from GFP-expressing cells and were found to have some CUT transgenes and some UNCUT transgenes underwent limiting dilution and were subsequently screened for the presence of the target hs3a and hs1,2 enhancers. The new isolates in this figure originated from the D2, GFP-expressing isolate. Several GFP-expressing isolates were also re-screened for the enhancers. In this figure, 11 of the new isolates still have the targeted enhancers while 19 do not. CH12.LX cells (LX) acted as negative control.

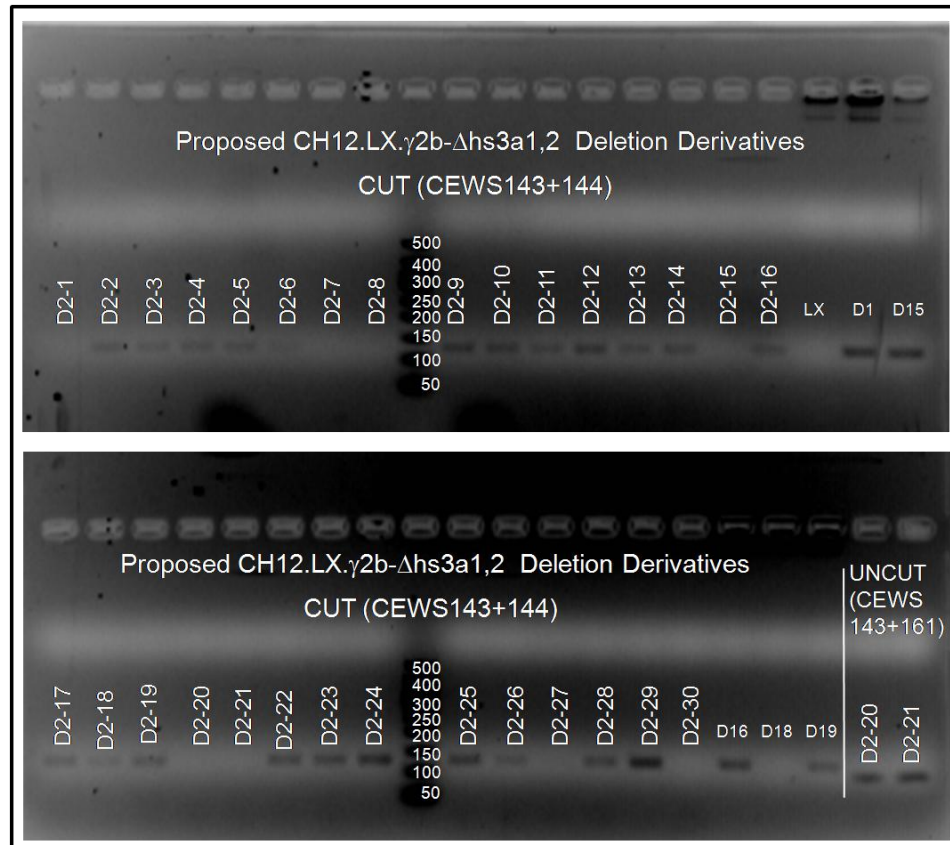


**Figure 16 PCR Test for hs3a and hs1,2 Deletion from Proposed Deletion Derivatives:** Cells which were isolated from GFP-expressing cells and were found to have some CUT transgenes and some UNCUT transgenes underwent limiting dilution and were subsequently screened for the deletion of the target hs3a and hs1,2 enhancers. Several previously screened GFP-expressing isolates and new isolates were also re-screened for the presence or deletion of the targeted enhancers. In this figure, 22 of the new isolates tested positive for deletion of the targeted enhancers, only 3 of which had also tested positive for presence of the enhancers. 7 did not test positive for deletion. CH12.LX cells acted as negative control.

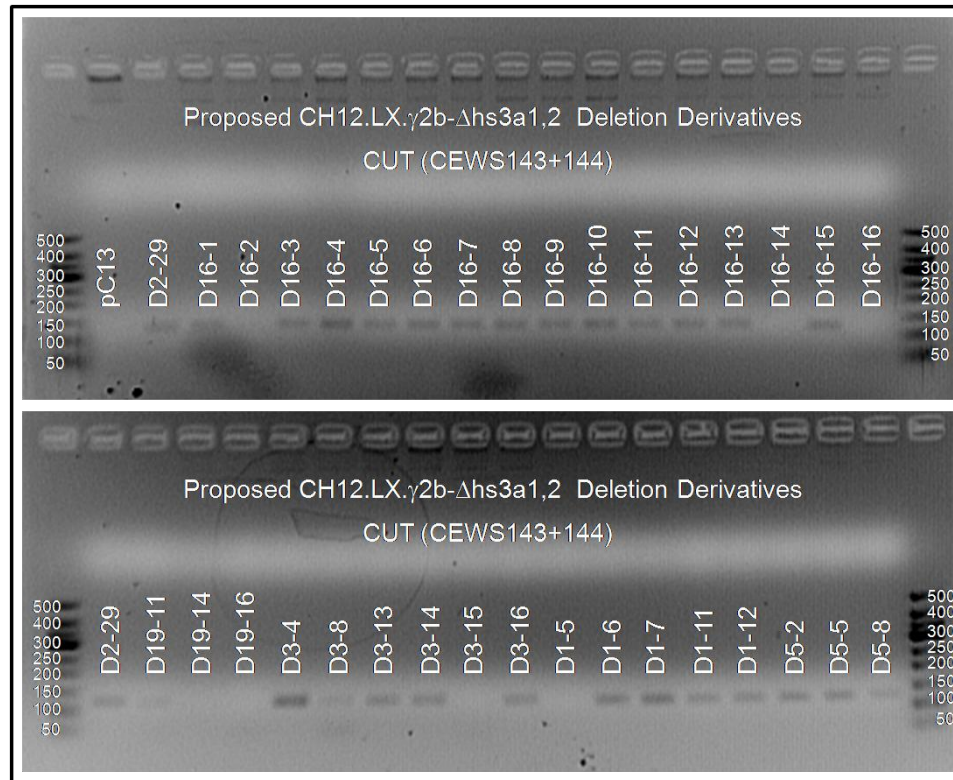


**Figure 17 PCR Test for hs3a and hs1,2 Deletion from Proposed Deletion Derivatives:** Cells derived from limiting dilution of GFP-expressing isolates were screened by PCR for deletion of the targeted enhancers (CUT). In this figure, the enhancer region was found to be deleted from 28 of the new clonal isolates. These new isolates came from the GFP-expressing isolates D1, D2, D3, D5, D16, and D19. The parental pC13 cells acted as negative control while D2-29 (positive in previous tests) acted as positive control.

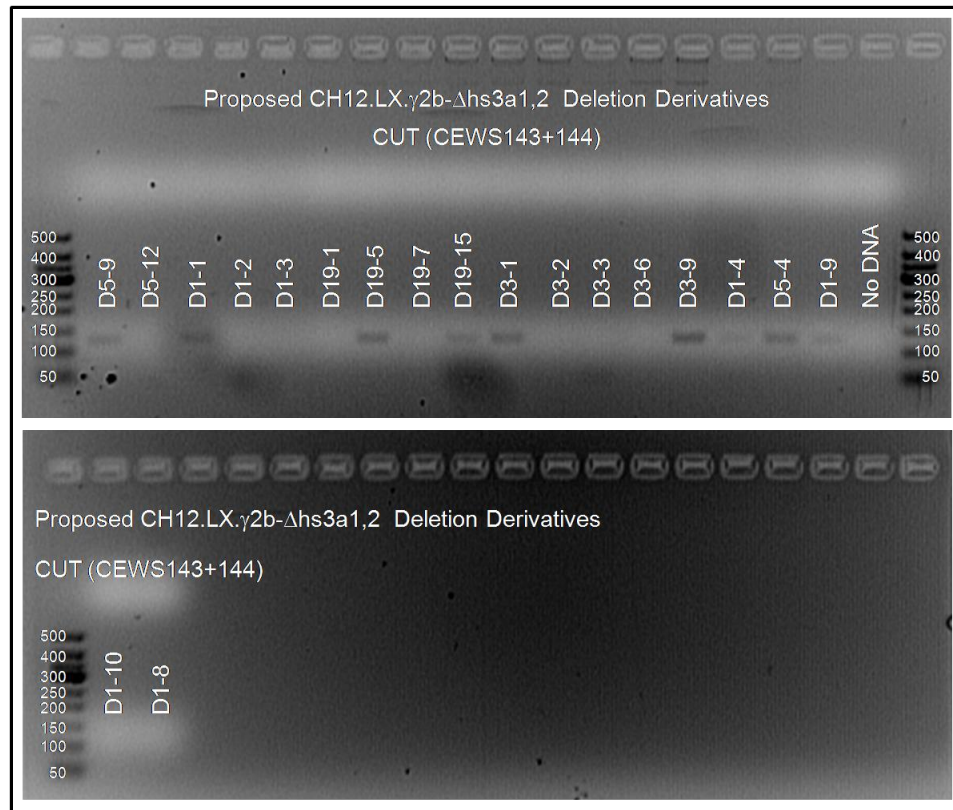


**Figure 18 PCR Test for hs3a and hs1,2 Deletion from Proposed Deletion Derivatives:** Cells derived from limiting dilution of GFP-expressing isolates were screened by PCR for deletion of the hs3a and hs1,2 enhancer region (CUT). In this figure, 9 of the new isolates tested positive for deletion of the targeted enhancers. These samples were amplified at the same time as the previous gels but there was no positive or negative control left to load to this gel.

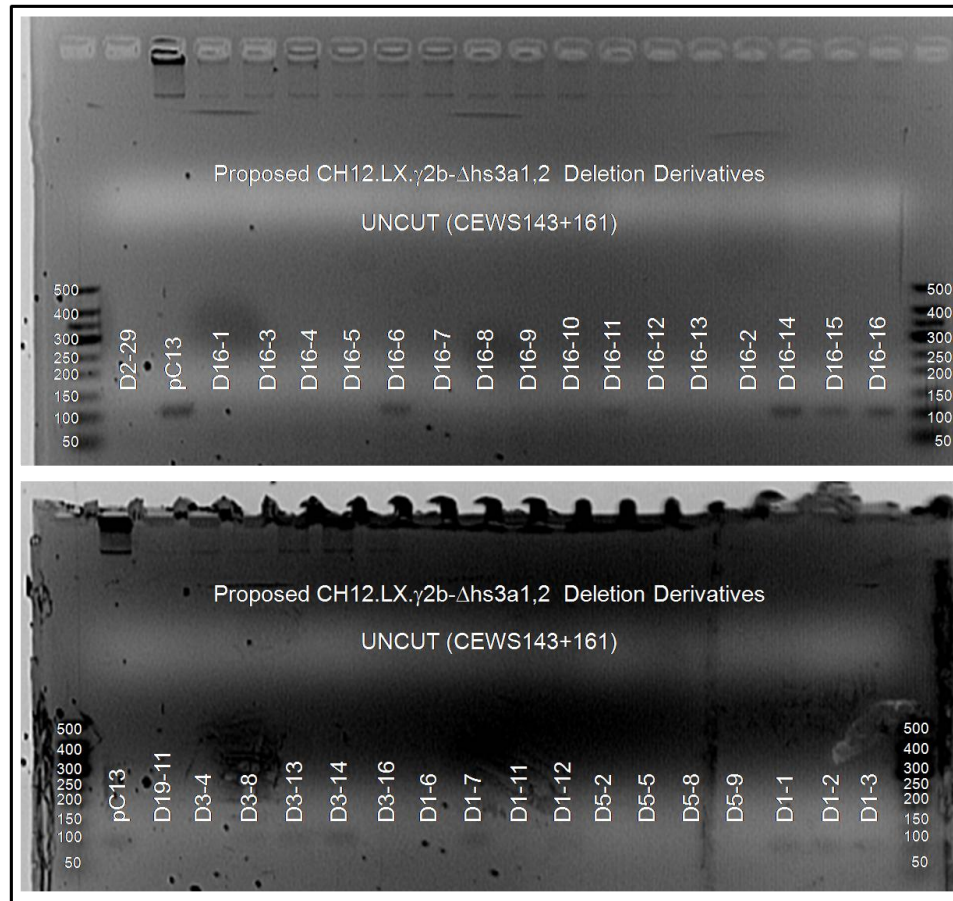


**Figure 19 PCR Test for the Presence of the hs3a and hs1,2 enhancers in Proposed Deletion Derivatives:** Cells derived from limiting dilution of GFP-expressing isolates were screened by PCR for presence of the hs3a and hs1,2 enhancer region (UNCUT). In this figure, thirteen of the new clonal isolates were found to contain the targeted enhancer region, 9 of which also tested positive for deletion. Some of the faint bands were verified by loading a larger volume on another gel. D2-29 which tested negative previously served as the negative control and pC13 acted as positive control.

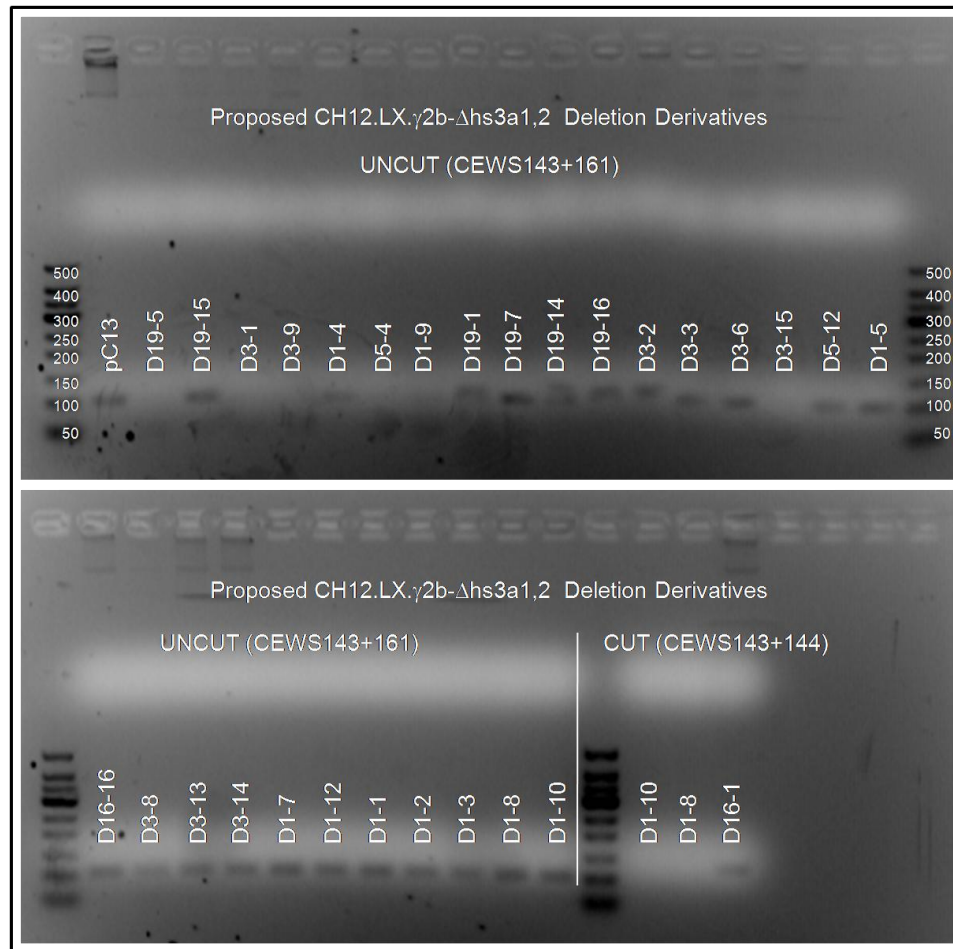


**Figure 20 PCR Test for the Presence of the hs3a and hs1,2 enhancers in Proposed Deletion Derivatives:** Cells derived from limiting dilution of GFP-expressing isolates were screened by PCR for presence of the hs3a and hs1,2 enhancer region (UNCUT). In this figure, 11 of the new isolates were found to contain the targeted enhancer region, only 2 of which also tested positive for enhancer deletion. Another 11 were verified here after their bands were too light in a previous gel. pC13 acted as positive control and the same negative control as the other gels, D2-29, did not have enough left to load here.

<b>CH12.LX.γ2b-Δhs3a1,2-D2 sub-clone number</b>	<b>Primers CEWS 143+144 CUT</b>	<b>Primers CEWS 143+161 UNCUT</b>
D2-1	-	+
D2-2	+	-
D2-3	+	-
D2-4	+	+
D2-5	+	-
D2-6	+	-
D2-7	-	+
D2-8	-	+
D2-9	+	-
D2-10	+	-
D2-11	+	-
D2-12	+	-
D2-13	+	-
D2-14	+	-
D2-15	-	+
D2-16	+	-
D2-17	+	+
D2-18	+	-
D2-19	+	-
D2-20	-	+

**Table 4 Results of PCR testing of the D2 Subclones:** Proposed deletion derivative D2 which tested positive for CUT and UNCUT underwent limiting dilution and subclone isolates were tested by PCR for modification of the  $\gamma$ 2b transgene. “+” indicates the presence of a PCR product while “-“ indicates absence of PCR product.

<b>CH12.LX.γ2b-Ahs3a1,2-D2 sub-clone number</b>	<b>Primers CEWS 143+144 CUT</b>	<b>Primers CEWS 143+161 UNCUT</b>
D2-21	-	+
D2-22	+	-
D2-23	+	-
D2-24	+	-
D2-25	+	-
D2-26	+	+
D2-27	-	+
D2-28	+	-
D2-29	+	-
D2-30	-	+
D3-1	+	-
D3-2	-	+
D3-3	-	+
D3-4	+	-
D3-6	-	+
D3-8	+	+
D3-9	+	-
D3-13	+	+
D3-14	+	+
D3-15	-	-
D3-16	+	-

**Table 5 Results of PCR testing of the Various Subclones I:** Proposed deletion derivatives, Dx, which tested positive for CUT and UNCUT underwent limiting dilution. Subclone isolates, Dx-y, were then tested by PCR for modification of the γ2b transgene. “+” indicates the presence of a PCR product while “-“ indicates absence of PCR product.

<b>CH12.LX.γ2b-Ahs3a1,2-Dx sub-clone number</b>	<b>Primers CEWS 143+144 CUT</b>	<b>Primers CEWS 143+161 UNCUT</b>
D16-1	+	-
D16-2	-	-
D16-3	+	-
D16-4	+	-
D16-5	+	-
D16-6	+	+
D16-7	+	-
D16-8	+	-
D16-9	+	-
D16-10	+	-
D16-11	+	+
D16-12	+	-
D16-13	+	-
D16-14	-	+
D16-15	+	+
D16-16	-	+
D19-1	-	+
D19-5	+	-
D19-7	-	+
D19-11	+	-
D19-14	-	+
D19-15	+	+
D19-16	-	+

**Table 6 Results of PCR testing of the Various Subclones II:** Proposed deletion derivatives, Dx, which tested positive for CUT and UNCUT underwent limiting dilution. Subclone isolates, Dx-y, were then tested by PCR for modification of the γ2b transgene. “+” indicates the presence of a PCR product while “-“ indicates absence of PCR product.

<b>CH12.LX.γ2b-Δhs3a1,2-Dx sub-clone number</b>	<b>Primers CEWS 143+144 CUT</b>	<b>Primers CEWS 143+161 UNCUT</b>
D1-1	+	+
D1-2	-	+
D1-3	-	+
D1-4	+	+
D1-5	-	+
D1-6	+	-
D1-7	+	+
D1-8	-	+
D1-9	+	-
D1-10	-	+
D1-11	+	-
D1-12	+	+
D5-2	+	-
D5-4	+	-
D5-5	+	-
D5-8	+	-
D5-9	+	-
D5-12	-	+

**Table 7 Results of PCR testing of the Various Subclones III:** Proposed deletion derivatives, Dx, which tested positive for CUT and UNCUT underwent limiting dilution. Subclone isolates, Dx-y, were then tested by PCR for modification of the γ2b transgene. “+” indicates the presence of a PCR product while “-“ indicates absence of PCR product.

CH12.LX. $\gamma$ 2b- $\Delta$ hs3a1,2-Dx clone number	Number of sub-clones in each category			
	+ CUT - UNCUT	- CUT + UNCUT	+ CUT + UNCUT	- CUT - UNCUT
D1	3	5	4	0
D2	19	8	3	0
D3	4	3	3	1
D5	5	1	0	0
D16	10	2	3	1
D19	2	4	1	0

**Table 8 Results of Subclone Testing for  $\gamma$ 2b Transgene Modification:** The table shows the number of subclones found to have cut transgenes (+CUT /- UNCUT) or uncut transgenes (- CUT/+UNCUT) or mixed cut and uncut (+CUT/+UNCUT) or no transgene (- CUT/- UNCUT).

Transcriptional inducibility of the  $\gamma$ 2b transgene was tested by activating cells with LPS and measuring  $\gamma$ 2b protein by ELISA. D15 was the only deletion derivative from the initial limiting dilution (isolated after cell sorting and PCR test indicated that the LoxP flanked sequence was deleted) did not express  $\gamma$ 2b after LPS activation. The initial ELISA for that deletion derivative was conducted with 1  $\mu$ g of total protein, so the assay was repeated two more times with various amounts of total protein up to 40  $\mu$ g. No  $\gamma$ 2b was detected at any amount of total protein. The parent assayed on the same date was induced by LPS to express  $\gamma$ 2b and that expression was inhibited by TCDD (Figure 21), so the assay conditions did not prevent  $\gamma$ 2b expression by D15.

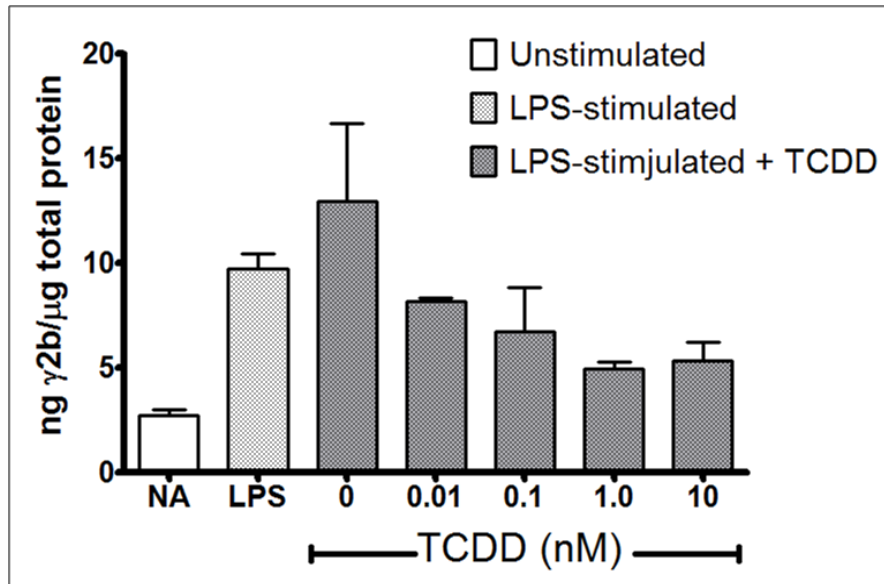


**Figure 21 LPS-Induced  $\gamma$ 2b-Expression and Inhibition by TCDD in CH12.LX. $\gamma$ 2b-LoxPhs3a1,2-pC13 Cells:** The pC13 parental cells were assayed by ELISA for  $\gamma$ 2b expression without treatment (NA) after treatment with LPS or LPS + Vehicle (0.01% DMSO – 0 nM TCDD) or LPS + TCDD at different concentrations (0.01, 0.1, 1.0, or 10 nM). LPS induced the cells to express  $\gamma$ 2b (LPS and LPS + 0 nM TCDD were significantly greater than NA). There was no vehicle effect (LPS and LPS + 0 nM TCDD treatments were not significantly different from each other). Expression of  $\gamma$ 2b was inhibited by TCDD at concentrations greater than 0.01 nM (LPS + 0.1, 1.0, or 10 nM were significantly less than LPS + 0 nM TCDD). Even at 10 nM TCDD,  $\gamma$ 2b expression was not completely eliminated since it was still significantly greater than NA ( $\alpha=0.05$ ). Error bars represent the standard deviation.

Since the initial characterization studies were run concurrent with PCR confirmation of enhancer deletion, D1 which was initially confirmed as a correctly cut clone but later identified as a mixed population of cut and uncut, was tested twice for LPS activation. In one test (5/1/09),  $\gamma$ 2b appeared to be induced at higher LPS concentrations, but differences between doses were not statistically significant, and the second test showed no increase in  $\gamma$ 2b at all (Figure 22). In anticipation of transfecting additional parental clones for deletion of the hs3a and hs1,2 enhancers, LPS-mediated

activation of pC14 and pC15 was confirmed (Figure 23). In addition, CH12.LX cells were tested for  $\gamma 2b$  expression and I found that despite the rtPCR results that show the  $\gamma 2b$  gene sequence may be present in CH12.LX cells, they are not induced to produce  $\gamma 2b$  by LPS (data not shown). Even when loading 5  $\mu\text{g}$  of total protein to the ELISA plate, the levels of  $\gamma 2b$  at LPS concentrations up to 10  $\mu\text{g}/\text{mL}$  were equal to or lower than background (negative control).

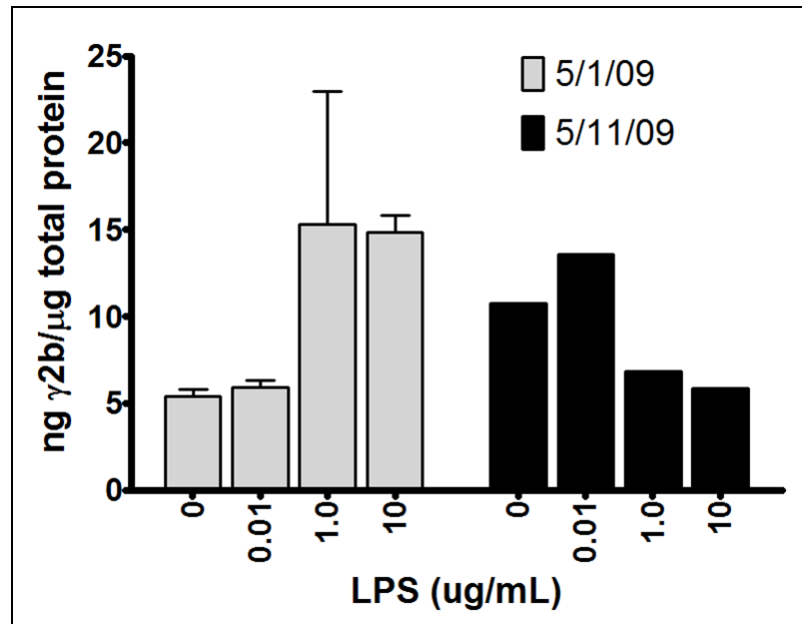


**Figure 22 LPS Does not Induce D1 Deletion Derivative to Express  $\gamma 2b$ :** D1 cells were a GFP-expressing isolate which initially appeared in PCR tests to have the hs3a and hs1,2 enhancers deleted. They were tested twice for LPS-induced  $\gamma 2b$  expression by ELISA. The data from 5/1/09 represents the mean and standard deviation of duplicate samples at each concentration of LPS. There is no significant difference between treatments. The data from 5/11/09 represents a single sample at each concentration, and there is no increase in  $\gamma 2b$  expression with increasing concentrations of LPS. Subsequent PCR tests proved that D1 was a mixed population of cells: some with an uncut  $\gamma 2b$  transgene and some with the hs3a and hs1,2 enhancers deleted.

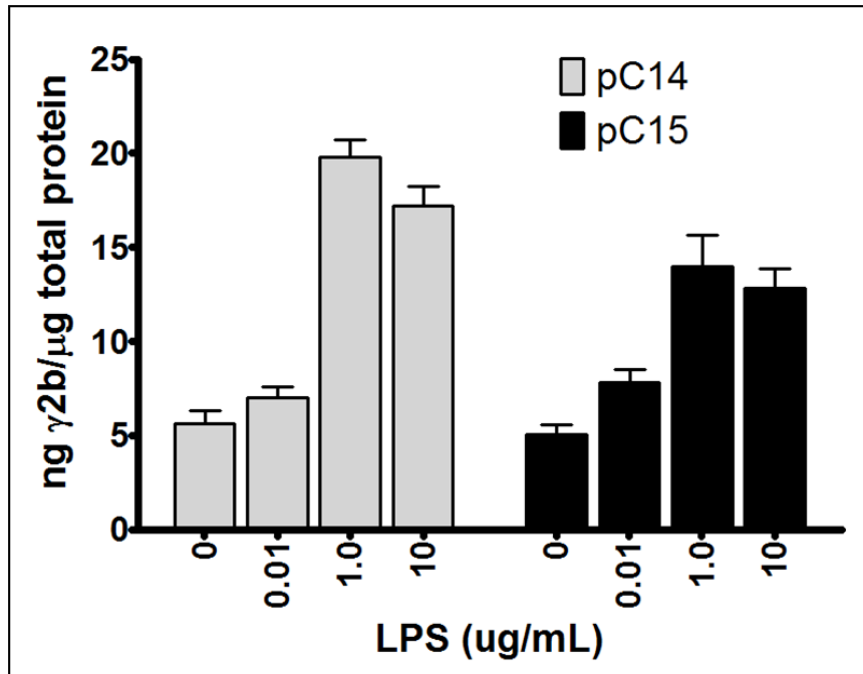


**Figure 23 LPS Induced  $\gamma$ 2b Expression in CH12.LX. $\gamma$ 2b-LoxPhs3a1,2-pC14 and -pC15 Cells:** These parental clones, transfected with the  $\gamma$ 2b transgene, were re-tested for activation by LPS in preparation for making additional Cre-recombinant derivatives.

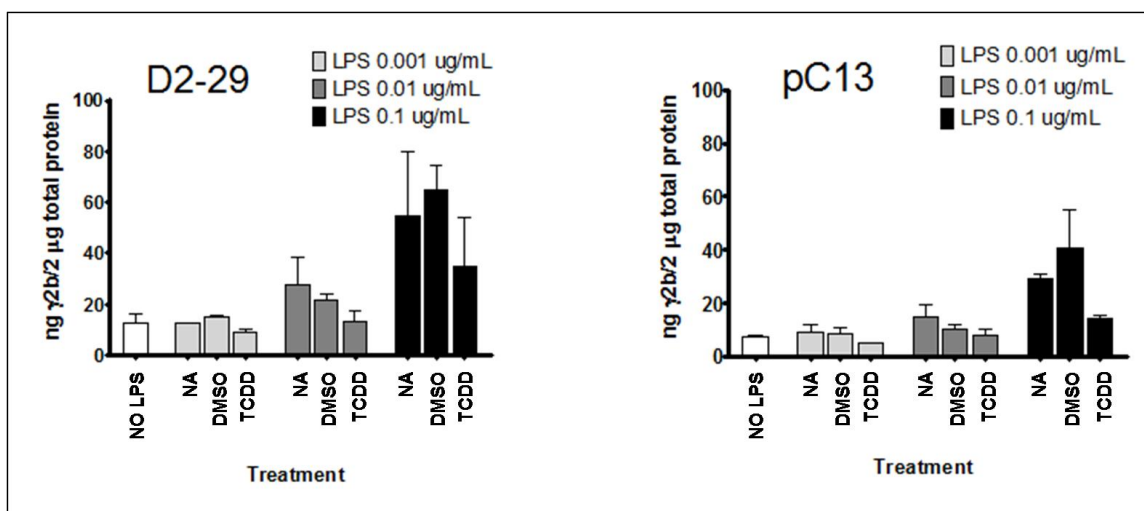


**Figure 24 First Study of the Effect of LPS and TCDD on Deletion Derivative D2-29 and Its Parental pC13:** Confirmed deletion derivative D2-29 and its parental pC13 were treated with different concentrations of LPS alone or with vehicle (0.01% DMSO) or TCDD (10 nM). Expression of  $\gamma$ 2b was measured by ELISA using 2  $\mu$ g total protein per well. “NO LPS” refers to unstimulated cells. “NA” cells were stimulated by the concentration of LPS indicated but not treated with vehicle or TCDD. Duplicate treatments are represented here by their mean and standard deviation. LPS only induced a significant increase in  $\gamma$ 2b at 0.1  $\mu$ g/mL LPS in D2-29 cells, and the apparent decreases in  $\gamma$ 2b at 0.01 and 0.1  $\mu$ g/mL LPS after TCDD treatment were not statistically significant ( $\alpha=0.10$ ). pC13 cells were similar to D2-29 in that LPS induced a significant increase in  $\gamma$ 2b only at 0.1  $\mu$ g/mL, but in pC13 cells, the decrease in  $\gamma$ 2b after TCDD treatment is significant ( $\alpha=0.05$ ).

Several deletion derivatives from the second limiting dilution (separating mixed populations of cut and uncut derivatives) were found not to express  $\gamma$ 2b after LPS-activation: no  $\gamma$ 2b protein was found even after loading 5 times (5  $\mu$ g) the total protein normally used in the ELISA. (data not shown). The deletion derivative D2-29 was then tested for transgene induction at 3 concentrations of LPS and for inhibition by 10 nM TCDD, using its parent, pC13, as a control. The results are shown in Figure 24. I observed previously that the  $\gamma$ 2b response reached a plateau in response to LPS at 1

$\mu\text{g/mL}$ , so in order to preserve the lot of LPS that I was using, I used the LPS concentrations of 0.001, 0.01, and 0.1  $\mu\text{g/mL}$ . Each treatment was done in triplicate, but there was high variability in the total protein determination for the first sample in most treatments, so any sample greater than 15% CV in total protein determination was removed from the final ELISA results. For both pC13 and D2-29, the only significant increase in  $\gamma 2\text{b}$  expression was at the highest concentration of LPS (0.1  $\mu\text{g/mL}$ ). In addition, only at that concentration, TCDD caused a significant decrease in  $\gamma 2\text{b}$  expression for both pC13 and D2-29. The LPS concentration response of D2-29 and pC13 with 10 nM TCDD was repeated with similar results. Figure 25 shows that  $\gamma 2\text{b}$  expression by D2-29 is significantly inhibited by TCDD when activated by 0.01 and 0.1  $\mu\text{g/mL}$  LPS. Even at 0.001  $\mu\text{g/mL}$  LPS, where  $\gamma 2\text{b}$  expression is not significantly greater than basal (0.0  $\mu\text{g/mL}$ ), it is significantly less in the 10 nM TCDD treatment than its vehicle control. The pC13 cells had a lower than usual level of  $\gamma 2\text{b}$  expression after LPS treatment, and TCDD only inhibited  $\gamma 2\text{b}$  expression significantly at the highest concentration of LPS, which is also the only concentration at which  $\gamma 2\text{b}$  expression was significantly greater than basal. There was less variability in the total protein analysis for the repeat experiment, and a second protein determination conducted after diluting the samples to the concentration used in the ELISA revealed that the D2-29 samples were consistently just under the 2  $\mu\text{g}$  total-protein target while the pC13 samples were consistently just over the 2  $\mu\text{g}$  target.

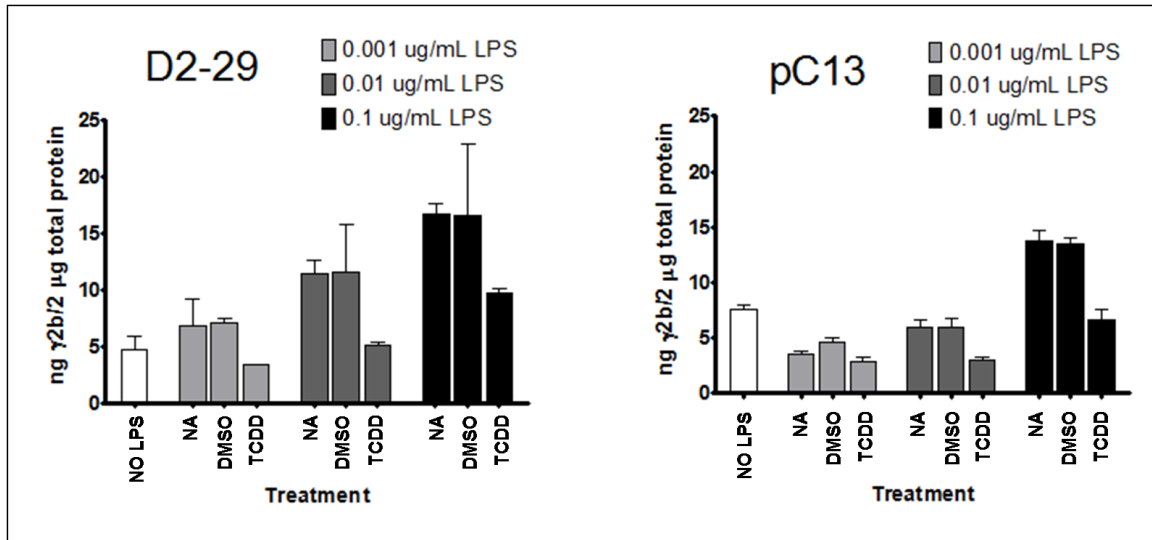


**Figure 25 Second Study of the Effect of LPS and TCDD on Deletion Derivative D2-29 and Its Parental pC13:** Confirmed deletion derivative D2-29 and its parental pC13 were treated with different concentrations of LPS alone or with vehicle (0.01% DMSO) or TCDD (10 nM). Expression of  $\gamma$ 2b was measured by ELISA using 2  $\mu$ g total protein per well. “NO LPS” refers to unstimulated cells. “NA” cells were stimulated by the concentration of LPS indicated but not treated with vehicle or TCDD. Duplicate treatments are represented here by their mean and standard deviation. With 95% confidence ( $\alpha=0.05$ ),  $\gamma$ 2b in the pC13 cells only increases significantly over basal expression at 0.1  $\mu$ g/mL LPS, while in the D2-29 cells  $\gamma$ 2b is significantly increased at 0.01 and 0.1  $\mu$ g/mL LPS. In this study, TCDD caused a significant decrease in  $\gamma$ 2b at 0.1  $\mu$ g/mL LPS in both the pC13 parents and the D2-29 deletion derivatives. In the D2-29 cells,  $\gamma$ 2b is also significantly inhibited by TCDD at 0.01  $\mu$ g/mL TCDD.

I hoped to see a synergistic increase in  $\gamma$ 2b expression in the D2-29 clone, similar to that which was seen previously in transient transfection studies, but the transgene in my first deletion derivative (D2-29) appeared to be inhibited by TCDD, so I conducted a screen of all the deletion derivatives in which each was either untreated, treated with 1  $\mu$ g/mL LPS, or treated with 10 nM TCDD and 1  $\mu$ g/mL LPS. My hope was to identify several clones with a cut  $\gamma$ 2b transgene which was further stimulated by TCDD. Each

treatment was conducted in duplicate with plans to further characterize any cells that screened positive for activation with TCDD. The 20 isolates of deletion derivatives were all treated on the same day and analyzed by ELISA in 4 plates over 2 days. The isolates were expected to represent up to 5 different deletion derivative cell lines: D16 was represented by 10 isolates; D19 by one isolate; D3 by 4 isolates; D5 by 3 isolates; and D1 was represented by two isolates. Since each set of isolates had a cut  $\gamma$ 2b transgene and was obtained by limiting dilution of a single mixed population (from mixed populations D16, D19, D3, D5, or D1), those derived from the same mixed population but confirmed to have a cut transgene were likely to be identical clones, so I expected them to respond similarly (each identical clone being affected similarly). That proved true for 3 of the 5 deletion derivative clones. None of the isolates from D16 expressed  $\gamma$ 2b. Deletion of the hs3b and hs4 enhancers from the  $\gamma$ 2b-LoxPhs3b4 transgene also produced many clonal isolates that no longer expressed  $\gamma$ 2b (Fernando, personal communication), so it was no surprise to find a deletion derivative that did not express  $\gamma$ 2b. The single isolate from D19 and the 3 isolates from D5 also did not express  $\gamma$ 2b. Surprisingly, one of the two isolates from D1 did not express  $\gamma$ 2b, nor did one out of the 4 isolates from D3. D1-11 which expressed  $\gamma$ 2b increased expression by 4 fold when treated with LPS, and was significantly inhibited by TCDD (Figure 26). Of the 3 isolates from D3 which expressed  $\gamma$ 2b, D3-4 and D3-9 responded similarly with about a 2 fold increase in expression after LPS treatment and not a significant change when TCDD was added (Figure 26). D3-16 had a 4 fold increase in expression with LPS and not a significant change when TCDD was added. Expression of  $\gamma$ 2b in pC13, the parental cells tested on the same day, was significantly inhibited by TCDD (Figure 26).

No deletion derivative was found to have a synergistic increase in  $\gamma$ 2b expression with LPS and TCDD, but one deletion derivative, with at least 2 differently responding subtypes, does not appear to be significantly inhibited by TCDD under these treatment conditions.

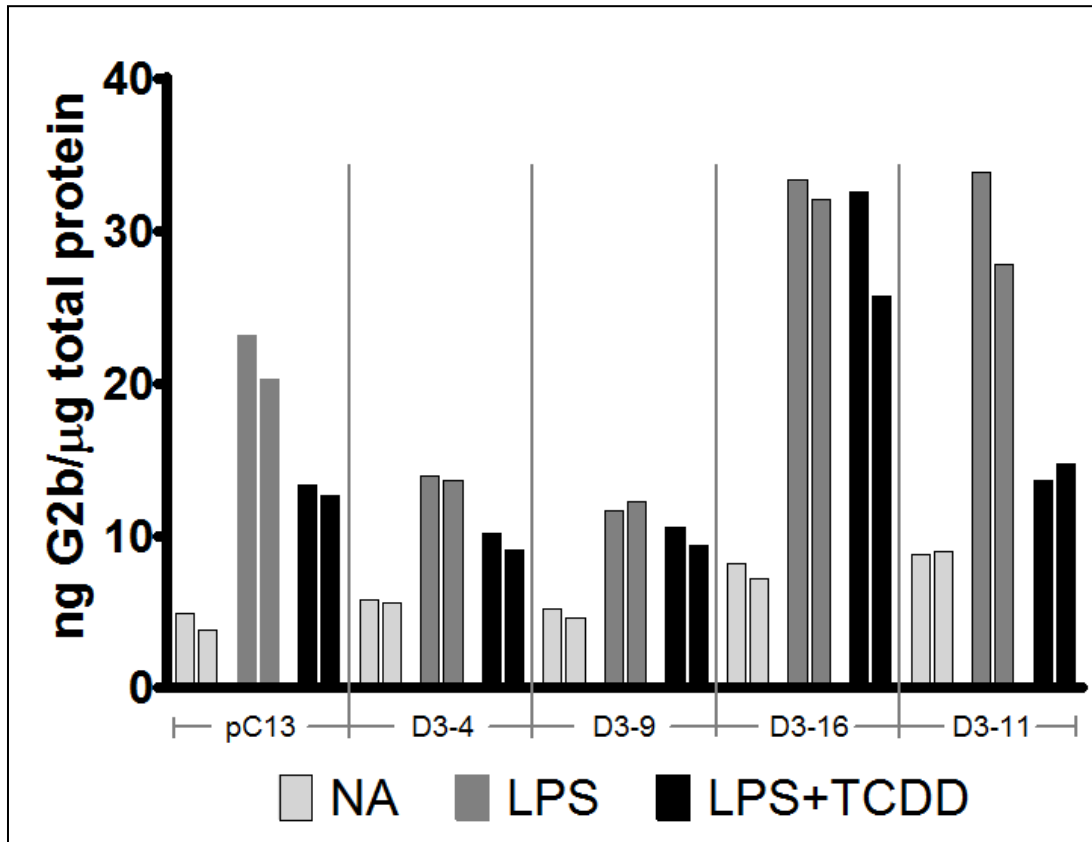


**Figure 26 The Effect of LPS and TCDD on Various Deletion Derivatives and Their Parental**

**pC13:** 20 isolates of confirmed deletion derivatives and their parental pC13 were either untreated, treated with LPS alone or with 10 nM TCDD. Expression of  $\gamma$ 2b was measured by ELISA using 2  $\mu$ g total protein per well. Only 4 of the 20 isolates tested expressed  $\gamma$ 2b: 3 came from the same proposed deletion derivative (D3) and one came from another (D1). There was also one isolate from D3 and one from D1 which did not express  $\gamma$ 2b. In this figure duplicate measurements are presented side by side instead of presenting them as a mean and standard deviation. Expression of  $\gamma$ 2b in all of the deletion derivative isolates and pC13 increased significantly after LPS treatment but only pC13 and D1-11 were significantly inhibited by TCDD ( $\alpha=0.05$ ).

The second specific aim proposing a qualitative shift in the binding of NF $\kappa$ B/Rel proteins to the hs4 and hs1,2 enhancers after TCDD exposure was addressed using the Electrophoretic Mobility Shift Assay (EMSA). This study began with optimization of binding conditions for the hs4 probe in an attempt to replicate published results (Sulentic, et al., 2000) with the addition of stimulation by LPS, which was not tested previously. My first EMSA (Figure 27) used nuclear protein from CH12.LX cells treated with 10 nM TCDD. Poly[d(I-C)] concentrations were 0.5, 1, and 2  $\mu$ g and the KCl was meant to vary between 90 and 110 mM, but a miscalculation resulted in concentrations ranging from 129 to 165 mM. In addition, because of the method used to put together the binding reaction and dilute the proteins, the HEPES and EDTA concentrations varied between groups of samples from 15 to 20 mM HEPES and 0.6 to 0.8 mM EDTA. The glycerol percentage also varied between samples. This experiment did show that proteins will bind the hs4 probe under diverse and less than optimal conditions.

The mistakes were not realized until later, so my next two experiments also had incorrect salt, HEPES, EDTA, and glycerol concentrations (Figure 28). In addition, the phosphoimager plates were causing lines and varying densities of response within the gels which eventually caused me to change to autoradiography film. Although a light spot on the imaging plate interfered with the results, a time course for the binding reaction suggested that there was not much difference in binding between 15, 30, 45 and 60 minute incubation times (Figure 28, right gel, right end of gel), so subsequent binding reactions were incubated between 30 and 45 minutes.

The calculation mistakes were corrected and the method for making the binding reaction improved by making a reaction mix with the HED, glycerol, DTT, poly[d(I-C)],

and HEDK, so that each diluted protein got the intended reagent concentrations (10 mM HEPES, 1 mM EDTA, variable KCl). Figure 29 shows the first optimization-EMSA with correct reagent concentrations. It also shows that binding appeared to increase when cells were treated with TCDD or LPS and decrease approximately back to baseline (NA) when cells were treated with both TCDD and LPS. Those differences between treatments are most apparent at 90 mM KCl.

Published work with the hs4 enhancer (Sulentic, et al., 2000) suggested that the band caused by AhR binding and the band caused by NF $\kappa$ B/Rel binding should be somewhat distinguishable from each other. Since two bands were not distinguishable in my results, I added conditions to try and tease apart those bands while continuing to optimize binding conditions. Figure 30, left gel, shows a study optimizing poly[d(I-C)] concentration while also adding excess unlabeled DRE3 probe to bind up AhR and see if the binding pattern changed. Antibodies to AhR or p65 or p50 were also added to some reactions to try and change the migration of bands (supershift) corresponding to those proteins. I chose 90 mM KCl for this experiment because of a clear difference in binding between treatments in the previous experiment at 90 mM KCl (Figure 29) and the lack of a vehicle effect at 90 mM that is apparent at 100 and 110 mM KCl. In this experiment, the proteins from vehicle treated cells have a more intense band than NA cells (Figure 30, left gel), suggesting a vehicle effect at 90 mM KCl that was not apparent in the previous experiment. DRE3 unlabeled competitor seemed to affect band intensity only slightly, suggesting that there may be some DRE binding, but its band was not discernable from overlapping bands. The antibodies did not appear to supershift any bands, suggesting that either those proteins were not binding, or that conditions needed to be optimized to see a

supershift. There was also no apparent difference between poly[d(I-C)] concentrations, so I chose 1 µg/mL for most subsequent studies to replicate the published data. Interestingly, the gel on the right in Figure 30 which did not have unlabeled competitors or antibodies to differentiate the binding of multiple proteins, appears to have two distinguishable bands. Also note that this experiment involved an altered hs4 probe: the top strand had additional nucleotides (GAT) on its 5-prime end to create an overhang of unmatched nucleotides. Use of overhangs had been recommended to the lab for improved labeling efficiency. Two additional experiments were conducted with this “overhang” probe in which electrophoresis ran longer and the gels were unreadable (not shown), likely due to increased resistance in the ion-depleted buffer which generated heat in the gel. Thereafter, the buffer in the upper reservoir was periodically replaced with fresh buffer. In published literature, overhangs are used to label probes by filling them with radio-labeled dNTP using Klenow enzyme (Liao, et al., 1992; Singh, et al., 1993; Sovak, et al., 1997; Tian, et al., 1999; Urban, et al., 1990; Grant, et al., 1992; Kretzschmar, et al., 1992; Davarinos, et al., 1999; Ruby, et al., 2002; Lin, et al., 1992; Woo, et al., 2002) and I was concerned about proteins sticking non-specifically to the unfilled overhangs on our probe, so I discontinued use of the hs4 overhang probe. One additional change was that glycerol was removed from the binding reaction. Since I had been using a loading dye to transfer samples from the reaction tubes to the gel, I did not need glycerol in the reaction itself.

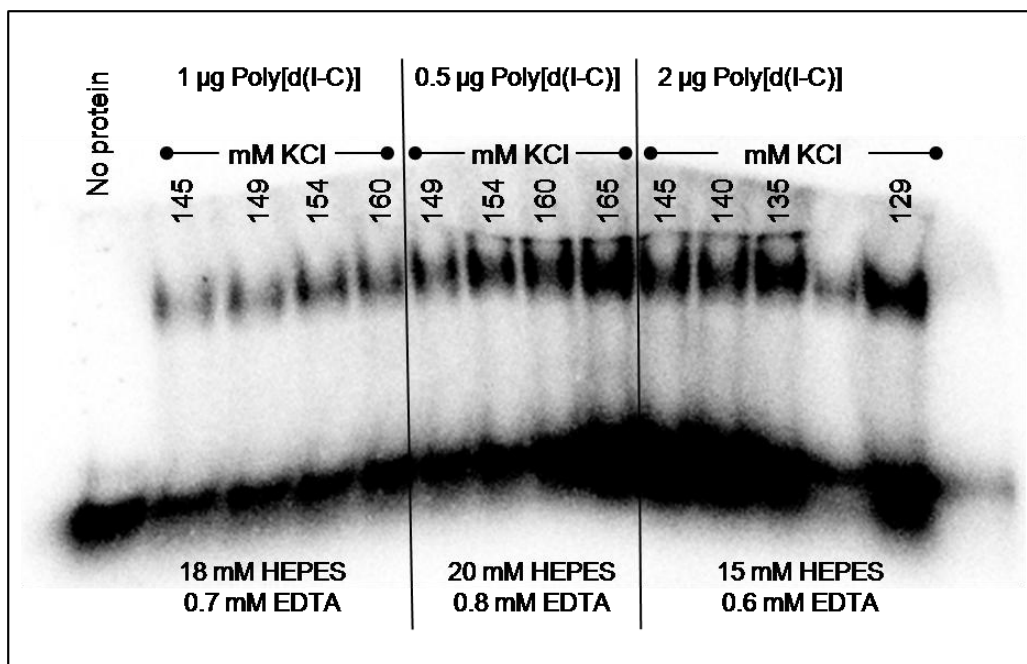


**Figure 27 Initial EMSA Optimization with Variable Reagent Concentrations:** Due to miscalculation and the method by which the binding reaction was put together, this initial EMSA had too much reagent variability; however, this shows that under diverse conditions, proteins will still bind the probe. Nuclear proteins from TCDD treated CH12.LX cells were collected by the homogenizer method. Reaction products were separated on a 4% polyacrylamide gel and documented on a FujiFilm FLA5100.

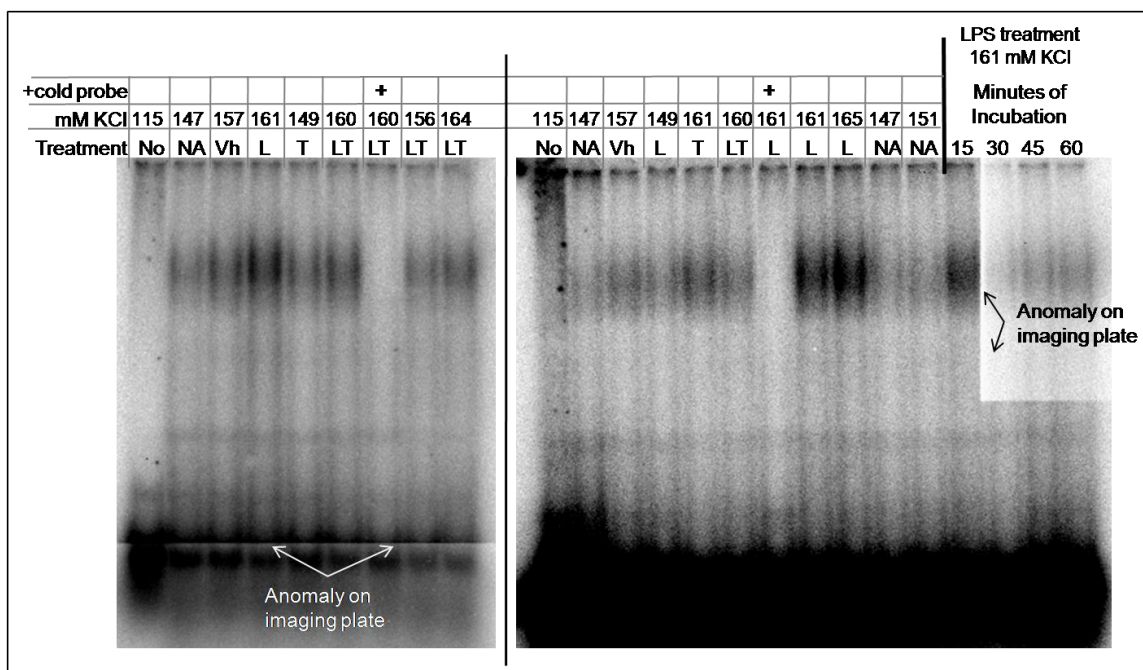


**Figure 28 Initial EMSA Optimization Showing Variable Reagent Concentrations and Imager Anomalies:** Miscalculation and method development issues caused reagent variability in these EMSA results. Nuclear proteins were collected from CH12.LX cells by the homogenizer method after no treatment (NA), treatment with vehicle (Vh), 1  $\mu\text{g}/\text{mL}$  LPS (L), 10 nM TCDD (T), or with both LPS and TCDD (LT). “No” indicates there was no protein added to that binding reaction. Reaction products were separated on 4% polyacrylamide gels and documented on a FujiFilm FLA5100. Note the lines and variable image density which continued to be a problem with the phosphoimaging plates, leading to an eventual change to autoradiography film.

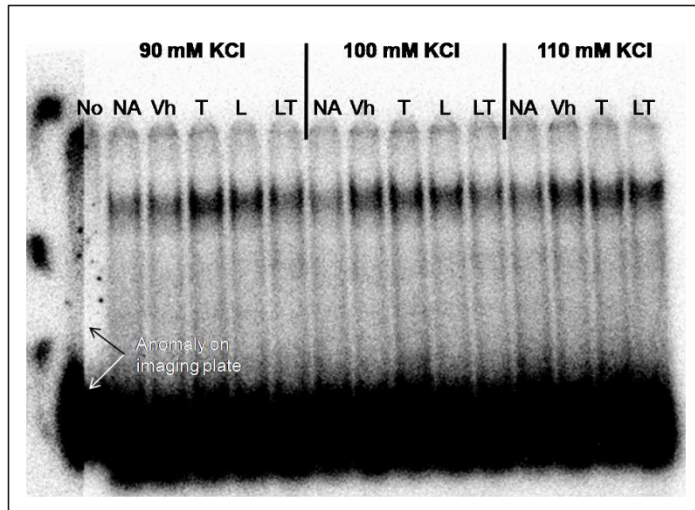


**Figure 29 Optimization of the EMSA for the hs4 probe:** Nuclear proteins from CH12.LX cells were collected by the homogenizer method after no treatment (NA) or treatment with vehicle (Vh), 10 nM TCDD, 1  $\mu$ g/mL TCDD, or LPS and TCDD (LT). They were incubated with the hs4 probe in 25mM HEPES, 1 mM EDTA, 1 mM DTT, 10% glycerol, and either 90, 100, or 110 mM KCl. “No” indicates no protein was added to the binding reaction. Reaction products were separated on a 4% polyacrylamide gel and documented on a FujiFilm FLA5100.

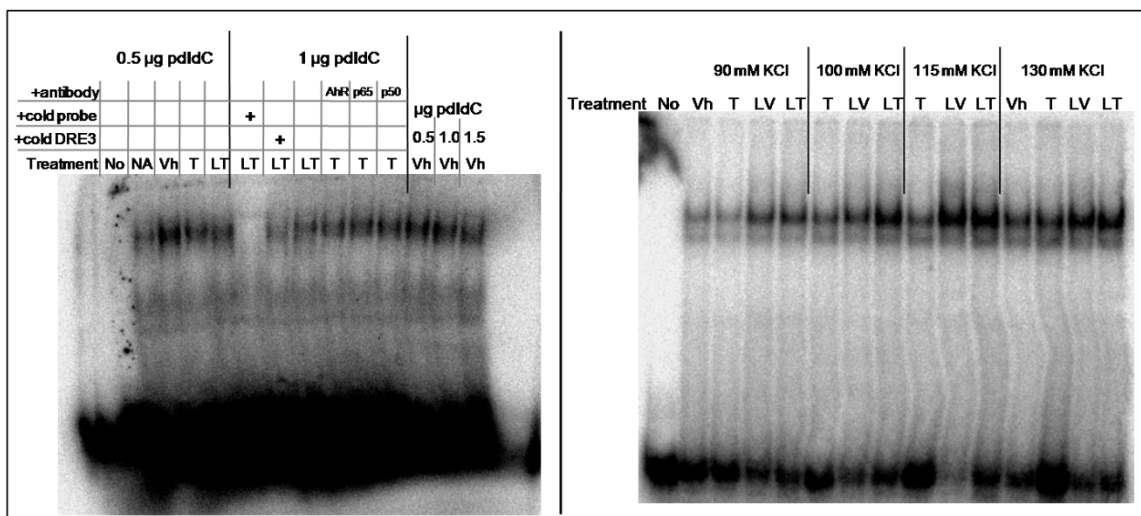


**Figure 30 Optimization and Characterization of the hs4 Probe with an Overhang:** The probe use in these experiments had an “overhang” of unpaired nucleotides. Nuclear protein was isolated from CH12.LX cells by the homogenizer method after no treatment (NA) or treatment with vehicle (Vh), 10 nM TCDD, 1  $\mu$ g/mL LPS and vehicle, or 1  $\mu$ g/mL LPS and 10 nM TCDD. “No” indicates that no protein was added to the binding reaction. The proteins were incubated with the overhung hs4 probe in 10 mM HEPES, 1 mM EDTA, 1 mM DTT, variable amounts of poly[d(I-C)], and variable concentrations of KCl. Where indicated, unlabeled probes were added as binding competitors or antibodies were added for a supershift. Reaction products were separated on a 4% polyacrylamide gel and documented on a FujiFilm FLA5100.

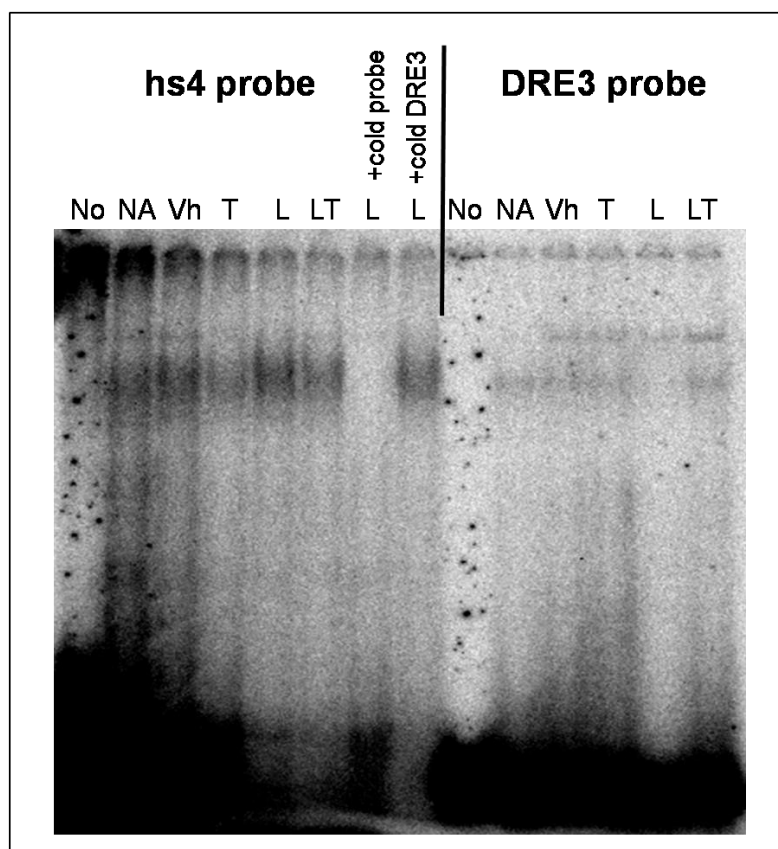


**Figure 31 EMSA with hs4 and DRE3 probes:** Nuclear proteins from CH12.LX were collected by the homogenizer method after no treatment (NA) or treatment with vehicle (Vh), 10 nM TCDD (T), 1  $\mu\text{g}/\text{mL}$  LPS (L), or LPS and TCDD (LT). “No” indicates that no protein was added to the binding reaction. Proteins were incubated with the hs4 probe or DRE3 probe in 10 mM HEPES, 1 mM EDTA, 1 mM DTT, 1  $\mu\text{g}/\text{mL}$  poly[d(I-C)], and 90 mM KCl. Where indicated, unlabeled probe was added as a binding competitor. Reaction products were separated on a 4% polyacrylamide gel and documented on a FujiFilm FLA5100.

I next labeled the DRE3 probe, hoping to confirm that the protein samples did have AhR, since only the AhR protein (and binding partner) should bind to the DRE3 probe. Figure 31 shows that nuclear proteins bound the DRE3 probe form two differently migrating bands. The upper band was missing for the untreated cells but present for cells treated with vehicle, TCDD, LPS, or LPS and TCDD. TCDD and LPS are both known to

stimulate AhR expression(Sulentic, et al., 1998; Marcus, et al., 1998; Sulentic, et al., 2000), so the upper band appeared to correspond to AhR binding; however, that same band appears in most of the samples across the gel including the proteins from untreated (NA) cells bound to the hs4 probe. The band's intensity does seem reduced when unlabeled DRE3 is present with the hs4 probe, but not when the unlabeled hs4 probe is the competitor, which is suggestive of non-specific binding or differing affinity of the binding complex for DRE sites. The faster migrating band in this gel acts similar to previous experiments with the hs4 probe, but its appearance with the DRE3 probe is different: not as wide, nor as dense, nor as predictable of a pattern.

I decided to change to autoradiography film and use a higher concentration of KCl (130 mM) hoping that more total binding at the higher KCl concentrations would allow easier teasing out of AhR binding. In Figure 32, I used the hs4 and DRE3 labeled probes in combination with unlabeled hs4, DRE3, DRE4, or  $\kappa$ B (huhs1,2kb – see Table 1- was used because I did not have the consensus  $\kappa$ B probe yet) to discern which proteins correspond to different bands or areas within a band. I used proteins from cells exposed to 1  $\mu$ g/mL LPS and 10 nM TCDD (LT), in which I expected to have both NF $\kappa$ B/Rel and AhR proteins in high concentration, and cells exposed to 1  $\mu$ g/mL LPS and vehicle (LV) because I wanted to see what proteins were binding in the apparent vehicle effect.

I included the hs4s probe as an unlabeled competitor because its 5-prime end starts at the  $\kappa$ B site and I wondered if that might alter the  $\kappa$ B binding of that probe. There was no difference in results between the LT and LV samples for the hs4 probe. When unlabeled hs4 or hs4s probe was included, proteins did not bind the labeled probe, so the bands

were likely caused by specific binding. When the DRE3 or DRE4 unlabeled probes were used as competitors, there was no change in the bands from hs4 probe without unlabeled competitor. When the  $\kappa$ B unlabeled probe was used, the bands were eliminated, which indicated that the bands were likely caused by NF $\kappa$ B/Rel proteins. Interestingly, when a LV sample was incubated with DRE3 probe, no binding occurred, suggesting that the vehicle effect does not involve AhR protein; however, there is a bright residual band at the loading well for that lane which I am unable to explain. In summary, only probes with  $\kappa$ B binding sites appear to compete for binding of proteins with the hs4 probe, in these samples.

The published study which I was trying to reproduce and develop further, treated cells with 30 mM TCDD, so I increased my treatment concentration. I also tested 1 hour treatment versus 2 hour treatment. The results are shown in Figure 33. The hs4s probe had less binding than the hs4 and was not utilized after this study. While there was no clear difference for any sample between its binding of labeled probe and binding in the presence of unlabeled competitor with a DRE binding site, the binding was reduced for each sample when the unlabeled competitor had a  $\kappa$ B binding site. The labeled DRE3 probe was clearly bound by proteins from TCDD treated cells, indicating there is AhR in the sample which is available to bind a DRE site. Perhaps the NF $\kappa$ B/Rel binding was so great for these samples that the DRE binding was overwhelmed so that eliminating DRE binding through unlabeled competition did not impact band intensity. Furthermore, the hs4 probe has overlapping DRE and  $\kappa$ B binding sites. Competing out the DRE binding does not necessarily mean that less total probe is bound: it means that less probe is bound by AhR, which could leave room for more  $\kappa$ B binding.

I conducted an EMSA/Western to better identify the proteins and where their bands were migrating in the gel. In the published study(Sulentic, et al., 2000), the EMSA/Western showed that the AhR band migrated slightly slower than the NFκB band. In my first EMSA/Western (Figure 34) the EMSA gel was documented on autoradiography film but the Western blot was digitally documented on the FujiFilm LAS 3000 Image Reader, and that caused great problems in trying to match the image sizes and line up the loading wells. Assuming the line-up was correct, AhR appears to migrate close but slightly slower than RelA. AhR appears to increase binding with TCDD or LPS treatment more than with the combined treatment. RelA appears to only increase binding with TCDD treatment.

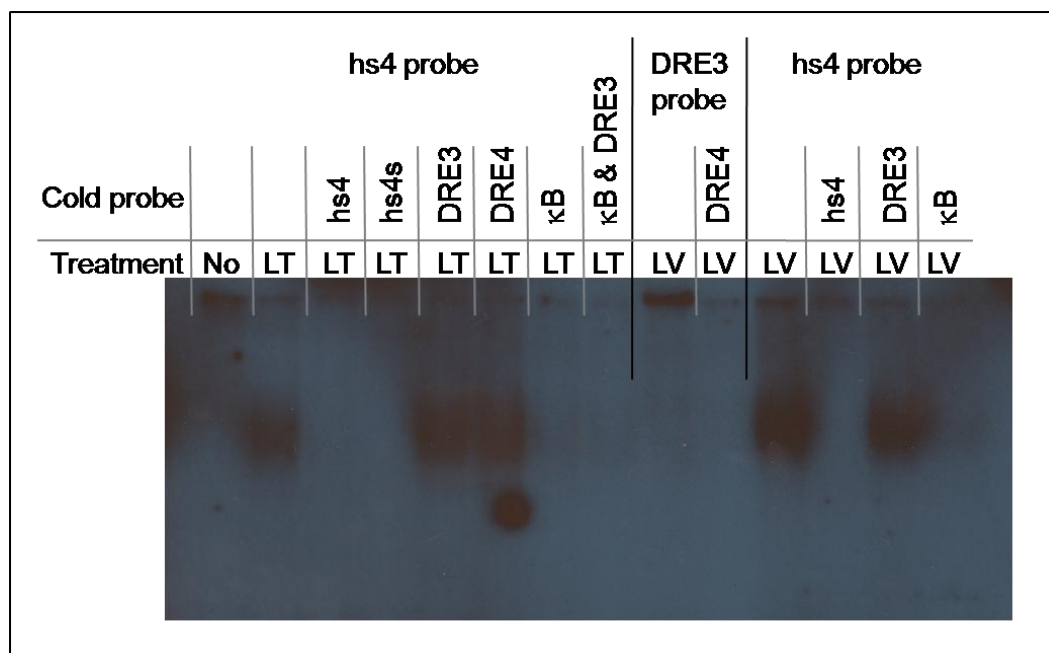


**Figure 32 EMSA with the hs4 and DRE3 Probes and Various Unlabeled Competitors:** Nuclear proteins from CH12.LX cells were collected by the homogenizer method after treatment with 1  $\mu\text{g}/\text{mL}$  LPS and 10 nM TCDD (LT) or 1  $\mu\text{g}/\text{mL}$  LPS and vehicle (LV). “No” indicates no protein was added to the binding reaction. Proteins were incubated with the hs4 probe or DRE3 probe in 10 mM HEPES, 1 mM EDTA, 1 mM DTT, 1  $\mu\text{g}/\text{mL}$  poly[d(I-C)], and 130 mM KCl. Where indicated unlabeled competitor probes were added. The unlabeled  $\kappa\text{B}$  probe was CEWS80+81, huhs1,2 $\kappa\text{B}$ . Reaction products were separated on a 4% polyacrylamide gel and documented on autoradiography film.

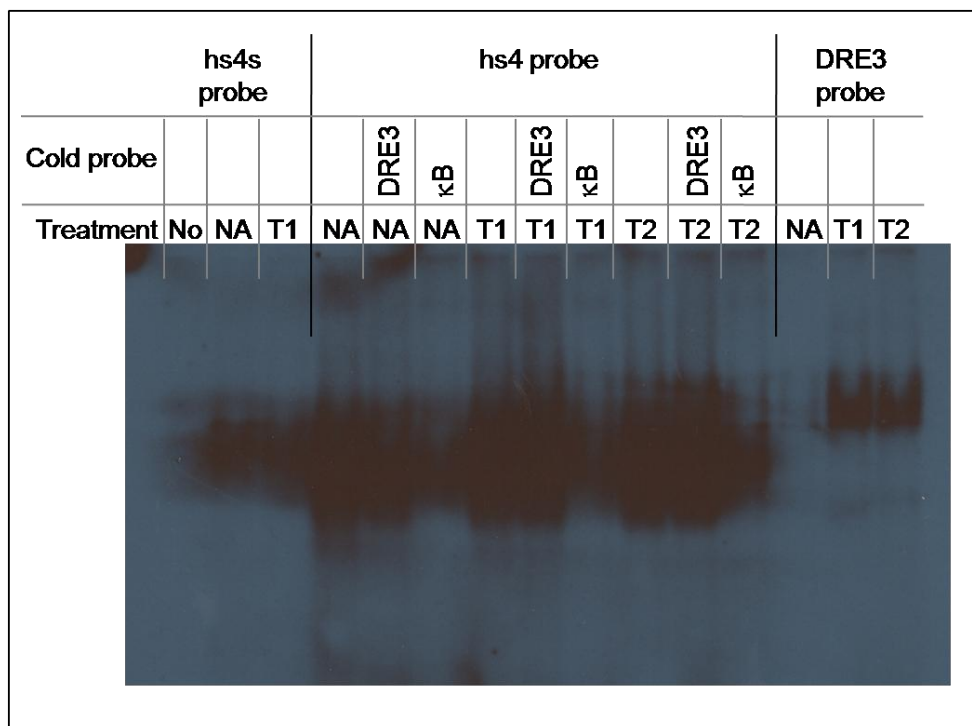


**Figure 33 EMSA with the hs4 and DRE3 Probes and Unlabeled Competitors at a 30 nM TCDD Treatment:** Nuclear proteins were collected from CH12.LX cells by the homogenizer method after no treatment (NA) or treatment with 30 nM TCDD for 1 hour (T1) or for 2 hours (T2). Proteins were incubated with the hs4, hs4s, or DRE3 probe in 10 mM HEPES, 1 mM EDTA, 1 mM DTT, 1 μg poly[d(I-C)], and 130 mM KCl. Where indicated, unlabeled DRE3 or κB (huhs1,2κB) probe was added. Reaction products were separated on a 4% polyacrylamide gel and documented on autoradiography film.

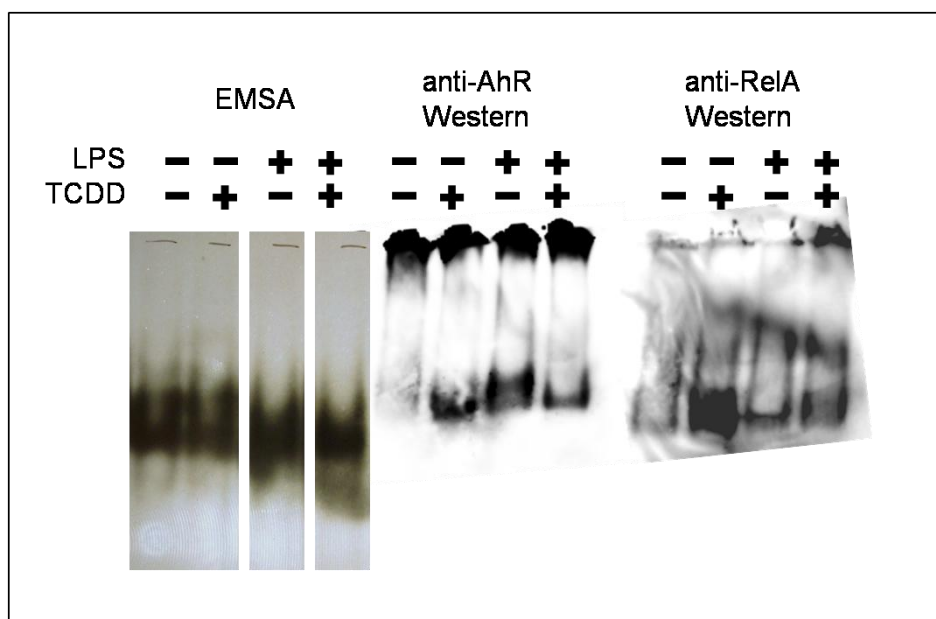


**Figure 34 EMSA/Western to Study the Binding of AhR and RelA:** Nuclear proteins from CH12.LX cells were collected by the homogenizer method after no treatment or treatment with 30 nM TCDD or 1  $\mu$ g/mL LPS or both LPS and TCDD. Proteins were incubated with the hs4 probe with or without radio-label, in 10 mM HEPES, 1mM EDTA, 1 mM DTT, 1  $\mu$ g poly[d(I-C)], and 130 mM KCl. Unlabeled competitors were used in the EMSA portion of this experiment but here the lanes were removed from the gel image (scanned autoradiography film) to simplify the picture. Reaction products were separated on a 4% polyacrylamide gel and documented on autoradiography film. The Western blot was accomplished with antibody to AhR or RelA (p65) after transfer of unlabeled, bound probe from the polyacrylamide gel to a PVDF membrane. The Western blots were documented on a FujiFilm LAS 3000 Image Reader .

I decided to increase the amount of polyacrylamide in my EMSA gels because molecules that are close in size are better separated in gels with smaller pore sizes. In addition, I started testing the hs1,2 probe to see if the same binding patterns would be found with that probe, whose  $\kappa$ B and DRE binding sites are further apart than the hs4. I thought that perhaps the NF $\kappa$ B/Rel proteins were out-competing AhR for binding to the overlapping sites on the hs4 probe, so that in the presence of a  $\kappa$ B unlabeled competitor, more AhR could bind but in the presence of a DRE unlabeled competitor, no change in

binding could be detected. Figure 35 shows two EMSA/Western experiments with duplicate reaction conditions whose products are separated on a 4% or 6% polyacrylamide gel. Although the autoradiography film may have been overexposed, it is still apparent that the bands were better defined on the 6% gel; however, only one band could be distinguished for the hs1,2 probe and one large banding area for the hs4. The gel to the right shows the Western blot results of this study which was documented on autoradiography film. There are spots that seem to correspond to AhR and to RelA at the same migration as the EMSA bands for 6% polyacrylamide and the hs4 probe, and possibly for the 4% gel with hs1,2 probe, but other spots do not match the migration of their EMSA counterpart, which causes doubt as to the identity of all the spots. Markings for the loading wells poorly transferred to the film, so lining up the Western gel image with the EMSA gel image was difficult. It was also difficult to label the Western gel during transfer to the membrane so that the order of wells was not inverted. In addition, because the sample volume was limited for this experiment, I had to use protein from LPS treated cells in the EMSA but from LPS and TCDD treated cells in the Western. Since my main purpose was to see the assay work and identify different migrations for the NF $\kappa$ B/Rel and AhR proteins, the differing samples were not a concern, but with limited success in the assay, interpretation became even more difficult with unmatched samples.

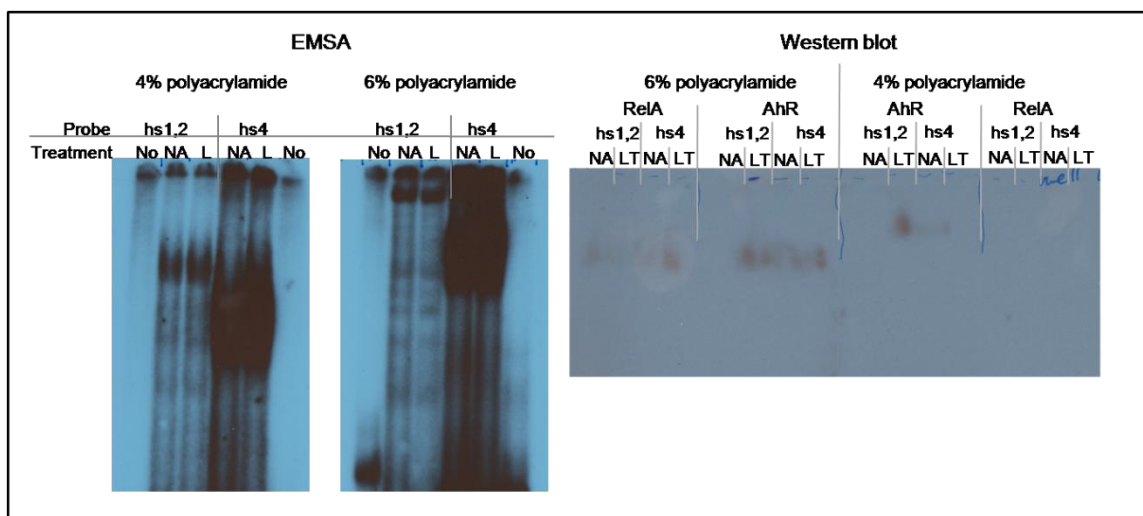


**Figure 35 EMSA/Western with 4% or 6% Polyacrylamide Gels:** Nuclear proteins from CH12.LX cells were collected by the homogenizer method after no treatment (NA) or treatment with 1  $\mu\text{g}/\text{mL}$  LPS (L) or with 1  $\mu\text{g}/\text{mL}$  LPS and 30nM TCDD. “No” indicates no protein was added to the binding reaction. Proteins were incubated with the hs4 probe or hs1,2 probe in 10 mM HEPES, 1 mM EDTA, 1 mM DTT, 1  $\mu\text{g}$  poly[d(I-C)], and 130 mM KCl (hs4 probe) or 106 mM KCl (hs1,2 probe). Reaction products were separated on either a 4% or 6% polyacrylamide gel and documented on autoradiography film. The Western blot was accomplished with antibody to AhR or RelA (p65) after transfer of unlabeled, bound probe from the polyacrylamide gel to a PVDF membrane. The Western blots were documented on autoradiography film.

Having somewhat mixed results, I wanted to increase my protein yield from each treatment so that multiple EMSA experiments could be run using the same protein batch, thus eliminating one possible source of variation. In the literature, some conduct nuclear protein extraction for EMSA using non-ionic detergent to lyse the cell membrane (Ruby, et al., 2002; Feng, et al., 2004; DiDonato, et al., 1995; Kistler, et al., 1998; Ruby, et al., 2002) and some use a homogenizer (Ashida, et al., 1998; Sulentic, et al., 2000) and some use both (Grumont, et al., 1999). Other graduate students in this laboratory indicated that their protein yield was much greater using a non-ionic detergent, so I developed a method similar to the homogenizer method I was using, but using the non-ionic detergent

IGEPAL CA630 to lyse cell membranes. In addition, some EMSA binding reactions in the literature contain non-ionic detergents (Fujita, et al., 1992; Grigoriadis, et al., 1996), so I was not concerned about carryover from the protein extraction affecting my EMSA results.

I also questioned my choice of 130 mM KCl, and conducted a study with the new protein extraction method comparing 100 and 130 mM KCl with the hs4 and DRE3 probes, adding DRE3 unlabeled competitor, and including the protein from treated primary splenocytes to see if there was any binding from those samples. I also wanted to check the difference between 10 and 30 nM TCDD treatments. Figure 36 shows the two gels from that experiment. In the 10 nM TCDD gel, the band representing bound probe is generally denser at 100 mM KCl than at 130 mM KCl; however, there is no difference between protein from cell treated with vehicle, TCDD, or LPS and TCDD. In the 30 nM TCDD gel, there is no obvious difference between 100 mM or 130 mM KCl. There is also no discernible difference between treatments. While it appears that at 100 mM, unlabeled DRE3 probe competed for binding of the hs4 probe, the wells of that gel were poorly formed and that sample may have combined with the splenocyte sample next to it. Likewise for well 12 of the 30 nM TCDD gel (130 mM KCl, DRE3 probe): it may have combined with some of the LT sample with hs4 probe next to it. The altered migration in that lane may be a reaction between the two different probes and protein samples. Consistent with previous studies, the DRE3 probe was bound in samples from cells treated with 30 nM TCDD but not with 10 nM TCDD. The only well in the 10 nM TCDD gel with DRE3 probe and no unlabeled competitor is at 130 mM KCl, because there was

not enough probe for the 100 mM KCl sample, but no proteins appear to bind the probe from cells treated with 10 nM TCDD under those conditions.

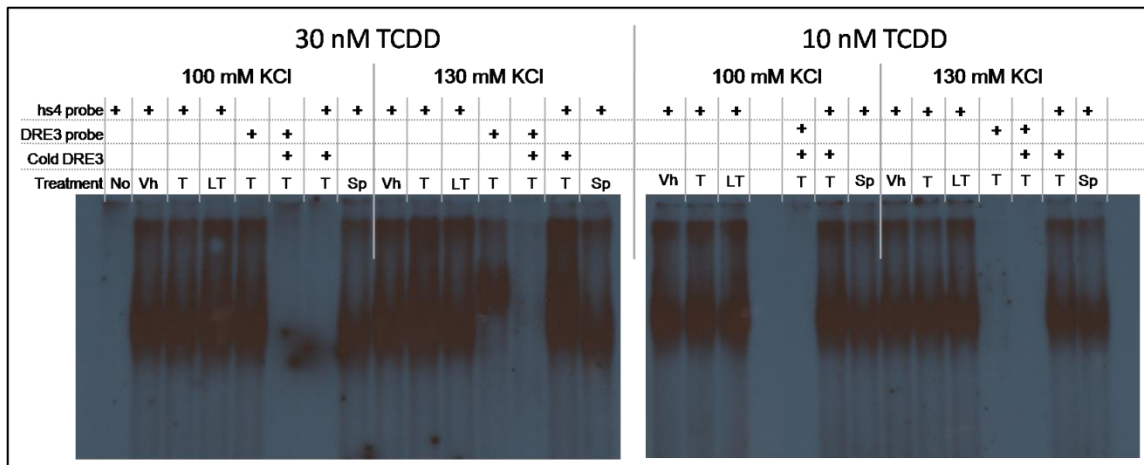


**Figure 36 EMSA Comparing 100 and 130 mM KCl and 10 and 30 nM TCDD with the hs4 and DRE3 Probes:** Nuclear proteins collected by the nonionic detergent method, from CH12.LX cells treated with vehicle (Vh) or TCDD (T) or 1 µg/mL LPS and TCDD (LT) or from mouse splenocytes treated with 30 nM TCDD (Sp) were incubated with hs4 or DRE3 probe in 10 mM HEPES, 1 mM EDTA, 1 mM DTT, 1 µg poly[d(I-C)], and 100 or 130 mM KCl. Reaction products were separated on a 4% polyacrylamide gel and documented on autoradiography film. “No” indicates no protein was added to the binding reaction.

I was still getting variability with the hs4 probe and still not able to replicate what had been published for that probe, so I chose to optimize conditions for the hs1,2 probe while deliberating options for the hs4. Discussions with other researchers helped me realize that I did not need to reduce the HEPES concentration in my samples from the protein extraction to the binding reaction, so I used 25 mM HEPES for subsequent reactions. I was also advised that DNA loading dyes might interfere with migration of my EMSA products, so I stopped using loading dye and starting adding 10% glycerol to the binding reaction. Figure 37 shows the optimization of KCl concentration for the hs1,2 probe along with the other new conditions just mentioned. At 175 mM, the bands and the

entire lane are darker than all the other samples. That sample may have received too much probe since the unbound probe appears more abundant at the bottom of the gel as well. Looking at the lower bands, I might have chosen 200 mM KCl as optimal because the bands are darkest and there is a clear difference between treatments. The upper band, though, is more likely the relevant band here because in the 30 nM TCDD lane, only the upper band remains visible. I did not employ an unlabeled-probe competitor lane to help distinguish between specific and non-specific bands this time because there was not room on the gel. I chose 100 mM KCl as optimal because the upper bands are darkest and lower bands are still visible. Protein from cells treated with 10 nM TCDD was used because there was more available, but the single lane with protein from 30 nM TCDD treated cells demonstrates that binding is clearly increased at that concentration.

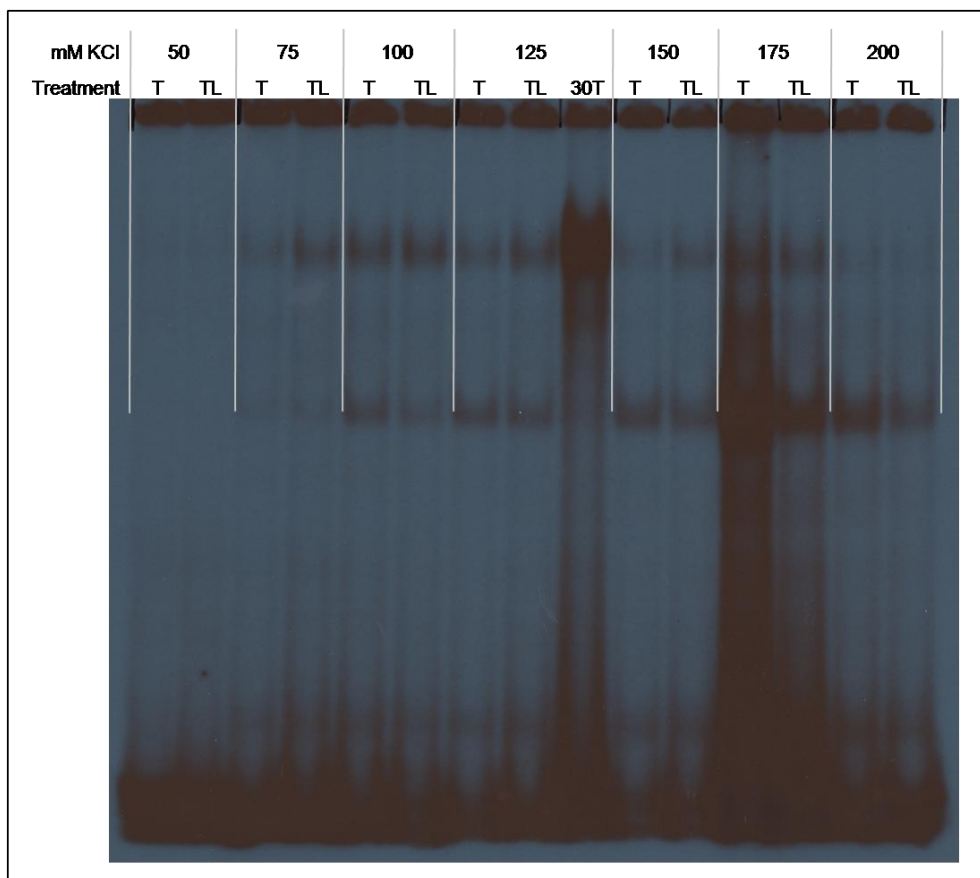


**Figure 37 Optimization of the KCl Concentration for EMSA of the hs1,2 Probe:** Nuclear protein was isolated from CH12.LX cells by the non-ionic detergent method after treatment with 10 nM (T) or 30 nM (30T) TCDD or 10 nM TCDD and 1  $\mu$ g/mL LPS. Proteins were incubated with the hs1,2 probe in 25 mM HEPES, 1 mM EDTA, 1 mM DTT, 1  $\mu$ g poly[d(I-C)], 10% glycerol and variable concentrations of KCl. Reaction products were separated on a 4% polyacrylamide gel and documented on autoradiography film.

Turning back to the hs4 probe, I studied the binding of proteins from cells exposed to other AhR ligands. Indolo(3,2,b)carbazole, Primaquine, Carbaryl, and Omeprazole are known to alter expression of a transient reporter regulated by the 3-prime enhancers (Henseler, et al., 2009), so I tested them in the EMSA to see if they affected binding of the hs4 probe in a different way than TCDD which would help me understand the EMSA binding profiles. The initial EMSA with these compounds showed the same

effect as TCDD: binding of the hs4 probe which was not reduced by a unlabeled competitor with a DRE site (data not shown). Figure 38 shows quite variable results, but in general, even when an unlabeled  $\kappa$ B competitor is present to inhibit binding of rel proteins to the probe, there is binding to the hs4 probe which is not eliminated by addition of unlabeled DRE competitor. Antibody for AhR seemed to cause a large increase in binding.

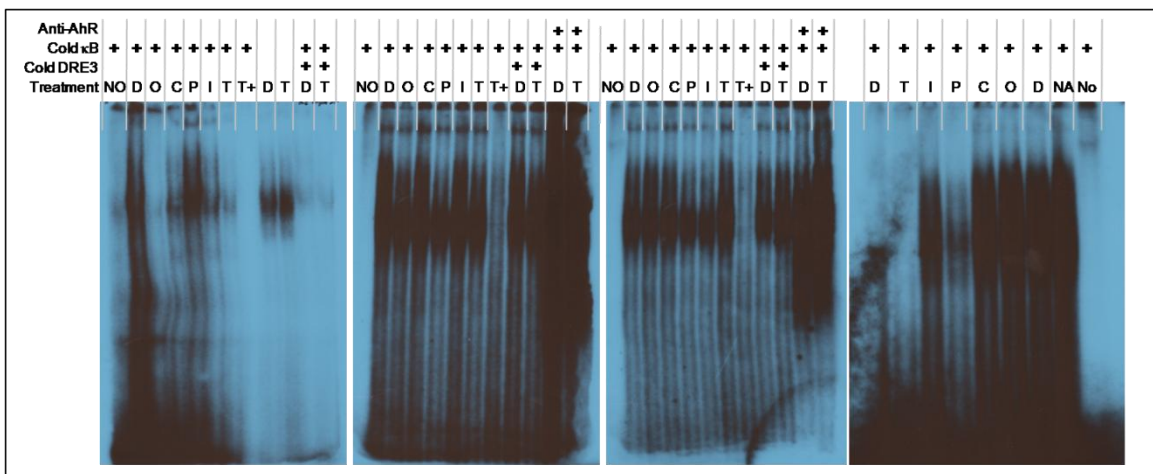


**Figure 38 EMSA with the hs4 Probe and Cells Treated with AhR Ligands:** Nuclear proteins were isolated by the non-ionic detergent technique from CH12.LX cells after treatment with DMSO vehicle (D), or Omeprazole (O), or Carbaryl (C), or Primaquine (P) or Indolo(3,2,b)carbazole (I) or TCDD (T). “No” indicates no protein was added to the binding reaction. “T+” indicates that the protein came from TCDD treated cells and unlabeled hs4 probe was added to the binding reaction. The proteins were incubated with the hs4 probe in 25 mM HEPES, 1 mM EDTA, 1 mM DTT, 1  $\mu$ g poly[d(I-C)], 10% glycerol, and 100 mM KCl. Unlabeled competitor probe or anti-AhR antibody was added where indicated. The unlabeled  $\kappa$ B competitor was the consensus  $\kappa$ B probe. Product was separated on a 4% polyacrylamide gel and documented on autoradiography film.

Hoping that reducing the total amount of binding would help me see the differences in binding between treatment groups, I conducted a study to see if increasing

the amount of poly[d(I-C)] would help reduce the total binding. Figure 39 shows the results of this experiment. For both the hs4 and hs1,2 probes, increasing the amount of poly[d(I-C)] caused a decrease in total binding and an apparent shift in band migration, although the bands may not actually shift, but simply become more visible as the large non-specific band close to it disappears. Moreover, at the highest amount of poly[d(I-C)], two bands were distinguishable for each probe, and the hs4 band looked more like the “shouldered” bands I was trying to reproduce from the publication. Clearly, using a greater amount of non-specific competitor would clarify my EMSA results.

In collaboration with another graduate student, and confident that I knew the optimal binding conditions for the hs1,2 probe, I turned my EMSA efforts toward the human hs1,2 probe sequences. Figure 40 shows an EMSA comparing the binding of proteins from untreated (NA) cells or cells treated with vehicle (Vh) or 30 nM TCDD (T) to the human and mouse hs1,2 probes. In this experiment, it appears that the mouse hs1,2 sequence was greatly bound in each treatment. The human hs1,2 sequence containing both a  $\kappa$ B and DRE site was bound greater with NA samples than with Vh or T samples, but less than when the probe only contained one or the other binding site. In fact, the greatest binding occurs when only the  $\kappa$ B site was present on the probe. Note that the “DRE only” and “ $\kappa$ B only” probes used in this experiment were half the length of the “DRE &  $\kappa$ B” probe. This is because the binding sites are sufficiently distant that simply cutting the “DRE &  $\kappa$ B” probe in half provided the single site probes. That difference in size may have contributed to the difference in binding between the double and single site probes. The figure also shows with the single-site probes that less AhR is bound than the NF $\kappa$ B/Rel proteins.

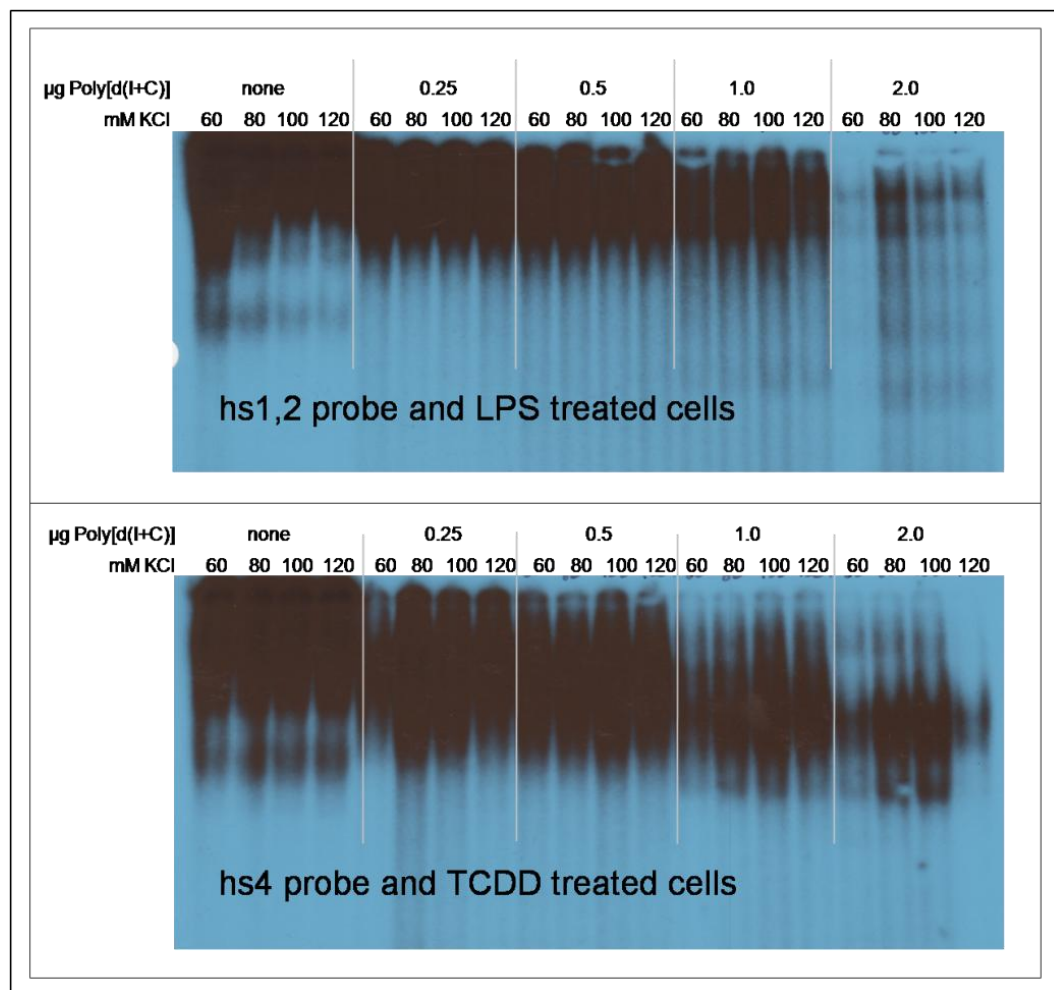


**Figure 39 Re-optimization of the hs4 and hs1,2 Probes:** Nuclear proteins were isolated by the non-ionic detergent technique from CH12.LX cells after treatment with 1 µg/mL LPS (for the hs1,2 probe) or 30 nM TCDD (for the hs4 probe) and incubated with either the hs4 or hs1,2 probe. The binding reaction was 25 mM HEPES, 1 mM EDTA, 1 mM DTT, 10% glycerol, and the poly[d(I+C)] and KCl concentrations varied as indicated. Reaction products were separated on a 6% polyacrylamide gel and documented on autoradiography film.

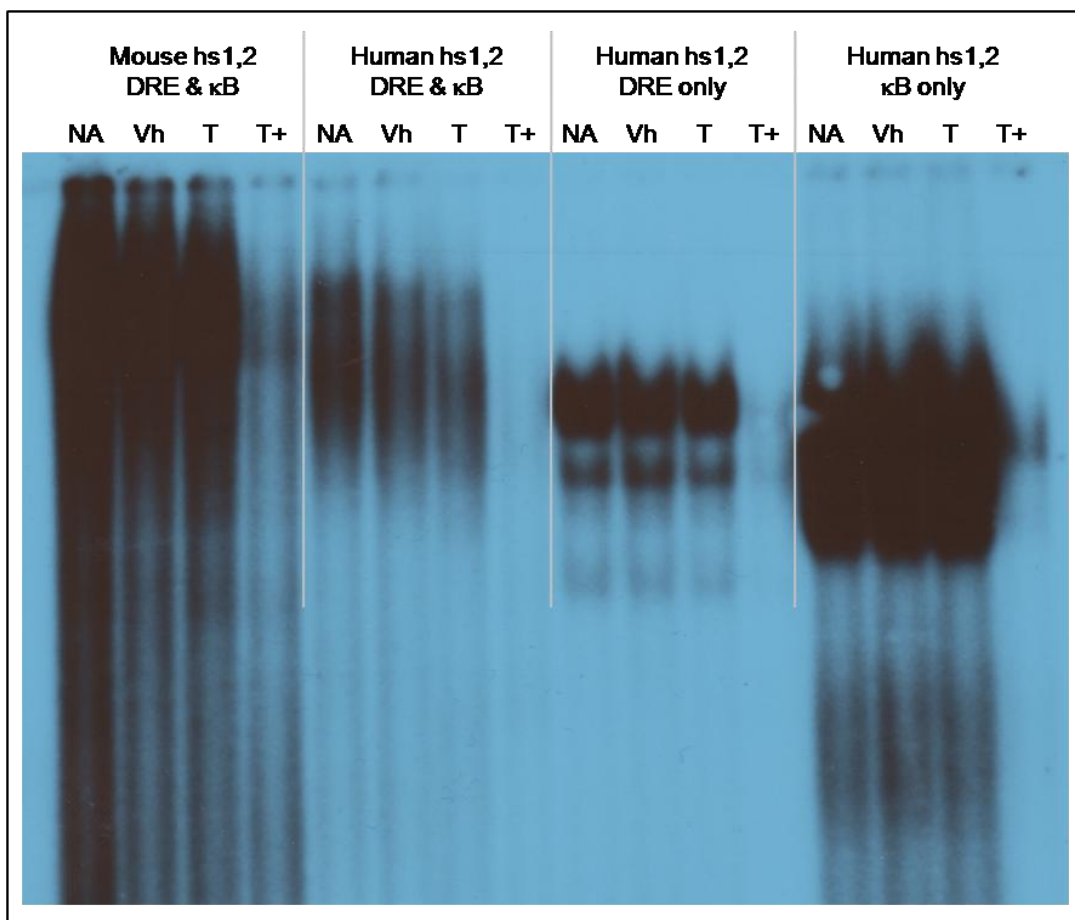


**Figure 40 EMSA with Mouse and Human hs1,2 Probes:** Nuclear proteins were isolated by the non-ionic detergent technique from CH12.LX cells after no treatment (NA) or after treatment with vehicle (Vh) or 30 nM TCDD (T) and incubated with one of the hs1,2 probes: the mouse hs1,2 has both a DRE and κB binding site; the human hs1,2 probes either have one or both binding sites. The binding reaction was 25 mM HEPES, 1 mM EDTA, 1 mM DTT, 10% glycerol, 2 μg poly[d(I+C)], 80 mM KCl. Reaction products were separated on a 5% polyacrylamide gel and documented on autoradiography film.

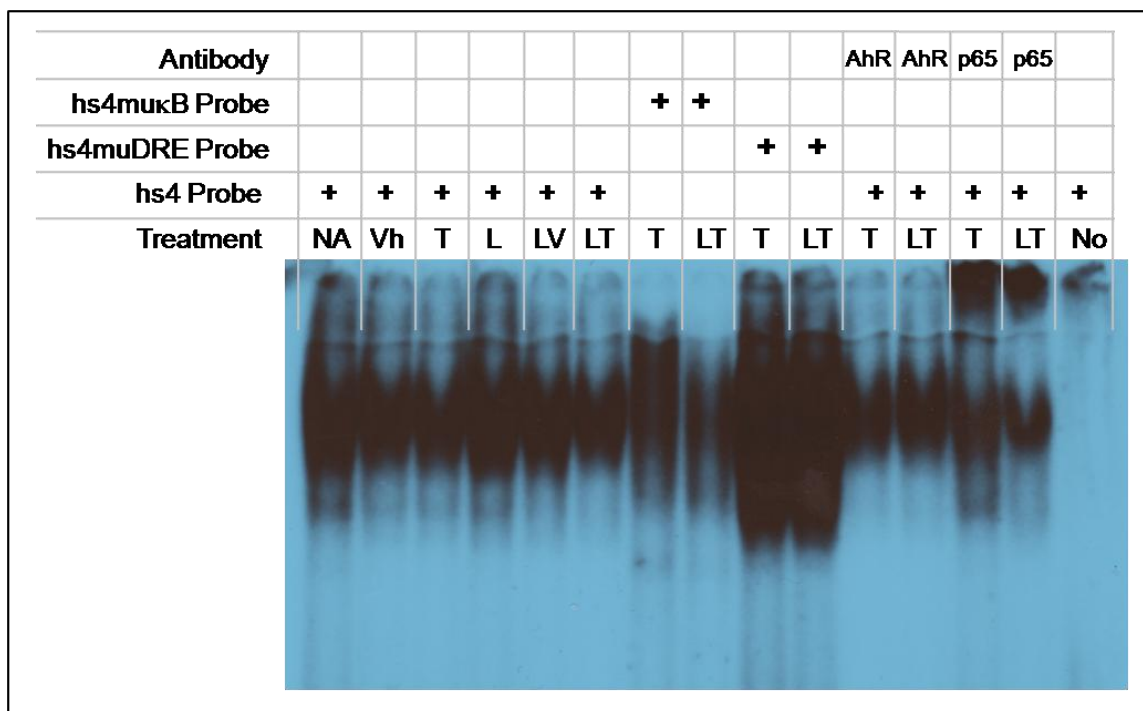


**Figure 41 EMSA Comparing the Binding of Altered hs4 Sequences:** Nuclear proteins were isolated from CH12.LX cells by the non-ionic detergent method after no treatment (NA) or treatment with vehicle (Vh) or 30 nM TCDD (T), or 1 μg/mL LPS, or LPS and vehicle (LV) or LPS and TCDD (LT). “No” indicates no protein was added to the binding reaction. Proteins were incubated with probes for the mouse hs4 enhancer with altered binding sites in 25 mM HEPES, 1 mM EDTA, 1 mM DTT, 1 μg poly[d(I-C)], 10% glycerol, and 100 mM KCl. Antibody to AhR or RelA (p65) was added where indicated for supershift. Reaction products were separated on a 5% polyacrylamide gel and documented on autoradiography film.

Concurrent with the human sequence and poly[d(I-C)] optimization studies I decided to see if altering the binding sites on the hs4 probe would help me understand what changes might be occurring in binding patterns between treatments. Figure 41 shows the result of that experiment. Although it is still difficult to make comparisons between treatments for the wild type hs4 probe, the probe with a mutated κB site clearly has an altered binding pattern: with TCDD treatment, there appears to be more binding

with the missing  $\kappa$ B site while with LPS and TCDD treatment there appears to be less binding with the missing  $\kappa$ B site. In both treatment groups, there was a great increase in binding when the DRE site was mutated. This supports the theory I explained earlier in which NF $\kappa$ B proteins and AhR compete for binding of the overlapping sites of the hs4 enhancer. When one is not able to bind, binding of the other increases, so long as sufficient protein is present. The addition of antibody to AhR did not change binding in the T or LT treatment groups, but antibody for RelA (p65) caused a supershift such that much of the labeled probe was still near the loading well in those lanes. I know from previous studies that AhR is in the nucleus and will bind a DRE site (DRE3 probe), and from published studies that AhR will bind the hs4 probe, but with experiments like that in Figure 41, it seems that the amount of AhR binding the hs4 probe is very small when NF $\kappa$ B/Rel proteins are also bound. Furthermore, binding to the hs4 probe which has a mutated  $\kappa$ B site is reduced to a greater extent when cells are co-treated with LPS and TCDD than with TCDD alone. Since LPS treatment should cause an increase in NF $\kappa$ B/Rel proteins in the nucleus, perhaps an interaction between AhR proteins and the abundant unbound NF $\kappa$ B/Rel proteins (because their binding site has been mutated) causes less AhR to bind the probe, and thus the enhancer. If that is true, and AhR inhibits the hs4 enhancer, such an interaction (which reduces the AhR binding to hs4) might explain the synergistic increase in reporter expression associated with published transient expression studies(Sulentic, et al., 2004).

## Conclusions

I was able to successfully produce deletion derivative clones which stably expressed hs3b/hs4-regulated  $\gamma$ 2b when activated by LPS. Unlike transient transfection studies, the cells stably expressing  $\gamma$ 2b under hs3a/hs4 regulation were either inhibited or not affected by TCDD. In this stable expression system, the hs3b enhancer is paired with the hs4 enhancer, but in the transient expression studies which showed synergistic activation, the hs4 enhancer were isolated on a luciferase reporter plasmid. The presence of hs3b may have altered the response of hs4 to TCDD treatment. In addition, the transgene may have responded differently because of its presence in the context of chromatin in this study or by the use of a full-length hs4 sequence while a truncated hs4 was used in the transient experiments. There may also have been unpredicted modifications caused by CRE-recombination that altered the response to TCDD.

I was unable to show a difference in NF $\kappa$ B/Rel subunits that bind to enhancer sequences after TCDD treatment. My results were highly variable; however, some of the experiments were conducted for optimization of assay conditions, and many were conducted to troubleshoot or clarify the binding that occurred, so every treatment condition was not included in each experiment, and controls such as probe alone or unlabeled competitor were sometimes left out to make room for more samples.

One possible reason for not seeing clear differences in binding is that in the EMSA, proteins have an abundance of binding sites in conditions that favor binding, so subtle differences in protein concentrations are masked. Moreover, if the difference in

binding is related to the different affinities of AhR and NFκB/Rel proteins for their binding sites, then competition for the overlapping binding sites in the hs4 enhancer may be masked by the excess of sites. One additional step I would like to try is altering the total amount of protein and the amount of labeled probe in the reaction. Perhaps if the ratio of protein to probe is properly balanced, the proteins will truly have to compete for binding sites.

Another possible explanation was pointed out by Tian in a recent review(Tian, 2009): interaction between NFκB/Rel and AhR does not necessarily inhibit binding of either protein to its DNA recognition site. The protein might bind, but because of an association with the other protein, another signal that is necessary to initiate transcription is blocked. If the dichotomy in effects of TCDD on individual enhancers is related to accessibility of binding sites for additional transcription factors, the EMSA would not reveal that difference.

The EMSA/Western was a difficult assay to master. Improvements to this technique might include using a larger membrane transfer rig to avoid cutting and handling the somewhat fragile EMSA gel or to use antibodies that have been validated to bind the target proteins while they are bound to DNA. I would much prefer to use supershifts, unlabeled probes, and the mutation of binding sites to identify bound proteins given the difficulties I experienced conducting the Western.

# Bibliography

Allan, L. L., & Sherr, D. H. (2005). Constitutive Activation and Environmental Chemical Induction of the Aryl Hydrocarbon Receptor/Transcription Factor in Activated Human B Lymphocytes. *Molecular Pharmacology* , 67, 17540-1750.

Altarawneh, M., Dlugogorski, B. Z., Kennedy, E. M., & Mackie, J. C. (2009). Mechanisms for formation, chlorination, dechlorination and destruction of polychlorinated dibenzo-p-dioxins and dibenzofurans (PCDD/Fs). *Progress in Energy and Combustion Science* , 35, 245-274.

Arnold, L. W., LoCascio, N. J., Lutz, P. M., Pennell, C. A., Klapper, D., & Haughton, G. (1983). Antigen-induced lymphomagenesis: Identification of a murine B cell lymphoma with known antigen specificity. *The Journal of Immunology* , 131 (4), 2064-2068.

Arulampalam, V., Furebring, C., Samuelsson, A., Lendahl, U., Borrebaeck, C., Lundkvist, I., et al. (1996). Elevated expression levels of an Ig transgene in mice links the IgH 3' enhancer to the regulation of IgH expression. *International Immunology* , 8 (7), 1149-1157.

Arulampalam, V., Grant, P. A., Samuelsson, A., Lendahl, U., & Pettersson, S. (1994). Lipopolysaccharide-dependent transactivation of the temporarily regulated immunoglobulin heavy chain 3' enhancer. *The European Journal of Immunology* , 24 (7), 1671-1677.

Ashida, H., & Matsumura, F. (1998). Effect of in vivo administered 2,3,7,8-tetrachlorodibenzo-p-dioxin on DNA-binding activity of nuclear transcription factors in liver of guinea pigs. *J Biochem Mol Toxicol* , 12 (4), 191-204.

Baglolle, C. J., Maggirwar, S. B., Gasiewicz, T. A., Thatcher, T. H., Phipps, R. P., & Sime, P. J. (2008). The aryl hydrocarbon receptor attenuates tobacco smoke-induced cyclooxygenase-2 and prostaglandin production in lung fibroblasts through regulation of the NF-kappaB family member RelB. *J Biol Chem* , 283 (43), 28944-28957.

- Bhattacharya, D., Lee, D. U., & Sha, W. C. (2002). Regulation of Ig class switch recombination by NF-kappaB: Retroviral expresssion of RelB in activated B cells inhibits switchiing to IgG1, but not to IgE. *Int Immunol* , 14 (9), 983-991.
- Bishop, G. A., & Haughton, G. (1986). Induced differentiation of a transformed clone of ly-1+ Bcells by clonal T cells and antigen. *Proceedings of the National Academy of Sciences USA* , 83 (19), 7410-7414.
- Bishop, G. A., & Hostager, B. S. (2001). B lymphocyte activation by contact-mediated interactions with T llymphocytes. *Current Opinion in Immunology* , 13, 278-285.
- Bonilla, F. A., & Oettgen, H. C. (2010). Adaptive Immunity. *Journal of Allergy and Clinical Immunology* , 125 (2), S33-S40.
- Buu-Hoï, N. P., Chanh, P.-H., Sesqué, G., Azum-Gelade, M. C., & Saint-Ruf, G. (1972). Organs as Targets of "Dioxin" (2,3,7,8-Tetrachlorodibenzo-p-dioxin) Intoxication. *Naturwissenschaften* , 59, 174-175.
- Cawthon, R. M. (2002). Telomere Measurement by quantitative PCR. *Nucl Acids Res* , 13 (10), e47.
- Chauveau, C., Pinaud, E., & Cogne, M. (1998). Synergies between regulatory elements of the immunoglobulin heavy chain locus and its pallindromic 3' locus control region. *The European Journal of Immunology* , 28, 3048-3056.
- Chen, F. E., Huang, D. B., Chen, Y. Q., & Ghosh, G. (1998). Crystal structure of p50/p65 heterodimer of trranscription factor NF-kappaB to DNA. *Nature* , 391 (6665), 410-413.
- Crawford, R. B., Holsapple, M. P., & Kaminski, N. E. (1997). Leukocyte Activation Induces Aryl Hydrocarbon Receptor Up-Regulation, DNA Binding, and Increased Cyp1a1 Expression in the Absence of Exogenous Ligand. *Molecular Pharmacology* , 52, 921-927.
- Dariavach, P., Williams, G. T., Campbell, K., Pettersson, S., & Neuberger, M. S. (1991). The mouse IgH 3'-enhancer. *The European Journal of Immunology* , 21, 1499-1504.

Davarinos, N. A., & Pollenz, R. S. (1999). Aryl hydrocarbon receptor imported into the nucleus following ligand binding is rapidly degraded via the cytoplasmic proteasome following nuclear export. *The Journal of Biological Chemistry* , 274 (40), 28708-28715.

Denison, M. S., & Nagy, S. R. (2003). Activation of the Aryl Hydrocarbon Receptor by Structurally Diverse Exogenous and Endogenous Chemicals. *Annu Rev of Pharmacol Toxicol* , 43, 309-334.

DiDonato, J. A., Mercurio, F., & Karin, M. (1995). Phosphorylation of I kappa B alpha preceeds but is not sufficient for its dissociation from NF-kappa B. *Mol Cell Biol* , 15 (3), 1302-1311.

Dikici, E., Qu, X., Rowe, L., Millner, L., Logue, C., Deo, S., et al. (2009). Aequorin variants with improved bioluminescence properties. *Protein Engineering Design and Selection* , 22 (4), 243-248.

Dooley, R. K., & Hosapple, M. P. (1988). Elucidation of cellular targets responsible for tetrachlorodibenzo-*p*-dioxin (TCDD)-induced suppression of antibody responses: I. The role of the B lymphocyte. *Immunopharmacology* , 16 (3), 167-180.

Dooley, R. K., Morris, D. L., & Hosapple, M. P. (1990). Elucidation of cellular targets responsible for tetrachlorodibenzo-*p*-dioxin (TCDD)-induced suppression of antibody responses: II. The role of the T-lymphocyte. *Immunopharmacology* , 19 (1), 47-58.

Durrin, L. K., Jones, P. B., Fisher, J. M., Galeazzi, D. R., & Whitlock, J. P. (1987). 2,3,7,8-Tetrachlorodibenzo-*p*-dioxin receptors regulate transcription of the cytochrome P1-450 gene. *The Journal of Cellular Biochemistry* , 35 (2), 153-160.

Dyke, P. H., Foan, C., Wenborn, M., & Coleman, P. J. (1997). A review of dioxin releases to land and water in the UK. *The Science of the Total Environment* , 207, 119-131.

Feng, B., Cheng, S., Pear, W. S., & Liou, H.-C. (2004). NF-kB inhibitor blocks B cell development at two checkpoints. *Medical Immunology* , 3 (1), 1.

Fernandez-Salguero, P. M., Hilbert, D. M., Rudikoff, S., Ward, J. M., & Gonzalez, F. J. (1996). Aryl-hydrocarbon Receptor-Deficient Mice Are Resistant to 2,3,7,8-Tetrachlorodibenzo-p-dioxin-Induced Toxicity. *Toxicology and Applied Pharmacology* , 140, 173-179.

Fujita, T., Nolan, G. P., Ghosh, S., & Baltimore, D. (1992). Independent modes of transcription activation by the p50 and p65 subunits of NF-kappa B. *Genes Dev* , 6 (5), 775-787.

Fukuda, I., Mukai, R., Kawase, M., Yoshida, K.-i., & Ashida, H. (2007). Interaction between the Aryl Hydrocarbon Receptor and Its Antagonists, Flavonoids. *Biochemical and Biophysical Research Communications* , 359, 822-827.

Gerondakis, S., Grumont, R., Rourke, I., & Grossmann, M. (1998). The regulation of roles of Rel/NF-kappa B transcription factors during lymphocyte activation. *Curr Opin Immunol* , 10 (3), 353-359.

Geusau, A., Schmaldienst, S., Derfler, K., Papke, O., & Abraham, K. (2002). Severe 2,3,7,8-tetrachlorodibenzo-p-dioxin (TCDD) intoxication: kinetics and trials to enhance elimination in two patients. *Archives of Toxicology* , 76, 316-325.

Giannini, S. L., Singh, M., Calvo, C.-F., Ding, G., & Birshstein, B. K. (1993). DNA Regions Flanking the Mouse Ig 3' a Enhancer Are Differentially Methylated and DNase I Hypersensitive during B Cell Differentiation. *The Journal of Immunology* , 150 (5), 1772-1780.

Grant, P. A., Arulampalam, V., Ahrlund-Richter, L., & Pettersson, S. (1992). Identification of ETS-like lymphoid specific elements within the immunoglobulin heavy chain 3' enhancer. *Nucleic Acids Research* , 20 (17), 4401-4408.

Grigoriadis, G., Zhan, Y., Grumont, R. J., Metcalf, D., Handman, E., Cheers, C., et al. (1996). The rel subunit of NF-kappaB-like transcription factors is a positive and negative regulator of macrophage gene expression: Distinct roles for rel in different macrophage populations. *EMBO J* , 15 (24), 7099-7107.

Grumont, R. J., Rourke, I. J., & Gerondakis, S. (1999). Rel-dependent induction of A1 transcription is required to protect B cells from antigen receptor ligation-induced apoptosis. *Genes Dev* , 13 (4), 400-411.

Grumont, R. J., Rourke, I. J., O'Reilly, L. A., Strasser, A., Miyake, K., Sha, W., et al. (1998). B lymphocytes differentially use the rel and nuclear factor kappa B1 (NF-kappaB1) transcription factors to regulate cell cycle progression and apoptosis in quiescent and mitogen-activated cells. *J Exp Med* , 187 (5), 66333-674.

Gugasyan, R., Grumont, R., Grossmann, M., Nakamura, Y., Pohl, T., Nesic, D., et al. (2000). Rel/NF-kappaB transcription factors: Key mediators of B-cell activation. *Immunol Rev* , 176, 134-140.

Gupta, B. M., Vos, J. G., Moore, J. A., Zinkl, J. G., & Bullock, B. C. (1973). Pathologic Effects of 2,3,7,8-Tetrachlorodibenzo-p-dioxin in Laboratory Animals. *Environmental Health Perspectives* , 5, 125-140.

Hansen, S., Baeuerle, P., & Blasi, F. (1994). Purification, reconstitution, and I kappa B association of the c-rel-p65 (RelA) complex, a strong activator of transcription. *Mol Cell Biol* , 14 (4), 2596.

Hansen, S., Nerlov, C., Zabel, U., Verde, P., Johnsen, M., Baeuerle, P., et al. (1992). A novel complex between the p65 subunit of NF-kappa B and c-rel binds to a DNA element involved in the phorbol ester induction of the human urokinase gene. *EMBO J* , 11 (1), 205.

Harris, M. W., Moore, J. A., Vos, J. G., & Gupta, B. N. (1973). General Biological Effects of TCDD in Laboratory Animals. *Environmental Health Perspectives* , 5, 101-109.

Henseler, R. A., Romer, E. J., & Sulentic, C. E. (2009). Diverse chemicals including aryl hydrocarbon receptor ligands modulate transcriptional activity of the 3' immunoglobulin heavy chain regulatory region. *Toxicology* , 261 (1-2), 9-18.

- Holsapple, M., & McCay, J. A. (1986). Immunosuppression without liver induction by subchronic exposure to 2,7-dichlorodibenzo-p-dioxin in adult female B6C3F1 mice. *Toxicology & Applied Pharmacology* , 83 (3), 445-455.
- Hosapple, M. P., Dooley, R. K., Mc Nerney, P. J., & McCay, A. J. (1986). Direct Suppression of Antibody Responses by Chlorinated Dibenzodioxins in Cultured Spleen Cells from (C57BL/6 x C3H)F1 and DBA/2 Mice. *Immunopharmacology* , 12, 175-186.
- Huang, H., & Buekens, A. (1995). On the mechanisms of dioxin formation in combustion processes. *Chemosphere* , 31 (9), 4099-4117.
- Jones, P. B., Durrin, L. K., Fisher, J. M., & Whitlock, J. P. (1986). Control of Gene Expression by 2,3,7,8-Tetrachlorodibenzo-p-dioxin. *The Journal of Biological Chemistry* , 261 (15), 6647-6650.
- Jones, P. B., Durrin, L. K., Galeazzi, D. R., & Whitlock, J. P. (1986). Control of Cytochrome P1-450 Gene Expression: Analysis of a Dioxin-Responsive Enhancer System. *Proceedings of the National Academy of Sciences USA* , 83 (9), 2802-2806.
- Ju, Z., Volpi, S. A., Hassan, R., Martinez, N., Giannini, S. L., Gold, T., et al. (2007). Evidence for physical interaction between the immunoglobulin heavy chain variable region and the 3' regulatory region. *J Biol Chem* , 282 (48), 35169-35178.
- Kazlauskas, A., Poellinger, L., & Pongratz, I. (1999). Evidence That the Co-chaperone p23 Regulates Ligand Responsiveness of the Dioxin (Aryl Hydrocarbon) Receptor. *The Journal of Biological Chemistry* , 274 (19), 13519-13524.
- Kazlauskas, A., Poellinger, L., & Pongratz, I. (2000). The Immunophilin-like Protein XAP2 Regulates Ubiquitination and Subcellular Localization of the Dioxin Receptor. *The Journal of Biological Chemistry* , 275 (52), 41317-41324.
- Kerger, B. D., Leung, H.-W., Scott, P., Paustenbach, D. J., Needham, L. L., Patterson, D. G., et al. (2006). Age- and Concentration-Dependent Elimination Half-Life of 2,3,7,8-Tetrachlorodibenzo-p-dioxin in Seveso Children. *Environmental Health Perspectives* , 114 (10), 1596-1602.

- Kerkvliet, N. J. (2009). AHR-mediated immunomodulation: The role of altered gene transcription. *Biochemical Pharmacology* , 77, 746-760.
- Kim, D., Gazourian, L., Quadri, S., Romieu-Mourez, R., Sherr, D., & Sonenshein, G. (2000). The RelA NF-kappaB subunit and the aryl hydrocarbon receptor (AhR) cooperate to transactivate the c-myc promoter in mammary cells. *Oncogene* , 19 (48), 5498.
- Kistler, B., Rolink, A., Marienfeld, R., Neumann, M., & Wirth, T. (1998). Induction of nuclear factor-kappa B during primary B cell differentiation. *J Immunol* , 160 (5), 2308-2317.
- Körner, W., Golor, G., Schulz, T., Wiesmüller, T., Hagenmaier, H., & Neubert, D. (2002). Tissue concentrations and induction of a hepatic monooxygenase in male Wistar rats after repeated doses of defined polychlorinated dibenzo-p-dioxin and dibenzofuran (PCDDs and PCDFs) mixtures. *Archives of Toxicology* , 75 (11-12), 653-664.
- Kretzschmar, M., Meisterernst, M., Scheidereit, C., Li, G., & Roeder, R. G. (1992). Transcriptional regulation of the HIV-1 promoter by NF-kappaB in vitro. *Genes and Development* , 6 (5), 761-774.
- Kumar, S., O'Dowd, C., Dunckley, M., & Lund, T. (1994). A comparative evaluation of three transfection procedures as assessed by resistance of G418 conferred to HEPG2 cells. *Biochemistry (NY)* , 32 (6), 1059.
- Kunsch, C., Ruben, S., & Rosen, C. A. (1992). Selection of optimal kappa B/Rel DNA-binding motifs: Interaction of both subunits of NF-kappa B with DNA is required for transcriptional activation. *Mol Cell Biol* , 12 (10), 4412.
- Lanier, L. L., Arnold, L. W., Raybourne, R. B., Russell, S., Lynes, M. A., Warner, N. L., et al. (1982). Transplantable B-cell lymphomas in B10. H-2aH-4bp/Wts mice. *Immunogenetics* , 16 (4), 367-371.
- Lees, M. J., & Whitelaw, M. L. (1999). Multiple Roles of Ligand in Transforming the Dioxin Receptor to an Active Basic Helix-Loop-Helix/PAS Transcription Factor

Complex with the Nuclear Protein Arnt. *Molecular and Cellular Biology* , 19 (8), 5811-5822.

Lees, M. J., Peet, D. J., & Whitelaw, M. L. (2003). Defining the Role for XAP2 in Stabilization of the Dioxin Receptor. *The Journal of Biological Chemistry* , 278 (38), 35878-35888.

Liao, F., Giannini, S. L., & Birshstein, B. K. (1992). A nuclear DNA-binding protein expressed during early stages of B cell differentiation interacts with diverse segments within and 3' of the IgH chain gene cluster. *The Journal of Immunology* , 148 (9), 2909-2917.

Lieberson, R., Giannini, S. L., Birshstein, B. K., & Eckhardt, L. A. (1991). An enhancer at the 3' end of the mouse immunoglobulin heavy chain locus. *Nucleic Acids Research* , 19 (4), 933-937.

Lieberson, R., Ong, J., Shi, X., & Eckhardt, L. A. (1995). Immunoglobulin gene transcription ceases upon deletion of a distant enhancer. *The EMBO Journal* , 14 (24), 6229-6238.

Lin, S. C., Wortis, H. H., & Stavnezer, J. (1998). The ability of CD40L, but not lipopolysaccharide, to initiate immunoglobulin switching to immunoglobulin G1 is explained by differential induction of NF-kappaB/Rel proteins. *Mol Cell Biol* , 18 (9), 5523-5532.

Lin, Y., & Stavnezer, J. (1992). Regulation of transcription of the germ-line Ig-alpha constant region gene by an ATF element and by novel transforming growth factor-beta 1-responsive elements. *The Journal of Immunology* , 149 (9), 2914.

Liou, H. C., Sha, W. C., Scott, M. L., & Baltimore, D. (1994). Sequential induction of NF-kappa B/Rel family proteins during B-cell terminal differentiation. *Mol Cell Biol* , 14 (8), 5349-5359.

- Liu, X., Shi, T., Ren, H., Su, H., Yan, W., & Suo, X. (2008). Restriction enzyme-mediated transfection improved transfectin efficiency in vitro in apicomplexan parasite *eimeria tenella*. *Molecular Biochemistry and Parasitology* , 161 (1), 72.
- Livák, F. (2004). In vitro and in vivo studies on the generation of the primary T cell receptor repertoire. *Immunological Reviews* , 200, 23-35.
- Madisen, L., & Groudine, M. (1994). Identification of a locus control region in the immunoglobulin heavy-chain locus that deregulates c-myc expression in plasmacytoma and Burkitt's lymphoma cells. *Genes & Development* , 8, 2212-2226.
- Manis, J. P., van der Stoep, N., Tian, M., Ferrini, R., Davidson, L., Bottaro, A., et al. (1998). Class Switching in B Cells Lacking 3' Immunoglobulin Heavy Chain Enhancers. *The Journal of Exploratory Medicine* , 188 (8), 1421-1431.
- Marcus, R. S., Holsapple, M. P., & Kaminski, N. E. (1998). Lipopolysaccharide Activation of Murine Splenocytes and Splenic B Cells Increased the Expression of Aryl Hydrocarbon Receptor and Aryl Hydrocarbon Receptor Nuclear Translocator. *The Journal of Pharmacology and Experimental Therapeutics* , 287 (3), 1113-1118.
- McGuire, J., Whitelaw, M. L., Pongratz, I., Gustafsson, J.-Å., & Poellinger, L. (1994). A Cellular Factor Stimulates Ligand-Dependent Release of hsp90 from the Basic Helix-Loop-Helix Dioxin Receptor. *Molecular and Cellular Biology* , 14 (4), 2438-2446.
- Medjakovic, S., & Jungbauer, A. (2008). Red Clover Isoflavones Biochanin A and Formononetin are Potent Ligands of the Human Aryl Hydrocarbon Receptor. *Journal of Steroid Biochemistry and Molecular Biology* , 108 (1-2), 171-177.
- Michaelson, J. S., Giannini, S. L., & Birshtein, B. K. (1995). Identification of 3'a-hs4, a novel Ig Heavy chain enhancer element regulated at multiple stages of B cell differentiation. *Nucleic Acids Research* , 23 (6), 975-981.
- Michaelson, J. S., Singh, M., Snapper, C. M., Sha, W. C., Baltimore, D., & Birshtein, B. K. (1996). Regulation of 3' IgH Enhancers by a Common Set of Factors, Including kB-Binding Proteins. *The Journal of Immunology* , 156, 2828 - 2839.

Mills, F. C., Harindranath, N., Mitchell, M., & Max, E. E. (1997). Enhancer Complexes Located Downstream of Both Human Immunoglobulin Ca Genes. *The Journal of Experimental Medicine* , 186 (6), 845-858.

Nakayama, K., Shimizu, H., Mitomo, K., Watanabe, T., Okamoto, S., & Yamamoto, K. (1992). A lymphoid cell-specific nuclear factor containing c-rel-like proteins preferentially interacts with interleukin-6 kappa B-related motifs whose activities are repressed in lymphoid cells. *Mol Cell Biol* , 12 (4), 1736.

Neumann, M., Wohlleben, G., Chuvpilo, S., Kistler, B., Wirth, T., Serfling, E., et al. (1986). CD40, but not lipopolysaccharide and anti-IgM stimulation of primary B lymphocytes, leads to a persistent nuclear accumulation of RelB. *The Journal of Immunology* , 157 (11), 4862-4869.

Okey, A. B., Riddick, D. S., & Harper, P. A. (1994). The Ah Receptor: Mediator of the Toxicity of 2,3,7,8-Tetrachlorodibenzo-p-dioxin (TCDD) and Related Compounds. *Toxicology Letters* , 70 (1), 1-22.

Ong, J., Stevens, S., Roeder, R. G., & Eckhardt, L. A. (1998). 3' IgH enhancer elements shift synergistic interactions during B cell development. *J Immunol* , 160, 4896-4903.

Perdew, G. H. (1988). Association of the Ah receptor with the 90-kDa heat shock protein. *The Journal of Biological Chemistry* , 263, 13802-13805.

Perkins, N., Schmid, R., Duckett, C., Leung, K., Rice, N., & Nabel, G. (1992). Distinct combinations of NF-kappa B subunits determine the specificity of transcriptional activation. *Proc Nat Acad Sci* , 89 (5), 1529.

Pettersson, S., Cook, G. P., Brüggemann, M., Williams, G. T., & Neuberger, M. S. (1990). A second B cell-specific enhancer 3' of the immunoglobulin heavy-chain locus. *Nature* , 344 (6262), 165-168.

Phelan, D., Winter, G. M., Rogers, W. J., Lam, L. C., & Denison, M. S. (1998). Activation of the Ah Receptor Signal Transduction Pathway by Bilirubin and Biliverdin. *Archives of Biochemistry and Biophysics* , 357 (1), 155-163.

- Pinaud, E., Khamlichi, A. A., Le Morvan, C., Drouet, M., Nalesso, V., Le Bert, M., et al. (2001). Localization of the 3' IgH Locus Elements that Effect Long-Distance Regulation of Class Switch Recombination. *Immunity*, 16, 187-199.
- Pirkle, J. L., Wolfe, W. H., Patterson, D. G., Needham, L. L., Michalek, J. E., Miner, J. C., et al. (1989). Estimates of the half-life of 2,3,7,8-tetrachlorodibenzo-p-dioxin in Vietnam Veterans of Operation Ranch Hand. *Journal of Toxicology and Environmental Health*, 27 (2), 165-171.
- Pohjanvirta, R., & Tuomisto, J. (1994). Short-Term Toxicity of 2,3,7,8-Tetrachlorodibenzo-p-dioxin in Laboratory Animals: Effects, Mechanisms, and Animal Models. *Pharmacological Reviews*, 46 (4), 483-549.
- Poland, A., & Knutson, J. C. (1982). 2,3,7,8-Tetrachlorodibenzo-p-dioxin and Related Halogenated Aromatic Hydrocarbons: Examination of the Mechanism of Toxicity. *Annual Review of Pharmacology and Toxicology*, 22, 517-554.
- Pongratz, I., Mason, G. G., & Poellinger, L. (1992). Dual Roles of the 90-kDa Heat Shock Protein hsp90 in Modulating Functional Activities of the Dioxin Receptor. *The Journal of Biological Chemistry*, 267 (19), 13728-13734.
- Puga, A., Barnes, S. J., Chang, C., Zhu, H., Nephew, K. P., Khan, S. A., et al. (2000). Activation of transcription factors activator protein-1 and nuclear factor-kappaB by 2,3,7,8-tetrachlorodibenzo-p-dioxin. *Biochem Pharmacol*, 59 (8), 997-1005.
- Reisinger, H., Steinfeldner, W., Stern, B., Katinger, H., & Kunert, R. (2008). The absence of effect of gene copy number and mRNA level on the amount of mAb secretion from mammalian cells. *Applied Microbiology*, 81 (4), 701.
- Rojo, J. M., Bello, R., & Portolés, P. (2008). T-Cell Receptor. In A. Sigalov (Ed.), *Multichain Immune Recognition Receptor Signaling: From Spatiotemporal Organization to Human Disease Series from Advances in Experimental Medicine and Biology* (Vol. 640, pp. 1-11). New York: Springer.

Ruby, C. E., Leid, M., & Kerkvliet, N. I. (2002). 2,3,7,8-tetrachlorodibenzo-p-dioxin suppresses tumor necrosis factor-alpha and anti CD40-induced activation of NF-kappaB/Rel in dendritic cells: P50 homodimer activation is not affected. *Molecular Pharmacology* , 62 (3), 722-728.

Ruby, C. E., Leid, M., & Kerkvliet, N. I. (2002). 2,3,7,8-tetrachlorodibenzo-p-dioxin suppresses tumor necrosis factor-alpha and anti-CD40-induced activation of NF-kappaB/Rel in dendritic cells: P50 homodimer activation is not affected. *Molecular Pharmacology* , 62 (3), 722-728.

Ruby, C. E., Leid, M., & Kerkvliet, N. I. (2002). 2,3,7,8-tetrachlorodibenzo-p-dioxin suppresses tumor necrosis factor-alpha and anti-CD40-induced activation of NF-kappaB/Rel in dendritic cells: P50 homodimer activation is not affected. *Mol Pharmacol* , 62 (3), 722-728.

Schroeder, H. W., & Cavacini, L. (2010). Structure and function of immunoglobulins. *J ALLERGY CLIN IMMUNOL* , S41-S52.

Seidl, K. J., Manis, J. P., Bottaro, A., Zhang, J., Davidson, L., Kisselgof, A., et al. (1999). Position-dependent inhibition of class-switch recombination by PGK-neo cassettes inserted into the immunoglobulin heavy chain constant region locus. *Proceedings of the National Academy of Science USA* , 96, 3000-3005.

Shi, L. Z., Faith, N. G., Nakayama, Y., Suresh, M., Steinberg, H., & Czuprynski, C. J. (2007). The aryl hydrocarbon receptor is required for optimal resistance to listeria monocytogenes infection in mice. *J Immunol* , 179 (10), 6952-6962.

Shi, X., & Eckhardt, L. A. (2001). Deletional analyses reveal an essential role for the hs3b/hs4 IgH 3' enhancer pair in an IG-secreting but not an earlier-stage B cell line. *International Immunology* , 13 (8), 1003-1012.

Sinal, C. J., & Bend, J. R. (1997). Aryl Hydrocarbon Receptor-Dependent Induction of Cyp1a1 by Bilirubin in Mouse Hepatoma Hepa 1c1c7 Cells. *Molecular Pharmacology* , 52, 590-599.

- Singh, M., & Birshstein, B. K. (1993). NF-HB (BSAP) is a repressor of the murine immunoglobulin heavy-chain 3' alpha enhancer at stages of B-cell differentiation. *Molecular and Cellular Biology* , 13 (6), 3611-3622.
- Sovak, M. A., Bellas, R. E., Kim, D. W., Zanieski, G. J., Rogers, A. E., Traish, A. M., et al. (1997). Aberrant nuclear factor-kappaB/Rel expression and pathogenesis of breast cancer. *The Journal of Clinical Investigation* , 100 (12), 2952-2960.
- Sulentic, C. E., Holsapple, M. P., & Kaminski, N. E. (1998). Aryl Hydrocarbon Receptor-Dependent Suppression by 2,3,7,8-Tetrachlorodibenzo-p-dioxin of IgM Secretion in Activated B Cells. *Molecular Pharmacology* , 53, 623-629.
- Sulentic, C. E., Holsapple, M. P., & Kaminski, N. E. (2000). Putative Link between Transcriptional Regulation of IgM Expression by 2,3,7,8-Tetrachlorodibenzo-p-dioxin and the Aryl Hydrocarbon Receptor/Dioxin-Responsive Enhancer Signaling Pathway. *The Journal of Pharmacology and Experimental Therapeutics* , 295, 705-716.
- Sulentic, C. E., Kang, J. S., Na, Y. J., & Kaminski, N. E. (2004). Interactions at a dioxin responsive element (DRE) and an overlapping kappaB site within the hs4 domain of the 3'alpha immunoglobulin heavy chain enhancer. *Toxicology* , 200 (2-3), 235-246.
- Sulentic, C. E., Zhang, W., Na, Y. J., & Kaminski, N. E. (2004). 2,3,7,8-Tetrachlorodibenzo-p-dioxin, an Exogenous Modulator of the 3' alpha Immunoglobulin Heavy Chain Enhancer in the CH12.LX Mouse Cell Line. *J Pharmacol Exp Ther* , 309 (1), 71-78.
- Thigpen, J. E., Faith, R. E., McConnell, E. E., & Moore, J. A. (1975). Increased Susceptibility to Bacterial Infection as a Sequela of Exposure to 2,3,7,8-Tetrachlorodibenzo-p-dioxin. *Infection and Immunity* , 12 (6), 1319-1324.
- Tian, Y. (2009). Ah receptor and NF-kappaBinterplay on the stage of epigenome. *Biochem Pharmacol* , 77 (4), 670.

- Tian, Y., Ke, S., Denison, M. S., Rabson, A. B., & Gallo, M. A. (1999). Ah receptor and NF-kappaB interactions, a potential mechanism for dioxin toxicity. *The Journal of Biological Chemistry* , 274 (1), 510-515.
- Tumang, J. R., Owyang, A., Andjelic, S., Jin, Z., Hardy, R. R., Liou, M. L., et al. (1998). C-rel is essential for B lymphocyte survival and cell cycle progression. *Eur J Immunol* , 28 (12), 4299-4312.
- Urban, M. B., & Baeuerle, P. A. (1990). The 65-kD subunit of NF-kappaB is a receptor for I-kappaB and a modulator of DNA-binding specificity. *Genes and Development* , 4 (11), 1975-1984.
- van der Molen, G. W., Kooijman, S. A., Michalek, J. E., & Slob, W. (1998). The Estimation of Elimination Rates of Persistent Compounds: A Re-Analysis of 2,3,7,8-Tetrachlorodibenzo-p-dioxin Levels in Vietnam Veterans. *Chemosphere* , 37 (9-12), 1833-1844.
- Vecchi, A., Mantovani, A., Sironi, M., Luini, W., Cairo, M., & Garattini, S. (1980). Effect of Acute Exposure to 2,3,7,8-Tetrachlorodibenzo-p-dioxin on Humoral Antibody Production in Mice. *Chemical-Biological Interactions* , 30, 337-342.
- Vecchi, A., Sironi, M., Antonia Canegrati, M., Recchia, M., & Garattini, S. (1983). Immunosuppressive Effect of 2,3,7,8-Tetrachlorodibenzo-p-dioxin in Strains of Mice with Different Susceptibility to Induction of Aryl Hydrocarbon Hydroxylase. *Toxicology and Applied Pharmacology* , 68, 434-441.
- Vogel, C. F., Sciallo, E., Li, W., Wong, P., Lazennec, G., & Matsumura, F. (2007). RelB, a new partner of aryl hydrocarbon receptor-mediated transcription. *Mol Endocrinol* , 21 (12), 2941-2955.
- Vorderstrasse, B. A., Bohn, A. A., & Lawrence, B. P. (2003). Examining the relationship between impaired host resistance and altered immune function in mice treated with TCDD. *Toxicology* , 188, 15-28.

- Vos, J. G., Kreeftenberg, J. G., Engel, H. W., Minderhoud, A., & Van Noorle Jansen, L. M. (1978). Studies on 2,3,7,8-Tetrachlorodibenzo-p-dioxin-Induced Immune Suppression and Decreased Resistance to Infection: Endotoxin Hypersensitivity, Serum Zinc Concentrations and Effect of Thymosin Treatment. *Toxicology* , 9, 75-86.
- Vos, J. G., Moore, J. A., & Zinkl, J. G. (1973). Effect of 2,3,7,8-Tetrachlorodibenzo-p-dioxin on the Immune System of Laboratory Animals. *Environmental Health Perspectives* , 5, 149-162.
- Vos, J. G., Moore, J. A., & Zinkl, J. G. (1974). Toxicity of 2,3,7,8-Tetrachlorodibenzo-p-dioxin (TCDD) in C57B1/6. *Toxicology and Applied Pharmacology* , 29 (2), 229-241.
- Vos, Q., Lees, A., Wu, Z.-Q., Snapper, C. M., & Mond, J. J. (2000). B-cell activation by T-cell-independent type 2 antigens as an integral part of the humoral immune response to pathogenic microorganisms. *Immunological Reviews* , 176, 154-170.
- Warren, T. K., Mitchell, K. A., & Lawrence, B. P. (2000). Exposure to 2,3,7,8-Tetrachlorodibenzo-p-dioxin (TCDD) Suppresses the Humoral and Cell-Mediated Immune Responses to Influenza A Virus without Affecting Cytolytic Activity in the Lung. *Toxicological Sciences* , 56, 114-123.
- Wihelmsson, A., Cuthill, S., Denis, M., Wikström, A.-C., Gustafsson, J.-Å., & Poellinger, L. (1990). The specific DNA binding activity of the dioxin receptor is modulated by the 90 kd heat shock protein. *The EMBO Journal* , 9 (1), 69-76.
- Williams, C. E., Crawford, R. B., Holsapple, M. P., & Kaminski, N. E. (1996). Identification of Functional Aryl Hydrocarbon Receptor and Aryl Hydrocarbon Receptor Nuclear Translocator in Murine Splenocytes. *Biochemical Pharmacology* , 52, 771-780.
- Woo, A., Dods, J., Susanto, E., Ulgiati, D., & Abraham, L. (2002). A proteomics approach for the identification of DNA binding activities observed in the electrophoretic mobility shift assay. *Molecular and Cellular Proteomics* , 1 (6), 472-478.

Xie, T. D., Sun, L., Zhao, H. G., Fuchs, J. A., & Tsong, T. Y. (1992). Study of mechanisms of electric field-induced DNA transfection. IV. effects of DNA topology on cell uptake and transfection efficiency. *Biophysical Journal* , 63 (4), 1026-1031.

Xie, T., & Tsong, T. Y. (1993). Study of mechanisms of electric field-induced DNA transfection. V. effects of DNA topology on surface binding, cell uptake, expression, and integration into host chromosomes of DNA in the mammalian cell. *Biophysical Journal* , 65 (4), 1684.

Zelazowski, P., Shen, Y., & Snapper, C. M. (2000). NF- $\kappa$ B/p50 and NF- $\kappa$ B/c-Rel differentially regulate the activity of the 3'aE-hs1,2 enhancer in normal murine B cells in an activation-dependent manner. *International Immunology* , 12 (8), 1167 - 1172.